Theoretical study of mixing in liquid clouds.

Part 1: classical concept

(revised version, 14 March 2016)

Alexei Korolev[1], Alex Khain[2], Mark Pinsky[2], and Jeffrey French[3]

[1] Environment Canada, Cloud Physics and Severe Weather Section, Toronto, Canada

[2] Department of Atmospheric Sciences, the Hebrew University of Jerusalem, Israel

[3] University of Wyoming, Laramie, WY, USA

Correspondence to: A. ~~Korolev (alexei.korolev@ec.gc.ca)~~Korolev (alexei.korolev@canada.ca)

Abstract

~~Relationships between basic microphysical parameters are studied within~~ The present study considers final stages of in-cloud mixing in the framework of classical concept of homogeneous and extreme inhomogeneous mixing. ~~Analytical expressions~~ Simple analytical relationships between basic microphysical parameters were obtained for homogeneous and ~~numerical simulations of~~extreme inhomogeneous mixing based on the adiabatic consideration. It was demonstrated that during homogeneous mixing the functional relationships between ~~droplet concentration, extinction coefficient, liquid water content, and mean volume droplet~~the moments of the droplets size~~, formed at the final~~ distribution hold only during primary stage of mixing ~~are presented. The expressions are~~. Subsequent random mixing between already mixed parcels and undiluted cloud parcels breaks these relationships. However, during extreme inhomogeneous mixing the functional relationships between the microphysical parameters hold both for primary and subsequent mixing. The obtained relationships can be used to identify the type of mixing ~~for~~from in- situ observations ~~obtained~~. The effectiveness of the developed method was demonstrated using in-situ data collected in convective clouds. ~~The analysis suggests~~It was found that for the specific set of ~~observations investigated here, in-~~situ measurements the interaction between cloudy and entrained environments ~~is~~was dominated by ~~inhomogeneous mixing. Lastly, an analysis of different response times of the cloud environment~~

Style Definition: Normal: Font: (Default) Calibri, 11 pt, English (Canada)

Style Definition: Heading 1

Style Definition: Balloon Text: Font: English (Canada)

Style Definition: Hyperlink: Font color: Blue

Style Definition: Footnote Text

Style Definition: Header: Font: (Default) Calibri, 11 pt, English (Canada)

Style Definition: Footer: Font: (Default) Calibri, 11 pt, English (Canada), Tab stops: 8.25 cm, Centered + 16.51 cm, Right + Not at 7.62 cm + 15.24 cm

Style Definition: Comment Text: Font: (Default) Calibri, 10 pt, English (Canada)

Style Definition: Comment Subject: Font: (Default) Calibri, English (Canada)

Style Definition: HTML Address

Style Definition: Colorful Shading - Accent 11

Formatted: Font: Times New Roman

Formatted: Justified

Formatted: Font: Times New Roman

Formatted: Font: Times New Roman

Formatted: Font: Times New Roman, 12 pt

Formatted: Justified

Formatted: Justified, Line spacing: 1.5 lines

Formatted: Font: Times New Roman, 12 pt

Formatted: Font: Times New Roman, 12 pt

Formatted: Justified

Formatted: Indent: First line: 0.75 cm, Don't adjust space between Latin and Asian text, Don't adjust space between Asian text and numbers

Formatted: Font: Times New Roman, 12 pt

Formatted: Font: Times New Roman, 12 pt

Formatted: Font: Times New Roman, 12 pt

Formatted: Font: Times New Roman, 12 pt

Formatted: Font: Times New Roman, 12 pt

Formatted: Font: Times New Roman, 12 pt

Formatted: Font: Times New Roman, 12 pt

Formatted: Font: Times New Roman, 12 pt

Formatted: Font: Times New Roman, 12 pt

Formatted: Font: Times New Roman, 12 pt

Formatted: Font: Times New Roman, 12 pt

Formatted: Font: Times New Roman, 12 pt

Formatted: Font: Times New Roman, 12 pt

Formatted: Font: Times New Roman, 12 pt

~~undergoing mixing is presented. Comparisons of different characteristic times suggest that within the same mixing environment depending on mixing fraction some volumes may be dominated by homogeneous mixing whereas others by inhomogeneous mixing.~~extreme inhomogeneous mixing.

~~1.~~ 1 Introduction

Turbulent mixing is an important non-adiabatic process in the atmosphere that to a large extent determines spatial gradients of many thermodynamic (e.g. temperature, humidity) and cloud microphysical parameters (e.g. hydrometeor concentrations, extinction coefficient, condensed water content) and as such, needs to be properly described in numerical simulations of clouds and weather predictions. Entrainment and mixing occurs during the entire lifetime of a cloud and is active not only near cloud edges, but it is important throughout the whole cloud volume. Mixing of cloudy and entrained air results in changes to the shape of the droplet size distribution through partial droplet evaporation and can also lead to changes in droplet concentration through complete evaporation of some fraction of droplets~~.~~ and dilution. The shape of the droplet size distribution plays key role in the initiation of precipitation and radiative properties of clouds.

The treatment of mixing in numerical simulations of clouds and precipitation formation remains a challenging problem. Besides the issues related to the way to describe mixing in numerical schemes, there is a fundamental problem of identifying a scenario or path, that mixing events should follow. ~~Since~~Through the pioneering works of Latham and Reed (1977) and Baker et al. (1980) two explicitly alternative scenarios of mixing were identified. In the first scenario ~~the~~ turbulent mixing rapidly stirs the environment ~~unifying~~homogenizing the fields of temperature and humidity. ~~After~~Following that, all of the droplets undergo partial evaporation under the same conditions. The result of this mixing is ~~the~~a droplet population with reduced sizes, but ~~their~~a total ~~amount~~number that remains unchanged. This type of mixing is referred to as *homogeneous*. In the second scenario~~,~~ mixing occurs more slowly such that the population of droplets experiences different amount of sub-saturation. Some number of droplets completely evaporates, while others experience no evaporation until the entirety of the entrained air becomes saturated. ~~After~~Following

Formatted: Font: Times New Roman, 12 pt, Not Highlight

Formatted: Indent: First line: 0.75 cm, No bullets or numbering, Don't adjust space between Latin and Asian text, Don't adjust space between Asian text and numbers

Formatted: Font: Times New Roman, 12 pt

Formatted: Font: Times New Roman, 12 pt

Formatted: Font: Times New Roman, 12 pt

Formatted: Font: Times New Roman, 12 pt

Formatted: Font: Times New Roman, 12 pt

Formatted: Font: Times New Roman, 12 pt

Formatted: Font: Times New Roman, 12 pt

Formatted: Font: Times New Roman, 12 pt

Formatted: Font: Times New Roman, 12 pt

Formatted: Font: Times New Roman, 12 pt

Formatted: Font: Times New Roman, 12 pt

Formatted: Font: Times New Roman, 12 pt

Formatted: Font: Times New Roman, 12 pt

that, turbulence mixes the rest of the droplets with the saturated, but droplet-free environment. During this type of mixing the size of droplets remains unchanged; however, their ~~concentration~~total number is reduced. This type of mixing is called *extreme inhomogeneous*. The intermediate case when some fraction of droplets ~~evaporate~~evaporates partially, ~~the~~another other fraction evaporates completely, and ~~the~~a third fraction remains ~~without changes~~unchanged is in some works referred to as inhomogeneous (e.g. Baker and Latham, 1980).

The conditions for homogeneous and extreme inhomogeneous mixing and their effects on precipitation formation have been debated in cloud physics over forty years. There are a number of numerical simulations and theoretical efforts on studying different aspects of mixing and its effect on cloud microphysics (e.g. Baker and Latham, 1982; Jensen and Baker, 1989; Su et al., 1989; Lasher-Trapp et al., 2005; Jeffrey, 2007; Andrejczuk et al., 2009; Kumar et al., 2013; Jarecka et al, 2013 and many others). A comprehensive review of the works on the effect of turbulence and mixing on cloud ~~droplets~~droplet formation can be found in Devenish et al. (2012).

A number of studies were dedicated to identifying type of mixing based on in-situ observations. Most of the previous ~~in-situ~~ observations ~~provide~~provided evidence supporting inhomogeneous mixing (e.g. Hill and Choularton, 1985; Paluch, 1986; Bower and Choularton, 1988; Blyth and Latham, 1991; Gerber et al., 2008, Lu et al. 2011; Beals et al. 2016). However, works of Jensen and Baker (1989), Paluch and Baumgardner (1989), Burnet and Brenguier (2007), Lehmann et al. (2009~~) suggest~~), Lu et al. (2011) suggested occurrence of homogeneous mixing. So, at the moment it appears that both types of mixing may occur in liquid clouds. However, the environmental conditions ~~resulting from~~governing one or the other type of mixing remain not well understood.

Early experimental work on identifying type of mixing from in-situ observations were based on the analysis of spatial variability of the shapes of individual droplet size distributions (e.g. Paluch and Knight, 1984; Paluch, 1986; Bower and Choularton, 1988). ~~However, the~~The effectiveness of this method involving the analysis of ~~overly~~a large number of individual size spectra turned out to be quite low. Another technique utilized expected functional relationships between droplet concentration ~~(N)~~(N) and droplet ~~radius (r), which is~~diameter (D) specific to each type of mixing. Thus, during extreme inhomogeneous mixing the droplet size is expected to remain unchanged, whereas the concentration will vary. ~~However, during~~During homogeneous mixing the droplet size and concentration in cloud will be related to each other in a certain way, depending on

the mixing fraction and the humidity of the entrained air. This fact was used in observational studies ~~on~~for identifying the type of mixing from "mixing diagrams" that related ~~N~~ N and ~~r~~ D_v for different regimes of mixing (e.g. Burnet and Brenguier, 2007; Gerber et al~~.~~., 2008; Lehmann et al~~.~~., 2009).

The use of ~~the~~ mixing diagrams to some extent facilitated identification of type of mixing. However, in many cases scatter in the relationships between ~~N versus r~~ N vs. D_v was too large, ~~which hindered identifying~~hindering identification of the type of mixing (Burnet and Brenguier, 2007). To resolve this problem many researchers used other complementary measurements supporting identification of the type of mixing (e.g. Gerber et al~~.~~., 2008; Lehmann et al~~.~~., 2009~~)~~).

Besides the effect on ~~N~~ N and ~~r~~ D_v, the type of mixing is anticipated to manifest itself in relationships between other moments of the droplet size distribution, ~~$f(r)$~~ $f(D)$. Such relationships may provide insight into the mixing process and identify type of mixing. With the exception of the work by Hill and Choularton (1985), who correlated concentration and liquid water content, there have been few attempts to use any other microphysical parameters for identification of type of mixing.

In order to fill this gap, this study presents a theoretical analysis of relationships between different moments of ~~$f(r)$~~ $f(D)$ within the framework of homogeneous and extreme inhomogeneous mixing. The analysis is focused on the first four moments of ~~$f(r)$~~ $f(D)$ corresponding to the droplet concentration ~~N~~ N (0^{th} moment), integral ~~radius~~ ~~Nr~~ diameter $N\bar{D}$ (1^{st} moment), extinction coefficient ~~β~~ β (2^{nd} moment~~) and~~), liquid water mixing ratio ~~q~~ q (3^{rd} moment) and mean volume ~~radius~~ ~~$\bar{r}_3$~~ diameter D_v (mixed 3^{rd} and 0^{th} moment). It is shown that the ~~set of~~ newly obtained relationships ~~obtained can be effectively used to identify~~between the moments provide a more robust identification of type of mixing from in-situ ~~observations.~~ measurements as compared to conventional $N - D_v^3$ relationships used in mixing diagrams. Relationships between moments may be useful for parameterization of mixing in numerical simulations of clouds and climate, interpretations of remote sensing measurements.

This paper constitutes the first in a series of three papers. ~~The present paper~~It considers the final stage of mixing based on the formal definitions of homogeneous and extreme inhomogeneous mixing. These two types of mixing present two extreme regimes of mixing. The following two papers provide a detailed analysis of the time dependent processes during

Formatted: Font: Times New Roman, 12 pt
Formatted: Font: Times New Roman, 12 pt
Formatted: Font: Times New Roman, 12 pt
Formatted: Font: Times New Roman, 12 pt, Italic
Formatted: Font: Times New Roman, 12 pt
Formatted: Font: Times New Roman, 12 pt
Formatted: Font: Times New Roman, 12 pt
Formatted: Font: Times New Roman, 12 pt
Formatted: Font: Times New Roman, 12 pt
Formatted: Font: Times New Roman, 12 pt
Formatted: Font: Times New Roman, 12 pt
Formatted: Font: Times New Roman, 12 pt
Formatted: Font: Times New Roman, 12 pt
Formatted: Font: Times New Roman, 12 pt
Formatted: Font: Times New Roman, 12 pt
Formatted: Font: Times New Roman, 12 pt, Italic
Formatted: Font: Times New Roman, 12 pt
Formatted: Font: Times New Roman, 12 pt
Formatted: Font: Times New Roman, 12 pt
Formatted: Font: Times New Roman, 12 pt
Formatted: Font: (Default) Times New Roman, 12 pt
Formatted: Font: Times New Roman, 12 pt, Italic
Formatted: Font: Times New Roman, 12 pt
Formatted: Font: Times New Roman, 12 pt, Italic
Formatted: Font: Times New Roman, 12 pt
Formatted: Font: Times New Roman, 12 pt, Italic
Formatted: Font: Times New Roman, 12 pt
Formatted: Font: Times New Roman, 12 pt
Formatted: Font: Times New Roman, 12 pt, Italic
Formatted: Font: Times New Roman, 12 pt
Formatted: Font: Times New Roman, 12 pt
Formatted: Font: Times New Roman, 12 pt
Formatted: Font: Times New Roman, 12 pt
Formatted: Font: Times New Roman, 12 pt
Formatted: Font: Times New Roman, 12 pt
Formatted: Comment Text, Left, Indent: First line: 0.75 cm
Formatted: Font: Times New Roman, 12 pt
Formatted: Font: Times New Roman, 12 pt
Formatted: Font: Times New Roman, 12 pt

homogeneous (Pinsky et al. 2015a., 2016a) and inhomogeneous (Pinsky et al. 2015b., 2016b) mixing. where non-extreme regimes are considered as well.

The present This paper is arranged in the following way. Section 2 presents analysis of the analytical relationship between $N, N\bar{r}, \beta, q, \bar{r}_3 N, N\bar{D}, \beta, q, D_v$ and mixing fraction μ for the cases of homogeneous and extreme inhomogeneous mixing. The In Sect. 3 the obtained analytical relationships are compared with the results of numerical simulation of $N, \beta, q, \bar{r}_3 N, \beta, q, D_v$ formed after at the final stage of mixing are discussed in section 3.. Section 4 presents results of simulation of progressive mixing and it effect of the relationships between moments. Examples of relationship between $N, \beta, q, \bar{r}_3 N, \beta, q$ and D_v from in-situ observations are presented in section 4. Section Sect. 5 presents analysis of characteristic response times of a cloud environment during homogeneous and inhomogeneous mixing. The. The discussion and concluding remarks are presented in section Sect. 6. and 7.

2. 2 Effect of mixing on microphysical variables

2.1. Phenomenological consideration

The conceptual diagrams of homogeneous and extreme inhomogeneous mixing are shown on Fig. 1. During the first stage of extreme inhomogeneous mixing the sub-saturated subsaturated parcel is engulfed into the cloudy environment (Fig. 1 a1 1a1). Then, the droplets at the interface of the sub-saturated parcel and the cloud environment undergo complete evaporation until the air within the engulfed volume reaches saturation (Fig. 1 a2 1a2). After that the saturated but droplet free parcel mixes with the rest of the cloud environment (Fig. 1 a3 1a3). The result of the inhomogeneous mixing is that the cloud parcel has reduced droplet concentration and the droplet sizes remain unchanged.

In the case of homogeneous mixing after entraining into a cloud (Fig. 1 b1 1b1), the sub-saturated subsaturated parcel "instantly" mixes up with its cloud environment (Fig. 1 b2), which leads 1b2) leading to undersaturation of the total volume. Then, all droplets throughout the mixed volume undergo simultaneous evaporation until the equilibrium state is reached. The result of homogeneous mixing is a cloud parcel volume with reduced concentration of droplets and droplets with reduced sizes (Fig. 1 b3). 1b3).

Formatted: Font: Times New Roman, 12 pt
Formatted: Font: Times New Roman, 12 pt
Formatted: Font: Times New Roman, 12 pt
Formatted: Indent: First line: 0.75 cm, Don't adjust space between Latin and Asian text, Don't adjust space between Asian text and numbers
Formatted: Font: Times New Roman, 12 pt
Formatted: Font: Times New Roman, 12 pt, Italic
Formatted: Font: Times New Roman, 12 pt
Formatted: Font: Times New Roman, 12 pt
Formatted: Font: Times New Roman, 12 pt
Formatted: Font: (Default) Times New Roman, 12 pt
Formatted: Font: Times New Roman, 12 pt
Formatted: Font: Times New Roman, 12 pt
Formatted: Font: (Default) Times New Roman, 12 pt
Formatted: Font: Times New Roman, 12 pt
Formatted: Font: Times New Roman, 12 pt
Formatted: Font: Times New Roman, 12 pt
Formatted: Font: Times New Roman, 12 pt
Formatted: Indent: First line: 0.75 cm, No bullets or numbering, Don't adjust space between Latin and Asian text, Don't adjust space between Asian text and numbers
Formatted: Font: Times New Roman, 12 pt
Formatted: Indent: First line: 0.75 cm, Don't adjust space between Latin and Asian text, Don't adjust space between Asian text and numbers
Formatted: Font: Times New Roman, 12 pt
Formatted: Font: Times New Roman, 12 pt
Formatted: Font: Times New Roman, 12 pt
Formatted: Font: Times New Roman, 12 pt
Formatted: Font: Times New Roman, 12 pt
Formatted: Font: Times New Roman, 12 pt
Formatted: Font: Times New Roman, 12 pt
Formatted: Font: Times New Roman, 12 pt
Formatted: Font: Times New Roman, 12 pt
Formatted: Font: Times New Roman, 12 pt
Formatted: Font: Times New Roman, 12 pt
Formatted: Font: Times New Roman, 12 pt
Formatted: Font: Times New Roman, 12 pt
Formatted: Font: Times New Roman, 12 pt

~~The difference between these two~~ Based on mass and energy conservation considerations the final state of the bulk parameters (i.e. liquid water mixing fraction, humidity, temperature, etc.) is the same for both types of mixing~~ is as follows:~~. However, in the case of extreme inhomogeneous mixing ~~the~~ saturation is reached through complete evaporation of some fraction of droplets, ~~whereas~~and their sizes remain constant. ~~In~~Whereas in case of homogeneous mixing ~~the~~ saturation is reached through a uniform evaporation of droplets, ~~whereas~~and the total number of droplets ~~in the diluted parcel~~ remains unchanged. It should be noted, that in both cases ~~of mixing~~ the droplet concentration decreases due to dilution by the ~~entrained~~mixed droplet free sub-saturated parcel.

The following discussion will be specifically focused ~~at~~on the microphysical properties formed at the final stage of the homogeneous and extreme inhomogeneous mixing. The processes occurring during mixing state (i.e. transition 1a→2a and 1b→2b in Fig. 1) remain outside the frame of this work. Following the formalism of homogeneous and extreme inhomogeneous mixing, the process of mixing reaches the final stage when (1) the entrained and cloud environment are mixed up and the spatial gradients of the microphysical ~~(N, β, q,~~(N, β, q, etc.) and environmental ~~(T, S, e,~~(T, S, e, etc.) parameters approach to zero; (2) the diffusional process related to droplet evaporation comes into equilibrium. The second condition is completed when (a) the environment reaches saturation state, or (b) the entire population of droplets is completely evaporated, if the ~~mixed~~entrained air is ~~too~~sufficiently dry.

The above description of homogeneous and extreme inhomogeneous mixing is highly idealized. Actual in-cloud mixing does not occur as a sequence of discrete events (Fig.1) that individually come to equilibrium only to be followed by next discrete mixing events. But rather it is occurring continuously on a cascade of different spatial and time scales. Broadwell and Breidenthal (1982) summarized the experimental evidence and proposed the following description of mixing in turbulent shear layers. Mixing takes place in a series of events. Two shear layers exchange mass by engulfing parcels from an opposite layer into localized zones. The initially large-scale filaments of the two gases break down towards smaller scales due to the action of turbulence. The turbulence stretches the interface between the gases and enhances the molecular diffusion across the increasing surface. The actual mixing of the engulfed volume is a molecular diffusion process that is most effective after the break down volumes reduce to the Kolmogorov viscosity scale. It is anticipated that the reaction of the ensemble of droplets~~ from entrainment~~ is a combination of homogeneous and inhomogeneous mixing with domination of one type of mixing

Formatted: Font: Times New Roman, 12 pt

Formatted: Font: Times New Roman, 12 pt

Formatted: Font: Times New Roman, 12 pt

Formatted: Font: Times New Roman, 12 pt

Formatted: Font: Times New Roman, 12 pt

Formatted: Font: Times New Roman, 12 pt

Formatted: Font: Times New Roman, 12 pt

Formatted: Font: Times New Roman, 12 pt

Formatted: Font: Times New Roman, 12 pt

Formatted: Font: Times New Roman, 12 pt

Formatted: Font: Times New Roman, 12 pt

Formatted: Font: Times New Roman, 12 pt

Formatted: Font: Times New Roman, 12 pt

Formatted: Font: Times New Roman, 12 pt

Formatted: Font: Times New Roman, 12 pt

Formatted: Font: Times New Roman, 12 pt

Formatted: Font: Times New Roman, 12 pt

Formatted: Font: Times New Roman, 12 pt

Formatted: Font: Times New Roman, 12 pt

Formatted: Font: Times New Roman, 12 pt

Formatted: Font: Times New Roman, 12 pt

Formatted: Font: Times New Roman, 12 pt

Formatted: Font: Times New Roman, 12 pt

Formatted: Font: Times New Roman, 12 pt

Formatted: Font: Times New Roman, 12 pt, Font color: Auto

Formatted: Font: Times New Roman, 12 pt

Formatted: Font: Times New Roman, 12 pt

over the other depending on the characteristic spatial and time scales of the environment determined by turbulence, cloud microphysics, state parameters and stage of mixing.

2.2~~.~~ Methodology

The foregoing discussion will be focused on mixing between saturated cloud parcels and out-of-cloud sub-saturated air. The cloud parcel contains droplets with ~~monodisperse radius r_0,~~ average diameter $\bar{D}_1$, liquid mixing ratio ~~q_0~~ q_1 and number concentration ~~N_0.~~ N_1. The initial temperature in the cloud parcel is ~~T_1,~~ T_1, relative humidity ~~$S_1 = 1$,~~ $RH_1 = 1$, where ~~$S = e / E_s(T)$ (The~~ $RH = e/e_s(T)$ (the explanation of ~~variables~~ variable notations is provided in ~~Appendix A~~ Table 1). The second parcel is droplet free ~~($N_2 = 0$),~~ $(N_2 = 0)$, sub-saturated with initial relative humidity ~~$S_2 < 1$~~ $RH_2 < 1$ and temperature ~~T_2.~~ T_2. The mixing occurs isobarically, i.e. ~~during mixing p=const.~~ $p = const$. At the ~~end~~ final stage of ~~the~~ mixing the temperature and humidity formed in the resulting parcel are ~~T_m~~ T and ~~S_m (Appendix B).~~ RH (appendix A). The process of mixing is completed when the mixed parcel reaches equilibrium due to the air saturation (i.e. ~~$S_m = 1$),~~ $RH = 1$,) or due to the complete evaporation of droplets. In the latter case the final humidity is ~~$S_m < 1$.~~ $RH \le 1$. The effect of the vertical velocity and vertical travel ~~of the mixing parcels on temperature T_m, humidity S_m,~~ on final T, RH, and ~~condensed water q_m~~ q is not considered here, i.e. vertical velocity ~~$u_z = 0$.~~ $u_z = 0$.

Without the loss of generality the masses of the cloudy and sub-saturated volumes prior to the mixing are assumed to have a unit masses, i.e. ~~$m_1 = 1$~~ $m_1 = 1$ and ~~$m_2 = 1$.~~ $m_2 = 1$. The mixing process will be considered as mixing of ~~the μ~~ μ fraction of the cloud ~~volume~~ parcel with ~~the $(1 - \mu)$~~ $(1 - \mu)$ fraction of the second (sub-saturated) ~~volume~~ parcel. The mixing cloud fraction ~~is changing~~ may vary within the range of ~~$0 \le \mu \le 1$.~~ $0 \le \mu \le 1$. Therefore, the mass of the resulting mixed parcel is equal to ~~$m_1\mu + (1 - \mu)m_2 = 1$.~~ $m_1\mu + (1 - \mu)m_2 = 1$. This approach simplifies the consideration of mixing and allows considering all possible proportions of the mixing of two volumes.

2.3 Effect of mixing on liquid water and temperature

Formatted: Font: Times New Roman, 12 pt
Formatted: Font: Times New Roman, 12 pt
Formatted: Font: Times New Roman, 12 pt
Formatted: Font: Times New Roman, 12 pt
Formatted: Font: Times New Roman, 12 pt
Formatted: Font: Times New Roman, 12 pt
Formatted: Font: Times New Roman, 12 pt
Formatted: Font: Times New Roman, 12 pt
Formatted: Font: Times New Roman, 12 pt
Formatted: Font: Times New Roman, 12 pt
Formatted: Font: Times New Roman, 12 pt
Formatted: Font: Times New Roman, 12 pt
Formatted: Font: Times New Roman, 12 pt
Formatted: Font: Times New Roman, 12 pt
Formatted: Font: Times New Roman, 12 pt
Formatted: Font: Times New Roman, 12 pt
Formatted: Font: Times New Roman, 12 pt
Formatted: Font: Times New Roman, 12 pt
Formatted: Font: Times New Roman, 12 pt
Formatted: Font: Times New Roman, 12 pt
Formatted: Font: Times New Roman, 12 pt
Formatted: Font: Times New Roman, 12 pt
Formatted: Font: Times New Roman, 12 pt
Formatted: Font: Times New Roman, 12 pt
Formatted: Font: (Default) Times New Roman, 12 pt
Formatted: Font: Times New Roman, 12 pt
Formatted: Font: Times New Roman, 12 pt, Italic
Formatted: Font: Times New Roman, 12 pt
Formatted: Font: Times New Roman, 12 pt
Formatted: Font: Times New Roman, 12 pt
Formatted: Font: Times New Roman, 12 pt
Formatted: Font: Times New Roman, 12 pt
Formatted: Font: Times New Roman, 12 pt
Formatted: Font: Times New Roman, 12 pt
Formatted: Font: Times New Roman, 12 pt
Formatted: Font: Times New Roman, 12 pt

The mixing ratio of liquid water q formed at the final stage of mixing is determined by the mass of the mixing cloud water μq_1 and amount of evaporated water required to saturate the newly formed mixed volume δq_m. The mass balance of liquid water for the mixing volume yields

$$q = \mu q_1 - \delta q_m , \quad (1)$$

where

$$\delta q_m = \frac{c_p R_v T_{m0}^2}{L^2} \ln\left(\frac{1 + \frac{e_s(T_{m0}) R_a L^2}{p c_{pa} R_v^2 T_{m0}^2}}{1 + RH_{m0} \frac{e_s(T_{m0}) R_a L^2}{p c_{pa} R_v^2 T_{m0}^2}} \right) \cong -\frac{S_{m0}}{A_2} \quad (2)$$

is the mixing ratio of liquid water required to saturate 1kg of volume with temperature T_{m0} and humidity RH_{m0} (appendix A); T_{m0}, RH_{m0} and S_{m0}, are the temperature, relative humidity formed and supersaturation formed in the volume after instantaneous air mixing, but before droplets start evaporating (appendix A); $e_S(T_{m0})$ is saturation vapor pressure at temperature T_{m0}.

Eq. (1) is a non-linear function of μ, since T_{m0}, e_{m0} and thus δq_m depend on μ. Eq.(1) can be simplified, if $T_1 = T_2$. In this case $T_{m0} = T_1 = T_2$, and $e_S(T_{m0}) = e_S(T_1) = e_S(T_2)$. Given that, the expression under logarithm in Eq.(2) can be expanded in series resulting in (appendix B)

$$\delta q_m = (1 - \mu)\delta q^* , \quad (3)$$

where

$$\delta q^* = \frac{c_p R_v T_2^2}{L^2} \ln\left(\frac{1 + \frac{e_S(T_2) R_a L^2}{p c_{pa} R_v^2 T_2^2}}{1 + RH_2 \frac{e_S(T_2) R_a L^2}{p c_{pa} R_v^2 T_2^2}} \right) \cong -\frac{S_2}{A_2} \quad (4)$$

is the mixing ratio of liquid water required to saturate 1 kg of the entrained dry air. Substituting Eq.(3) in Eq.(1) gives

$$q = \mu q_1 - (1 - \mu)\delta q^* , \quad (5)$$

The value of δq^* does not depend on μ, and Eq. (5) is a simple linear function of μ. The comparisons with numerical simulations showed, that Eq.(5) provides accuracy within few percent, when the temperature difference $|T_1 - T_2| < 2$°C. Although, in many cases $|T_1 - T_2|$ may

Field Code Changed

Field Code Changed

Field Code Changed

Formatted: Font: Times New Roman, 12 pt, Font color: Black

Field Code Changed

Field Code Changed

vary a wide range reaching 10°C or higher, clouds with $|T_1 - T_2| < 2$°C are quite common. Therefore, for the sake of simplicity, Eq.(5) and the assumption $T_1 \approx T_2$ will be used in the following consideration of mixing.

It should be noted that, Eqs (1) and (5) are valid for the cases, when $\mu > \mu_{cr}$. Here μ_{cr} is critical mixing fraction, which separates partial and complete evaporation of cloud water in the mixing volume (section 2.4). Cases when $\mu \le \mu_{cr}$ correspond to complete evaporation of droplets, and $q = 0$.

The temperature at the final stage of mixing can be estimated as (appendix C)

$$T = T_{m0} - \frac{(1-\mu)\delta q^* L}{c_{pa}}, \quad \text{when } \mu > \mu_{cr} \qquad (6a)$$

$$T = T_{m0} - \frac{\mu q_1 L}{c_{pa}} \quad \text{when } \mu \le \mu_{cr} \qquad (6b)$$

Eqs. (1), (5), (6) were obtained based on mass and energy conservation, and they do not depend on how mixing proceeds. Therefore, Eqs. (1), (5), (6) are valid for both homogeneous and inhomogeneous mixing.

2.4 Complete evaporation

As mentioned in section 2.2 the process of mixing is complete only after reaching equilibrium by saturating the mixed volume or by evaporating of all cloud droplets depending on the mixing fraction μ. The critical mixing fraction μ_{cr}, corresponding to evaporation of all droplets, can be found from Eq.(5) when $q = 0$, i.e.

$$\mu_{cr} = \frac{\delta q^*}{q_1 + \delta q^*} \qquad (7)$$

Critical mixing fraction separates μ in two subranges: (a) $1 \ge \mu > \mu_{cr}$ where q is described by Eqs.(1) or (5) and $RH_m = 1$; (b) $\mu_{cr} \ge \mu \ge 0$ where $q = 0$ and $RH_m \le 1$.

For the general case when $T_1 \ne T_2$, μ_{cr}, can be found by solving the non-linear equation

$$\mu_{cr} q_1 - \delta q_m(\mu_{cr}) = 0 \qquad (8)$$

Figure 2 shows comparisons of dependences of μ_{cr} vs. q_1 calculated from Eq. (7) and those deduced from a numerical model (Sect. 3). Critical mixing fraction μ_{cr} is also shown by black stars in Fig. 4. The locations of the stars in Fig.4 coincide well with the locations, where the

Field Code Changed

Field Code Changed

Formatted: Font: Times New Roman, 12 pt, Font color:

Formatted: Font color: Black

Field Code Changed

Field Code Changed

modeled microphysical moments become zero. The obtained agreement between analytical and modeled μ_{cr} in Figs. 2 and 4 validates the developed approach.

2.5 Extreme inhomogeneous mixing

Within the framework of ~~the~~ extreme inhomogeneous mixing some fraction of droplets undergo complete evaporation, whereas the rest of the droplets remain unchanged. Therefore, such a process results in scaling the droplet size distribution ~~$f(r)$,~~ $f(D)$, i.e.

~~$f(r) = kf_0(r)$ (1)~~

$$f(D) = kf_1(D) \qquad (9)$$

where ~~k~~ k is some coefficient dependent on ~~μ~~ μ and the initial environmental parameters of the mixing volumes, ~~$f_0(r)$~~ $f_1(D)$ is the droplet size distribution before mixing.

~~Eq.1~~Equation (9) yields ~~relationship~~relationships between pairs ~~n-th~~nth and ~~m~~k-th moments

~~$\frac{M_n}{M_{0n}} = \frac{M_m}{M_{0m}}$ (2)~~

$$\frac{M_n}{M_{n1}} = \frac{M_k}{M_{k1}} \qquad (10)$$

where ~~$M_n = \int_0^\infty f(r) r^n dr$~~ $M_n = \int_0^\infty f(D) D^n dD \Big/ \int_0^\infty f(D) dD$ is the ~~n-th~~nth moment of ~~$f(r)$.~~ $f(D)$.

Therefore, it is anticipated that for extreme inhomogeneous mixing droplet number concentration ~~N~~ (N (0th moment), extinction coefficient ~~β~~ β (2nd moment), liquid water ~~content q~~ mixing ratio q (3rd moment), along with other moments, will correlate with each other, i.e.

~~$\frac{N}{N_0} = \frac{\beta}{\beta_0} = \frac{q}{q_0}$ (3)~~

$$\frac{N}{N_1} = \frac{\beta}{\beta_1} = \frac{q}{q_1} \qquad (11)$$

One of the consequences of Eqs.~~1-3~~ (9)-(11) is ~~conservation of~~ that the characteristic droplet sizes~~, i.e. $\bar{r}$, $\bar{r}_2$, $\bar{r}_3$, r_{eff}~~ $\bar{D}$, D_2, D_v, D_{eff} will remain constant during inhomogeneous mixing.

~~The liquid water mixing ratio q resulting from extreme inhomogeneous mixing can be written based on~~ For the ~~mass balance of vapor~~case $T_1 = T_2$ and ~~liquid water as~~

$q = \mu q_0 - \delta q$, (4)

where δq is $\mu > \mu_{cr}$ Eqs. (5) and (11) yield the amount of liquid water per 1 kg of the dry air required to saturate the *volume formed as a result of mixing of the cloud and entrained parcels before droplet evaporation*. The value of δq can be found as (Appendix B)

$$\delta q = \frac{L^2}{c_p R_v T_2^2} \ln\left(\frac{1 + \frac{E_s(T_{m0}) R_a L^2}{p c_p R_v^2 T_{m0}^2}}{1 + S_{m0} \frac{E_s(T_{m0}) R_a L^2}{p c_p R_v^2 T_{m0}^2}} \right) \quad (5)$$

Here T_{m0} and S_{m0} are the temperature and relative humidity formed in the parcel after mixing, but before droplets start evaporating (Appendix B), $E_s(T_{m0})$ is saturation humidity at temperature T_{m0}. Since T_{m0}, S_{m0} and E_s are functions of the ratio of μ, then δq is function of μ as well.

Combining Eq.4 and Eq.3 yields dependence of N versus μ N vs. μ

$$N = N_0 \left(\mu - \frac{\delta q}{q_0} \right) \quad (6)$$

Eqs. 4 and 5 describe changes of q and δq for a general case, when the temperatures in the cloud (T_1) and sub-saturated (T_2) parcels are different. When $T_1 = T_2$, the temperature after mixing, but before droplet evaporation, remain the same, i.e. $T_{m0} = T_1 = T_2$. For this case the amount of liquid water evaporated after mixing can be estimated as the amount of evaporated liquid required to saturate the entrained parcel

$$\delta q = (1 - \mu) \delta q^*, \quad (7)$$

where

$$\delta q^* = \frac{L^2}{c_p R_v T_2^2} \ln\left(\frac{1 + \frac{E_S(T_2) R_a L^2}{p c_p R_v^2 T_2^2}}{1 + S_2 \frac{E_S(T_2) R_a L^2}{p c_p R_v^2 T_2^2}} \right) \quad (8)$$

is the amount of liquid water required to saturate 1kg of the entrained sub-saturated volume. Therefore, Eq.4 can be rewritten as

$$q = \mu q_0 - (1 - \mu) \delta q^*, \quad (9)$$

Formatted: Font: Times New Roman, 12 pt, Font color:

Formatted: Indent: First line: 0.75 cm, Don't adjust space between Latin and Asian text, Don't adjust space between Asian text and numbers

Formatted: Font: Times New Roman, 12 pt, Font color:

Formatted: Font: Times New Roman, 12 pt, Font color: Black

~~Eq.8 does not take into account the air temperature changes due to the latent heat of droplet evaporation. The comparisons of with numerical simulations showed that the~~ $N = N_1\left(\mu - \frac{(1-\mu)\delta q^*}{q_1}\right)$ (12)

$$\beta = \beta_1\left(\mu - \frac{(1-\mu)\delta q^*}{q_1}\right) \quad (13)$$

For a general case when $T_1 \neq T_2$ the term $(1-\mu)\delta q^*$ in Eqs. (12) and (13) should be replaced by $\delta q_m(\mu)$ (Eq.(2)).

~~2.6 Eqs. 8 and 9 provide accuracy within few percent when the temperature difference $|T_1 - T_2| < 2$°C.~~

~~It should be noted that the mass balance Eqs. 4 and 9 do not take into account changes of the size of the volume V due to changes of temperature caused by evaporation of droplets. The temperature depression $\Delta T = |T_1 - T_2|$ due to evaporation depends on δq and it may reach a few degrees depending on μ and q_0 (sections 3a,d). For isobaric processes the relative changes of volume can be estimated as $\frac{\Delta V}{V} = \frac{\Delta T}{T}$. So, for the lower troposphere ΔT =1C, would result in a relative changes of volume less than 0.3%. Therefore, the evaporative cooling within few degrees will not produce any significant effect on N, β and q during mixing, and the corrections of the volume changes can be neglected.~~

~~Similar to Eq.6 the dependence of concentration versus μ for the case $T_1 \approx T_2$ can be found as~~

$$N = N_0\left(\mu - \frac{(1-\mu)\delta q^*}{q_0}\right) \quad (10)$$

~~The dependences for other moments versus μ for extreme inhomogeneous mixing can be found the same way as in Eq.6 or Eq.10.~~

~~2.4.~~ Homogeneous mixing

~~Based on mass conservation one may conclude that the amount of evaporated water does not depend on how the mixing occurred. Therefore, the mass balance equations Eqs.4 and 9 are valid for both homogeneous and inhomogeneous mixing.~~

For homogeneous mixing, when $\mu > \mu_{cr}$, the droplet number concentration changes only due to dilution ~~of the cloud parcel~~ by the entrained air, i.e.

Field Code Changed

Field Code Changed

Formatted: Font: Times New Roman, 12 pt, Font color:

Formatted: Font color: Black

Formatted: Indent: First line: 0.75 cm, Don't adjust space between Latin and Asian text, Don't adjust space between Asian text and numbers

Formatted: Font: Times New Roman, 12 pt, Font color:

Formatted: Font: Times New Roman, 12 pt, Font color:

Formatted: Indent: First line: 0.75 cm, Don't adjust space between Latin and Asian text, Don't adjust space between Asian text and numbers

Formatted: Font: (Default) Times New Roman, 12 pt, Font color: Black

Formatted: Font: Times New Roman, 12 pt, Font color:

Formatted: Font: Times New Roman, 12 pt, Italic, Font color: Black

$$\frac{N}{N_0} = \mu \quad (11)$$

$$\frac{N}{N_1} = \mu \quad (14)$$

Assuming $T_1 \approx T_2$ $T_1 = T_2$, and substituting Eq.11 into Eq.9 yields dependence q versus N for homogeneous mixing (5) in (14) yields:

$$\frac{N}{N_0} = \frac{q + \delta q^*}{q_0 + \delta q^*} \quad (12)$$

Eq.12 suggests linear relationship between N and q $$\frac{N}{N_1} = \frac{q + \delta q^*}{q_1 + \delta q^*} \quad (15)$$

As follows from Eq. (15) N and q are linearly related for homogeneous mixing. However, no linear relationships exist between other moments. Thus, substituting the definition of the liquid water mixing ratio $q = 4\pi\rho_w N\bar{r}^3/3$ $q = \pi\rho_w N D_v^3/6\rho_a$ in Eq.12 (15) yields the relationship between changes ofmean volume droplet size and concentration

$$\frac{\bar{r}^3}{\bar{r}_{30}^3} = 1 + \frac{\delta q^*}{q_0}\left(1 - \frac{N_0}{N}\right) \quad (13)$$

$$\frac{D_v^3}{D_{v1}^3} = 1 + \left(1 - \frac{N_0}{N}\right)\frac{\delta q^*}{q_1} \quad (16a)$$

$$\frac{D_v^3}{D_{v1}^3} = \frac{q}{q_1}\left(\frac{q_1 + \delta q^*}{q + \delta q^*}\right) \quad (16b)$$

In a similar way the relationship between the extinction coefficient $\beta = Q\pi N\bar{r}_2^2$, concentration $\beta = Q\pi N D_2^2/4$, N, and liquid water$q$, can be obtainedwritten as

$$\frac{\beta}{\beta_0} = \frac{N}{N_0}\left(1 + \frac{\delta q^*}{q_0}\left(1 - \frac{N_0}{N}\right)\right)^{2/3} \quad (14a)$$

$$\frac{\beta}{\beta_0} = \frac{q}{q_0}\left(\frac{q + \delta q^*}{q_0 + \delta q^*}\right)^{5/3} \quad (14b)$$

Field Code Changed

Formatted: Font: Times New Roman, 12 pt, Font color:

Formatted: Font: Times New Roman, 12 pt, Font color:

Formatted: Indent: First line: 0.75 cm, Don't adjust space between Latin and Asian text, Don't adjust space between Asian text and numbers

Formatted: Font: Times New Roman, 12 pt, Font color:

Field Code Changed

Formatted: Font: Times New Roman, 12 pt, Font color:

Formatted: Indent: First line: 0.75 cm, Don't adjust space between Latin and Asian text, Don't adjust space between Asian text and numbers, Tab stops: Not at 10 cm

Formatted: Font: Times New Roman, 12 pt, Font color:

Formatted: Font: Times New Roman, 12 pt, Font color:

Formatted: Font: Times New Roman, 12 pt, Font color:

Formatted: Font: Times New Roman, 12 pt, Font color:

Field Code Changed

Field Code Changed

Formatted: Font: Times New Roman, 12 pt, Font color:

Formatted: Indent: First line: 0.75 cm, Don't adjust space between Latin and Asian text, Don't adjust space between Asian text and numbers

Formatted: Font: Times New Roman, 12 pt, Italic, Font color: Black

Formatted: Font: Times New Roman, 12 pt, Font color:

Formatted: Font: Times New Roman, 12 pt, Italic, Font color: Black

Formatted: Font: Times New Roman, 12 pt, Font color:

Formatted: Font: Times New Roman, 12 pt, Font color: Black

$$\frac{\beta}{\beta_1} = \frac{N}{N_1}\left(1+\left(1-\frac{N_0}{N}\right)\frac{\delta q^*}{q_1}\right)^{2/3} \quad (17a)$$

$$\frac{\beta}{\beta_1} = \left(\frac{q}{q_1}\right)^{2/3}\left(\frac{q+\delta q^*}{q_1+\delta q^*}\right)^{1/3} \quad (17b)$$

In Eqs. (17a) and (17b) it is assumed that $D_2 \approx D_v$.

Substituting in Eq. (16) the expression for the time of phase relaxation $\tau_p = 1/bN\bar{D}$ (e.g. Squires 1953; Korolev and Mazin, 2003)

$$\tau_p = \frac{1}{bN\bar{r}} \quad (15)$$

and assuming $\bar{D} \approx D_v$ yields

$$\frac{\tau}{\tau_0} = \frac{N_0}{N}\left(1+\frac{\delta q^*}{q_0}\left(1-\frac{N}{N_0}\right)\right)^{-1/3} \quad (16)$$

$$\frac{\tau}{\tau_1} = \frac{N_1}{N}\left(1+\left(1-\frac{N_1}{N}\right)\frac{\delta q^*}{q_1}\right)^{-1/3} \quad (18)$$

For the cases when the temperature difference $|T_1 - T_2|$ exceeds a few degrees, the effect of μ on T_m and S_m should be taken into consideration in the calculations of evaporated water. For such cases δq_m (Eq. (2)) should be used instead of δq^*.

Using Eq. (14) δq_m can be presented as a function of $\frac{N}{N_0}$, i.e. $\delta q(\mu) = \delta q\left(\frac{N}{N_0}\right)$. $\delta q_m(\mu) = \delta q_m\left(\frac{N}{N_1}\right)$. Replacing Eq. (5) by Eq. (1) in the above consideration, the equations Eqs. (15)-(18) can be rewritten as

$$\frac{N}{N_0} = \frac{q+\delta q\left(\frac{N}{N_0}\right)}{q_0} \quad (17)$$

[1] Equalities $\bar{r}_2 \approx \bar{r}_3$ and $\bar{r} \approx \bar{r}_3$ are valid for a relatively narrow droplet size distributions

Field Code Changed
Field Code Changed
Formatted: Font: Times New Roman, 12 pt, Font color:
Formatted: Don't adjust space between Latin and Asian text, Don't adjust space between Asian text and numbers
Formatted: Font: Times New Roman, 12 pt, Font color:
Field Code Changed
Formatted: Font: Times New Roman, 12 pt, Font color:
Formatted: Font color: Black
Formatted: Font color: Black
Formatted: Font color: Black
Formatted: Font: Times New Roman, 12 pt, Font color:
Formatted: Font color: Black
Formatted: Font: Times New Roman, 12 pt, Font color:
Formatted: Indent: First line: 0.75 cm, Don't adjust space between Latin and Asian text, Don't adjust space between Asian text and numbers
Formatted: Font: Times New Roman, 12 pt, Font color:
Field Code Changed
Formatted: Font: Times New Roman, 12 pt, Font color:
Formatted: Indent: First line: 0.75 cm, Don't adjust space between Latin and Asian text, Don't adjust space between Asian text and numbers
Formatted: Font: Times New Roman, 12 pt, Font color:
Formatted: Font: Times New Roman, 12 pt, Italic, Font color: Black
Formatted: Font: Times New Roman, 12 pt, Font color:
Formatted: Font: Times New Roman, 12 pt, Font color:
Formatted: Font: Times New Roman, 12 pt, Italic, Font color: Black
Formatted: Font: Times New Roman, 12 pt, Font color:
Formatted: Font: Times New Roman, 12 pt, Font color:
Formatted: Font: Times New Roman, 12 pt, Font color:
Formatted: Font: Times New Roman, 12 pt, Font color:
Formatted: Font: Times New Roman, 12 pt, Font color:
Formatted: Font: Times New Roman, 12 pt, Italic, Font color: Black
Formatted: Font: Times New Roman, 12 pt, Font color:
Formatted: Font: Times New Roman, 12 pt, Font color:
Formatted: Font: Times New Roman, 12 pt, Font color:
Formatted: Font: Times New Roman, 12 pt, Font color:
Formatted: Font: Times New Roman, 12 pt, Italic, Font color: Black

$$\frac{\bar{r}_3^3}{\bar{r}_{30}^3} = 1 - \frac{\delta q\left(\frac{N}{N_0}\right)}{q_0}\frac{N_0}{N} \quad (18)$$

$$\frac{\beta}{\beta_0} = \frac{N}{N_0}\left(1 - \frac{\delta q\left(\frac{N}{N_0}\right)}{q_0}\frac{N}{N_0}\right)^{2/3} \quad \frac{N}{N_1} = \frac{q + \delta q_m\left(\frac{N}{N_1}\right)}{q_1}$$

(19)

$$\frac{\beta}{\beta_0} = \frac{q^{1/3}\left(q + \delta q\left(\frac{\beta}{\beta_0}\right)\right)^{2/3}}{q_0} \quad \frac{D_v^3}{D_{v1}^3} = 1 - \frac{\delta q_m\left(\frac{N}{N_1}\right)}{q_1}\frac{N_1}{N} = \frac{q}{q + \delta q_m\left(\frac{q}{q_1}\right)}$$

(20)

$$\frac{\tau_p}{\tau_{p0}} = \frac{N_0}{N}\left(1 - \frac{\delta q\left(\frac{N}{N_0}\right)}{q_0}\frac{N_0}{N}\right)^{-1/3}$$

$$\frac{\beta}{\beta_1} = \frac{N}{N_1}\left(1 - \frac{\delta q_m\left(\frac{N}{N_1}\right)}{q_1}\frac{N}{N_1}\right)^{2/3} = \frac{q^{2/3}\left(q + \delta q_m\left(\frac{\beta}{\beta_1}\right)\right)^{1/3}}{q_1} \quad (21)$$

~~Equations 17-21 are non-linear and~~ $$\frac{\tau_p}{\tau_{p1}} = \frac{N_1}{N}\left(1 - \frac{\delta q_m\left(\frac{N}{N_0}\right)}{q_1}\frac{N_1}{N}\right)^{-1/3}$$

(22)

Eqs. (19)–(22) can be solved numerically.

2.7 Degenerate case

As follows from Eq.(5~~. Complete evaporation~~), if

Formatted: Font: Times New Roman, 12 pt
Field Code Changed
Formatted: Font: Times New Roman, 12 pt
Field Code Changed
Formatted: Font: Times New Roman, 12 pt
Formatted: Font: Times New Roman, 12 pt
Formatted: Font: Times New Roman, 12 pt
Formatted: Font: Times New Roman, 12 pt
Field Code Changed
Field Code Changed
Formatted: Indent: First line: 0.75 cm, Don't adjust space between Latin and Asian text, Don't adjust space between Asian text and numbers
Formatted: Font: Times New Roman, 12 pt, Font color:
Formatted: Font: Times New Roman, 12 pt, Font color:
Formatted: Font: Times New Roman, 12 pt, Not Italic, Font color: Black
Formatted: Font: Times New Roman, 12 pt, Font color:
Formatted: Indent: First line: 0.75 cm, Don't adjust space between Latin and Asian text, Don't adjust space between Asian text and numbers
Formatted: Font: Times New Roman, 12 pt, Not Bold, Font color: Black
Formatted: Font: Times New Roman, 12 pt, Not Bold, Font color: Black

~~The amount of evaporated water is determined by the initial and final values of the state parameters (e.g. T, e, p) in the mixed parcel, and it does not depend on the type of mixing. Therefore, Eqs. 4 and 9 are valid for both homogeneous and inhomogeneous mixing.~~

~~For the general case when $T_1 \neq T_2$ the value of δq is a function of μ, i.e. $\delta q(\mu)$ (Eq.5). Then, in order to find the critical value of μ_{cr}, when all liquid water evaporates (i.e. q=0) a non-linear equation should be solved~~

~~$$\mu_{cr} q_0 - \delta q(\mu_{cr}) = 0 \qquad (22)$$~~

~~If the temperature of the entrained and cloud parcels are the same (i.e. $T_1 = T_2$), then the critical mixing fraction for the case q=0 can be computed from Eq.9 as~~

~~$$\mu_{cr} = \frac{\delta q^*}{q_0 + \delta q^*} \qquad (23)$$~~

~~Eq.23 yields the condition for the mixing fraction of entrained and cloud parcels such that if $\mu < \mu_{cr}$ then all liquid water in the parcel after completing the mixing evaporates (q=0).~~

~~Figure 2 shows comparisons of dependences of μ_{cr} versus q_0 for different S_0 calculated from Eq.23 and those deduced from a numerical model. As it is seen the agreement appeared to be reasonably good.~~

~~Critical ratios of mixing are also shown by black stars in Figs.4ab (Eq.23). As seen from Figs.4ab the locations of the black stars coincide well with the locations~~ $\frac{(1-\mu)}{\mu}\frac{\delta q^*}{q_1} << 1$ (23)

then $q_1 \geq q \gg \delta q^*$. If the condition in Eq. (23) is valid, then the terms associated with δq^* in Eqs. (15)-(18) can be neglected. This results in correlation of all moments, i.e. $N/N_1 = \beta/\beta_1 = q/q_1$ (compare with Eq.(11)). This corresponds to the degenerate case, when the difference between the homogeneous and inhomogeneous mixing vanishes. Thus, the dimensionless parameter $\xi = \frac{1-\mu}{\mu}\frac{\delta q^*}{q_1}$ can be used for characterization of proximity of the homogeneous mixing moments to those formed during extremely inhomogeneous mixing.

The range of μ in ξ is limited by $\mu_{cr} < \mu \leq 1$, so that $0 < \frac{1-\mu}{\mu} \leq \frac{q_1}{\delta q^*}$. This gives the range of changes of ξ, i.e. $0 \leq \xi \leq 1$ for the mixing without complete evaporation of droplets. The degenerate case corresponds to $\xi \to 0$, whereas $\xi \to 1$ corresponds to maximum difference of the moments for homogeneous and extremely inhomogeneous mixing.

Field Code Changed

As follows from Eqs. (4) and (23) approaching to the degenerate case ($\xi \to 0$) occurs, when one of the following conditions or their combination is satisfied: (a) $RH_2 \to 1$; (b) $E_s(T) \to 0$ at low temperatures; (c) $q_1 \gg \delta q^*$; (d) $\mu \to 1$. The effect of RH, T, q_1 and μ on mixing will be demonstrated in Sect.3.

Figure 3 shows dependence of ξ vs. μ. The grey area in Fig.3 indicates the region where identification of type of mixing from in-situ measurements (Sect.5) may be hindered due to proximity of the moments for homogeneous and inhomogeneous mixing. Thus for $\delta q^*/q_1$ =0.01 identification of type of mixing is ambiguous for nearly the entire range of μ.

For the general case, when $T_1 \neq T_2$, it should be $\xi = \frac{|\delta q_m(\mu)|}{\mu q_1}$. An absolute value $|\delta q_m(\mu)|$ should be used in ξ since $\delta q_m(\mu)$ can be negative (Appendix A, Fig.A1) if mixing results in supersaturation Sect. 3.4).

The coefficient ξ may be useful for identification type of mixing from in-situ observations. It is worth nothing, that the ratio $\frac{\delta q^*}{q_1} \cong \frac{S_2}{A_2 q_1}$ is equal to the parameter R (Pinsky et al. 2015ab), which plays an important role in determining scenarios of droplet evaporation in turbulent environment.

3 Comparisons with numerical simulations

~~where modeled LWC and N become zero. The obtained agreement between analytical and modeled μ_{cr} in Figs. 3 and 4 validates the developed approach.~~

~~3. Modeling~~

Numerical simulations of the final stages of ~~homogeneous and inhomogeneous~~ mixing were performed in order to examine the accuracy and limitations of the analytical expressions obtained in the previous section. The simulations have been conducted with the help of a parcel model similar to that described in Korolev (1995). The ensemble of droplets in the simulation was assumed to be monodisperse. For the case of extreme inhomogeneous mixing the amount of evaporated water Δq required to saturate the mixed volume was calculated first. If $\Delta q < \mu q_1$, then the concentration of evaporated droplets was calculated as $N_{ev} = \frac{\Delta q}{m_d}\rho_a$, where $m_d = \pi\rho_w D^3/6$. Then, the concentration of the remaining droplets $N = N_1 - N_{ev}$ was

Formatted: Font: Times New Roman, 12 pt, Font color: Black

Formatted: Font: Times New Roman, 12 pt, Font color:

Formatted: Font: Times New Roman, 12 pt, Font color:

Formatted: Indent: First line: 0.75 cm, Don't adjust space between Latin and Asian text, Don't adjust space between Asian text and numbers

Field Code Changed

recalculated based of the calculation on the volume formed after mixing. If $\Delta q \geq \mu q_1$, then all droplets evaporate, and $N = 0$.

~~For the case of inhomogeneous mixing the amount of evaporated water Δq required to saturate the mixed volume was calculated first. If $\Delta q < q_0$, then the concentration of evaporated droplets was calculated as $N_{ev} = \frac{\Delta q}{\overline{m}_d}\rho_a$, where $\overline{m}_d = 4\pi\rho_w \bar{r}_3^3/3$ is the average mass of a droplet. Then the concentration of the remaining droplets $N = N_0 - N_{ev}$ was recalculated based of the calculation on the volume formed after mixing. If $\Delta q \geq q_0$, then all droplets evaporate and $N = 0$.~~

For the case of homogeneous mixing in the first step the engulfed parcel instantly mixes with the cloud parcel resulting in a new humidity ~~S_{m0}~~RH_{m0}, temperature ~~T_{m0}~~T_{m0} and volume ~~V_{m0}~~. ~~Then~~V_{m0}. After that the droplets start evaporating until either their complete evaporation or saturation over liquid is reached. The calculations stopped when, either ~~$r < D <$~~ 0.~~1μm~~2μm or ~~$(E_S - e)/E_S <$~~ $(E_S - e)/E_S <$ 0.001, respectively.

3.1. Effect of mixing ~~ratio~~fraction

Figure ~~3~~4 shows the results of the simulation of ~~the dependence of the droplet number concentration (N), droplet integral radius ($N\bar{r}$), extinction coefficient (β), liquid water mixing ratio (q) mean cube droplet radius ($\bar{r}_3$), and time of phase relaxation (τ_p), relative humidity (S_{m0}, S_m) and final temperature (T_m) versus mixing fraction μ.~~different moments and state parameters vs. μ. The calculations were performed for different ~~saturation ratios~~ relative humidity of the entrained parcel ~~$S_{20} = 0.2$~~, $RH_2 =$ 0.2, 0.5, 0.8 and 0.95. As seen from Fig.~~3~~4 for the case of homogeneous mixing only ~~N and q~~ N and q are linearly related with ~~μ~~, μ, the rest of the variables have non-linear dependences on ~~μ~~ μ. For the case of inhomogeneous mixing all ~~$f(r)$~~ $f(D)$ moments and droplet ~~size~~sizes linearly depend on ~~the mixing fraction when $\mu > \mu_{cr}$. When $\mu \leq \mu_{cr}$~~ μ. Note, for $\mu \leq \mu_{cr}$ all ~~liquid evaporates.~~ moments are equal to zero.

Since the amount of the evaporated liquid water does not depend on the type of mixing, the dependences of ~~$q(\mu)$~~ $q(\mu)$ are the same for both homogeneous and inhomogeneous mixing (Fig.~~3a~~4a). The type of mixing has the most pronounced effect on the droplet concentration

Formatted: Font: Times New Roman, 12 pt, Font color:
Formatted: Font: Times New Roman, 12 pt, Font color:
Formatted: Indent: First line: 0.75 cm, Don't adjust space between Latin and Asian text, Don't adjust space between Asian text and numbers
Formatted: Font: Times New Roman, 12 pt, Font color:
Formatted: Font: Times New Roman, 12 pt, Font color:
Formatted: Font: Times New Roman, 12 pt, Font color:
Formatted: Font: Times New Roman, 12 pt, Font color:
Formatted: Font: Times New Roman, 12 pt, Font color:
Formatted: Font: Times New Roman, 12 pt, Font color:
Formatted: Font: Times New Roman, 12 pt, Font color:
Formatted: Font: Times New Roman, 12 pt, Font color:
Formatted: Font color: Black
Formatted: Font: Times New Roman, 12 pt, Font color:
Formatted: Font color: Black
Formatted: Font: Times New Roman, 12 pt, Font color:
Formatted: Font color: Black
Formatted: Font: Times New Roman, 12 pt, Font color:
Formatted: Font color: Black
Formatted: Font color: Black
Formatted: Font: Times New Roman, 12 pt, Font color:
Formatted: Font color: Black
Formatted: Font: Times New Roman, 12 pt, Font color:
Formatted: Font color: Black
Formatted: Font color: Black
Formatted: Font: Italic, Font color: Black
Formatted: Font: Times New Roman, 12 pt, Font color:
Formatted: Font color: Black
Formatted: Font: Times New Roman, 12 pt, Font color:
Formatted: Font color: Black
Formatted: Font: Times New Roman, 12 pt, Font color:
Formatted: Font color: Black
Formatted: Font color: Black
Formatted: Font: Times New Roman, 12 pt, Font color:
Formatted: Font color: Black
Formatted: Font: Times New Roman, 12 pt, Font color:
Formatted: Indent: First line: 0.75 cm, Don't adjust space between Latin and Asian text, Don't adjust space between Asian text and numbers
Formatted: Font: Times New Roman, 12 pt, Font color:
Formatted: Font: Times New Roman, 12 pt, Font color: Black

(Fig.~~3b~~4b) and droplet sizes (Fig.~~3e). The obtained results are in a good agreement with the analytical predictions discussed in section 2.~~4e).

Figure ~~3g~~4g shows the dependences ~~$S_{m0}(\mu)$ and $S_m(\mu)$.~~ RH_{m0} and RH vs. μ. Here ~~$S_{m0}(\mu)$~~ RH_{m0} is the relative humidity at the initial stage of homogeneous mixing before droplets start evaporating (Fig. 1b2). Figure 3h presents ~~dependences of $T_m(\mu)$ for different S_2. It is worth noting that $S_m(\mu)$~~ comparisons of modeled $T(\mu)$ and those calculated from Eqs.(6a,b) and ~~$T_m(\mu)$ do not depend on the type of mixing and they are the same for homogeneous and inhomogeneous mixing. Basically the~~ (C4). The independence of ~~$q(\mu)$, $S_m(\mu)$~~ $q(\mu)$, $RH(\mu)$ and ~~$T_m(\mu)$~~ $T(\mu)$ on type of mixing (Fig.4a,g,h) is the consequence of the mass and energy conservation ~~laws~~, which are not contingent on type of mixing.

3.2. Effect of humidity of entrained air

The diagrams in Fig.~~4~~ 5a-c show the dependences of normalized ~~β, q and $\bar{r}_3$ versus N/N_0.~~ β, q and D_v vs. N/N_0, calculated from numerical simulations and analytical equations from ~~section~~Sect. 2. The calculations were performed for different humidity of the entrained air ~~S_2.~~ RH_2. As seen from Fig.~~4~~ 5a-c, the normalized dependences ~~$q(N)$, $\beta(N)$ and $\bar{r}_3(N)$~~ for homogeneous mixing $q(N)$, $\beta(N)$ and $D_v(N)$ tend to approach the line of extreme inhomogeneous mixing when relative humidity ~~S_2~~ RH_2 approaches to ~~100%. As it was indicated in previous studies (e.g. Burnet and Brenguier 2007), mixing with the entrained saturated air (S_2 =1) represents of~~ 1. This is consistent with the degenerate case, when ~~there is no difference between homogeneous or inhomogeneous mixing.~~ $\xi \to 0$ (Sect.2.7). In this case droplets behave as a passive admixture, and they do not interact with the environment. ~~This effect is clearly seen from the diagrams in Fig.4.~~

3.3. Effect of liquid water ~~content~~mixing ratio

Figure ~~5 presents the normalized dependences $q(N)$, $\beta(N)$ and $\bar{r}_3(N)$ calculated for different initial liquid water q_0 in the cloud parcel, but the same humidity of the entrained parcel S_2=0.5. Figure 5 shows~~ 5d-f demonstrate the sensitivity of $q(N)$, $\beta(N)$ and $D_v(N)$ to liquid water mixing ratio q_1. It is seen, that the increase of ~~q_0 results in $q(N)$, $\beta(N)$ and $\bar{r}_3(N)$ (which were q_1 results in~~ $q(N)$, $\beta(N)$ and $D_v(N)$ (calculated for homogeneous mixing) approaching towards ~~$q(N)$, $\beta(N)$~~ $q(N)$,

Formatted: Font: Times New Roman, 12 pt, Font color: Black
Formatted: Font: Times New Roman, 12 pt, Font color: Black
Formatted: Font: Times New Roman, 12 pt, Font color:
Formatted: Font: Times New Roman, 12 pt, Font color:
Formatted: Font: Times New Roman, 12 pt, Font color:
Formatted: Font: Times New Roman, 12 pt, Font color:
Formatted: Font: Times New Roman, 12 pt, Font color:
Formatted: Font: Times New Roman, 12 pt, Font color: Black
Formatted: Font: Times New Roman, 12 pt, Font color:
Formatted: Font: Times New Roman, 12 pt, Font color:
Formatted: Font: (Default) Times New Roman, 12 pt, Font color: Black
Formatted: Font: Times New Roman, 12 pt, Font color:
Formatted: Font: Times New Roman, 12 pt, Font color:
Formatted: Font: Times New Roman, 12 pt, Font color:
Formatted: Font: Times New Roman, 12 pt, Font color:
Formatted: Font: Times New Roman, 12 pt, Font color:
Formatted: Font: Times New Roman, 12 pt, Font color:
Formatted: Font: Times New Roman, 12 pt, Font color:
Formatted: Font: Times New Roman, 12 pt, Font color:
Formatted: Font: Times New Roman, 12 pt, Font color:
Formatted: Font: Times New Roman, 12 pt, Font color:
Formatted: Font: Times New Roman, 12 pt, Font color:
Formatted: Font: Times New Roman, 12 pt, Font color:
Formatted: Font: Times New Roman, 12 pt, Font color: Black
Formatted: Font: Times New Roman, 12 pt, Font color:
Formatted: Font: (Default) Times New Roman, 12 pt, Font color: Black
Formatted: Font: Times New Roman, 12 pt, Font color:
Formatted: Font: Times New Roman, 12 pt, Font color: Black
Formatted: Font: Times New Roman, 12 pt, Font color:
Formatted: Font: Times New Roman, 12 pt, Font color: Black
Formatted: Font: Times New Roman, 12 pt, Font color:
Formatted: Font: Times New Roman, 12 pt, Font color:

$\beta(N)$ and ~~$\bar{r}_3(N)$~~ $D_v(N)$ for the inhomogeneous mixing. In other words, the sensitivity of the microphysical parameters to the type of mixing increases with the decrease of ~~q_{l_0}~~ q_{l_1}. From a practical viewpoint it means, that from in-situ observations the difference between homogeneous and inhomogeneous mixing is anticipated to be more pronounced for the cases with a relatively low ~~LWC (q_0 <1 g~~liquid water mixing ratio (e.g. $q_1 \leq 1$g/m^3). Such behaviour is consistent with the consideration in Sect. 2.7.

3.4. Effect of temperature $T_1 = T_2$

Figure 5g-j shows the effect of temperature on the normalized $q(N)$, $\beta(N)$ and $D_v(N)$ for $T_1 = T_2$. Figure ~~6 shows the effect of temperature on the normalized dependences $q(N)$, $\beta(N)$ and $\bar{r}_3(N)$ calculated for the case $T_1 = T_2$. The relative humidity of the entrained parcel was assumed to be the same for all cases (S_2=0.5). Figure 6 suggests that the difference between the $f(r)$~~5g-j indicate that the difference between the moments becomes most pronounced at warm temperatures, whereas at cold temperatures (e.g. ~~T = 30C) $q(N)$, $\beta(N)$ and $\bar{r}_3(N)$~~ T= -30^{O}C), $q(N)$, $\beta(N)$ and $D_v(N)$ for homogeneous mixing are approaching those for the extreme inhomogeneous mixing limit.

Such behavior is explained by the fact that ~~the amount of~~ liquid water deficit ~~δq~~ δq_m decreases with decreasing temperature~~. The effect of T on δq is demonstrated in~~ (appendix A, Fig. ~~B1 (Appendix B~~A1). At low temperatures ~~(T < −30 °C~~(T=-30^{O}C) the amount of evaporated water ~~δq~~ δq_m is so small, that homogeneous mixing with ~~undersaturated~~dry out-of-cloud air will have approximately the same effect as mixing with saturated air (i.e. degenerate case, Sect. 2.7).

~~It is well-established that isobaric~~Overall, as follows from Fig.5 the results the analytical predictions (Sect. 2) turned out to be in a good agreement with numerical simulations.

3.5 Effect of temperature $T_1 \neq T_2$

Isobaric mixing of two nearly saturated ~~parcels having different temperatures results~~volumes with $T_1 \neq T_2$ may result in ~~the formation of~~ supersaturated ~~air~~environment (e.g. Rogers, 1976; Bohren and Albrecht, 1998). ~~However, as it was shown in Korolev and Isaac (2000), the isobaric~~ Mixing resulting in supersaturation is different in principle from the mixing ~~of saturated cloudy and~~

Formatted: Font: Times New Roman, 12 pt, Font color:
Formatted: Font: (Default) Times New Roman, 12 pt, Font color: Black
Formatted: Font: Times New Roman, 12 pt, Font color:
Formatted: Font: Times New Roman, 12 pt, Font color:
Formatted: Font: Times New Roman, 12 pt, Font color:
Formatted: Font: Times New Roman, 12 pt, Font color: Black
Formatted: Font: Times New Roman, 12 pt, Font color:
Formatted: Font: Times New Roman, 12 pt, Bold, Font color: Black
Formatted: Font: Times New Roman, 12 pt, Font color:
Formatted: Font: Times New Roman, 12 pt, Font color:
Formatted: Font: Times New Roman, 12 pt, Font color:
Formatted: Font: Times New Roman, 12 pt, Font color: Black
Formatted: Font: Times New Roman, 12 pt, Font color: Black
Formatted: Font: Times New Roman, 12 pt, Font color:
Formatted: Font: Times New Roman, 12 pt, Font color:
Formatted: Font: Times New Roman, 12 pt, Font color:
Formatted: Font: Times New Roman, 12 pt, Font color:
Formatted: Font: Times New Roman, 12 pt, Font color:
Formatted: Font: Times New Roman, 12 pt, Italic, Font color: Black
Formatted: Font: Times New Roman, 12 pt, Font color:
Formatted: Font: Times New Roman, 12 pt, Font color:
Formatted: Font: Times New Roman, 12 pt, Font color:
Formatted: Font: Times New Roman, 12 pt, Font color:
Formatted: Font: Times New Roman, 12 pt, Font color:
Formatted: Font: Times New Roman, 12 pt, Font color:
Formatted: Font: Times New Roman, 12 pt, Font color:
Formatted: Indent: First line: 0.75 cm, Don't adjust space between Latin and Asian text, Don't adjust space between Asian text and numbers
Formatted: Font: Times New Roman, 12 pt, Font color:
Formatted: Font: Times New Roman, 12 pt, Font color:
Formatted: Font: Times New Roman, 12 pt, Font color:
Formatted: Font: Times New Roman, 12 pt, Font color:
Formatted: Font: Times New Roman, 12 pt, Font color:
Formatted: Font: Times New Roman, 12 pt
Formatted: Font: Times New Roman, 12 pt, Font color:
Formatted: Font: Times New Roman, 12 pt, Font color: Black

~~undersaturated air may also result in supersaturated air. The formation~~with evaporating droplets. In this case the meaning of homogeneous and inhomogeneous mixing becomes ambiguous. Formation of ~~supersaturated air~~ supersaturation leads to different dependences between ~~$N\bar{r}$, β, q, $\bar{r}$ and N~~ $N\bar{D}$, β, q, $\bar{D}$ and N as compared to those shown in Figs. ~~3~~ 6 ~~–4~~, when ~~$T_1 = T_2$. In the cases discussed above, mixing between cloud and sub-saturated entrained air with $T_1 = T_2$ resulted in evaporation of some fraction of cloud liquid water, i.e. it was always $\delta q < 0$. However, mixing that causes supersaturation will result in condensation of liquid water (e.g. $\delta q > 0$), which is different of the cases considered above.~~ $T_1 = T_2$.

Figure ~~7~~6 presents a set of diagrams similar to those in Fig. ~~3~~4, but calculated for the ~~cloud and entrained sub-saturated parcels having different temperatures T_1 and T_2.~~ cases when $T_1 \leq T_2$. It turns out that for the case of extreme inhomogeneous mixing the temperature difference between ~~T_1 and T_2~~ T_1 and T_2 breaks down linear dependences ~~between μ and $f(r)$~~ of the microphysical moments (e.g. ~~$N\bar{r}$, β, q Fig. 7a,b,c). This happens because positive supersaturation ($S_{m0} > 1$), which may form after mixing, will result in an increase of q, β, $\bar{r}_3$, etc. The droplet concentration still holds the linear relationship with μ (Fig. 7b), since no formation of new droplets were allowed when $S_{m0} > 1$.~~ $N\bar{D}$, β, q Fig. 6a,c,d) vs. μ.

Figure ~~8~~7 presents the effect of the temperature difference ~~ΔT~~ ΔT on the normalized dependences ~~$q(N)$, $\beta(N)$ and $\bar{r}_3(N)$. As seen from Fig. 8 for large temperature differences $\Delta T = 10$ °C, the values of q, β, $\bar{r}$ for inhomogeneous mixing exceed those for inhomogeneous mixing for the same concentration N.~~

~~It is worth nothing that in real~~ $q(N)$, $\beta(N)$ and $D_v(N)$. In clouds, high supersaturation resulting from isobaric mixing may lead to activation of interstitial CCN, which may ~~slow down the growth of $\bar{r}_3$ and~~ increase ~~N~~ N and decrease D_v (Korolev and Isaac, 2000). However, no activation of new droplets during isobaric mixing was allowed in this study. For the cases when ~~$S_{m0} > 1$~~ $RH_{m0} > 1$ (Fig. ~~8, section AB~~ 7, AB on line 1) the condensed water was uniformly distributed between available droplets~~,~~. Therefore, $q(N)$, $\beta(N)$ and ~~therefore, $q(N)$, $\beta(N)$ and $\bar{r}_3(N)$~~ $D_v(N)$ calculated for homogeneous and extremely inhomogeneous mixing ~~to~~ coincide with each other.

Formatted: Font: Times New Roman, 12 pt, Font color:
Formatted: Font: Times New Roman, 12 pt, Font color:
Formatted: Font: Times New Roman, 12 pt, Italic, Font color: Black
Formatted: Font: Times New Roman, 12 pt, Font color:
Formatted: Font: Times New Roman, 12 pt, Font color:
Formatted: Font: Times New Roman, 12 pt, Font color: Black
Formatted: Font: Times New Roman, 12 pt, Font color:
Formatted: Font: Times New Roman, 12 pt, Font color:
Formatted: Font: Times New Roman, 12 pt, Font color:
Formatted: Font: Times New Roman, 12 pt, Font color:
Formatted: Font: Times New Roman, 12 pt, Font color:
Formatted: Font: Times New Roman, 12 pt, Font color:
Formatted: Font: Times New Roman, 12 pt, Font color: Black
Formatted: Font: Times New Roman, 12 pt, Font color:
Formatted: Font color: Black
Formatted: Font: Times New Roman, 12 pt, Italic, Font color: Black
Formatted: Font: Times New Roman, 12 pt, Font color:
Formatted: Font color: Black
Formatted: Font: Times New Roman, 12 pt, Font color:
Formatted: Font color: Black
Formatted: Indent: First line: 0.75 cm, Don't adjust space between Latin and Asian text, Don't adjust space between Asian text and numbers
Formatted: Font: Times New Roman, 12 pt, Font color:
Formatted: Font: Times New Roman, 12 pt, Font color:
Formatted: Font: Times New Roman, 12 pt, Font color:
Formatted: Font: Times New Roman, 12 pt, Font color:
Formatted: Font: Times New Roman, 12 pt, Font color:
Formatted: Font: (Default) Times New Roman, 12 pt, Font color: Black
Formatted: Font: (Default) Times New Roman, 12 pt, Font color: Black
Formatted: Font: Times New Roman, 12 pt, Font color:
Formatted: Font: Times New Roman, 12 pt, Font color:
Formatted: Font: Times New Roman, 12 pt, Font color: Black

Numerical simulations also showed, that the effect of temperature on ~~the result of~~ mixing is more pronounced for the cases when the cloud temperature is warmer than that of the entrained air, i.e. ~~$T_1 > T_2$~~, $T_1 > T_2$, as compared to the cases with ~~$T_1 < T_2$~~, $T_1 < T_2$.

~~**3.5. Multiple**~~**4. Progressive mixing** ~~**events**~~

4.1 Effect on microphysical parameters

In the previous sections the mixing ~~between cloud and sub-saturated volumes~~ was considered as a single event, i.e. μ fraction of the cloudy air mixed up with $(1-\mu)$ fraction of entrained dry air. Such mixing will be referred to as "primary" mixing. Primary mixing results in an ensemble of elementary volumes characterized by a set of microphysical and state parameters i.e. ~~$\bar{r}(\mu), N(\mu), S(\mu), T(\mu), \bar{D}(\mu)$~~, $N(\mu)$, $RH(\mu)$, $T(\mu)$, etc. Each of these parameters has a functional dependence on ~~μ~~, μ, and what is important, these parameters have functional relationships between each other.

In reality mixing is a continuous process. It does not stop after the primary mixing. The elementary volumes formed after primary mixing continue to progressively ~~mixing between~~mix with each other~~, cloud environment and newly entrained air~~.

The second stage of mixing will result in an ensemble of elementary volumes characterized by a set of parameters ~~$\bar{r}^{(2)}, N^{(2)}, S^{(2)}, T^{(2)}, D_v^{(2)}$~~, $N^{(2)}$, $RH^{(2)}$, $T^{(2)}$, etc. Here the superscript $^{(2)}$ indicates the stage of mixing. After the second stage the mixed volumes undergo subsequent stages of mixing. ~~The conceptual diagram of the progressive mixing is shown in Fig. 9. This is a highly idealized scheme of mixing. However, it helps understand some features of homogeneous mixing.~~

~~The progressive~~The idealised conceptual diagram of the progressive mixing is shown in Fig. 8. As mentioned in Sect. 2.1, the actual process of mixing is indeed much more complex than the sequence of discrete events portrayed in Fig.8. However, as it will be shown below, this simplified consideration of allows establishing main features of evolution of relationships between the microphysical moments affected by mixing. The obtained results facilitates identification of type of mixing from in-situ measurements.

Progressive mixing was simulated with the help of a numerical model, where parcels were randomly mixed with each other and with the cloud environment. The mixing fraction ~~μ~~ μ was also set to be random during each mixing event. Models of ~~random~~stochastic mixing have been

Formatted: Font: Times New Roman, 12 pt, Font color: Black

Formatted: Font: Times New Roman, 12 pt, Font color:

Formatted: Font: Times New Roman, 12 pt, Font color:

Formatted: Font: Times New Roman, 12 pt, Not Italic, Font color: Black

Formatted: Font: Times New Roman, 12 pt, Font color:

Formatted: Font: Times New Roman, 12 pt, Font color:

Formatted: Font: Times New Roman, 12 pt, Font color:

Formatted: Indent: First line: 0.75 cm, Don't adjust space between Latin and Asian text, Don't adjust space between Asian text and numbers

Formatted: Font: Times New Roman, 12 pt, Font color:

Formatted: Font: Times New Roman, 12 pt, Font color:

Formatted: Font: Times New Roman, 12 pt, Font color:

Formatted: Font: Times New Roman, 12 pt, Font color: Black

Formatted: Font: Times New Roman, 12 pt, Font color:

Formatted: Font: Times New Roman, 12 pt, Font color:

Formatted: Font: Times New Roman, 12 pt, Font color:

Formatted: Font: Times New Roman, 12 pt, Font color: Black

Formatted: Font: Times New Roman, 12 pt, Font color: Black

Formatted: Indent: First line: 0.75 cm, Don't adjust space between Latin and Asian text, Don't adjust space between Asian text and numbers

Formatted: Font: Times New Roman, 12 pt, Font color:

Formatted: Font: Times New Roman, 12 pt, Italic, Font color: Black

Formatted: Font: Times New Roman, 12 pt, Font color:

Formatted: Font: Times New Roman, 12 pt, Font color: Black

used in a number of studies (e.g. Krueger et al., 1997; Su et al., 1998; Burnet and Brenguier, 2007). Burnet and Brenguier (2007) allowed mixing between cloud and entrained parcels at each stage of mixing. In the present approachwork the mixing withanalysis of progressive mixing is expanded to examine its effect on the entrained environment was allowed only atrelationship between moments of the primary stage. After that the mixing continued with the cloud air and between the mixed volumesdroplet size distribution.

The results of the progressive mixing for the first four stages are presented in Fig.10 9. As seen from Fig.10 9 the functional relationship between the pairs of microphysical and state parameters exists only for the primary stage. However forFor higher mixing stages these functional relationships breakdownbreak down. Thus, cloud volumes with the same $N^{(2)}$ will be associated with an ensemble of droplets with$N^{(2)}$ may have different $\bar{r}^{(2)}$, $D_v^{(2)}$. Figure 109 also shows that the regions of scattering of $q(N)$, $\beta(N)$ $q(N)$, $\beta(N)$ and $\bar{r}_3(N)$ $D_v(N)$ for stages 2, 3 and 4 are limited from above by the inhomogeneous mixing (red dashed lines) and from below by primary homogeneous mixing (red solid lines).

Figure 10 presents a conceptual $N-q$ diagram explaining breaking the functional relationships during progressive homogeneous mixing. After the first stage of mixing the $N-q$ points will be scattered along the line OB and point C. The line OB corresponds to the ensemble of points with $RH=1$. Therefore, result of mixing between two saturated volumes randomly selected on AB, will remain on the same line. Point C corresponds to the ensemble of points with $N=0$, $RH_2 \le RH_C(\mu^{(1)}) \le 1$, where $0 \le \mu^{(1)} < \mu_{cr}$. Therefore, mixing between point A (Fig.10) and point C, when $RH=1$ will result in scattering along the line AC (degenerate case). Points resulted from mixing between A ($RH=1$) and point C, when $RH_2 \le RH_C < 1$, will scattered over the ensemble of dashed lines shown in Fig.10. These lines will fill the sector CAB. Random mixing between points on the line OB and C, will eventually fill the entire sector COB. The same consideration can be applied to progressive mixing between other moments.

During the progressive mixing $N^{(n)}$, $\beta^{(n)}$, $q^{(n)}$ and $\bar{r}_3^{(n)}$ $N^{(n)}$, $\beta^{(n)}$, $q^{(n)}$ and $D_v^{(n)}$ formed in the elementary parcels tend to approach those in the undiluted cloud, i.e. N_0, β_0, q_0 and $\bar{r}_{30}$ N_1, β_1, q_1 and D_{v1}. This process can be considered as a surrogate to the diffusion process between the cloud and sub-saturated out-of-cloud environment. The convergence of $N^{(n)}$, $\beta^{(n)}$, $q^{(n)}$ $\beta^{(n)}$, $q^{(n)}$

Formatted: Font: Times New Roman, 12 pt, Font color:
Formatted: Font: Times New Roman, 12 pt, Font color:
Formatted: Font: Times New Roman, 12 pt, Font color:
Formatted: Font: Times New Roman, 12 pt, Font color:
Formatted: Font: Times New Roman, 12 pt, Font color:
Formatted: Font: Times New Roman, 12 pt, Font color:
Formatted: Font: Times New Roman, 12 pt, Font color:
Formatted: Font: Times New Roman, 12 pt, Font color:
Formatted: Font: Times New Roman, 12 pt, Font color:
Formatted: Font color: Black
Formatted: Font color: Black
Formatted: Font color: Black
Formatted: Font color: Black
Formatted: Font: Times New Roman, 12 pt, Font color:
Formatted: Font color: Black
Formatted: Font color: Black
Formatted: Font color: Black
Formatted: Font color: Black
Formatted: Font color: Black
Formatted: Font: Times New Roman, 12 pt, Font color:
Formatted: Indent: First line: 0.75 cm, Don't adjust space between Latin and Asian text, Don't adjust space between Asian text and numbers
Formatted: Font: (Default) Times New Roman, 12 pt, Font color: Black
Formatted: Font: Times New Roman, 12 pt, Font color:
Formatted: Font: (Default) Times New Roman, 12 pt, Font color: Black

and ~~$\bar{r}_3^{(n)} D_v^{(n)}$~~ during the progressive mixing can be seen in Fig.~~10~~ 9, where the scattering of normalized ~~$q^{(n)}(N)$~~, ~~$\beta^{(n)}(N)$~~ $q^{(n)}(N)$, $\beta^{(n)}(N)$ and ~~$\bar{r}_3^{(n)}(N) D_v^{(n)}(N)$~~ $\bar{r}_3^{(n)} D_v^{(n)}(N)$ becomes denser towards the top-right corner (1,1) with the increase of the stage of mixing.

~~Another interesting feature of~~ It is worth noting that progressive mixing with the dry air does not break the functional relationships between the moments. This case is equivalent to detrainment of cloudy environment into dry air. It can be shown that Eq.(14) remain valid at any stage of progressive homogeneous mixing ~~is that it results in a population of points along the line corresponding to inhomogeneous mixing (dashed red line in Fig.10) In other words during homogeneous~~ with dry air only, i.e. $N_j/N_1 = \mu^{(1)} \cdots \mu^{(j-1)} \mu^{(j)}$ where $\mu^{(j)}$ is the mixing ~~some~~ fraction at the j-th stage of ~~elementary volumes may develop properties of inhomogeneous~~ mixing. ~~Similar conclusion was derived from a more comprehensive analysis of~~ Eqs. (15)-(24) also remain valid for the progressive mixing ~~in Pinsky et al. (2015b).~~ with the dry air only.

As follows from Eq.~~1~~ (9) for the case of extreme inhomogeneous mixing the progressive mixing does not affect the functional relations between ~~$N^{(n)}$~~, ~~$\beta^{(n)}$~~, ~~$q^{(n)}$~~, ~~$\bar{r}_3^{(n)} N^{(n)}$~~, $\beta^{(n)}$, $q^{(n)}$ and $D_v^{(n)}$ and other microphysical parameters. These relations remain the same regardless of the actual stage of mixing. This is one of the fundamental differences between homogeneous and inhomogeneous mixing, which can be used for identification of type of mixing from in-situ measurements.

~~3.6. Droplet~~4.2 Effect on droplet size ~~distribution~~distributions

Figure 11 shows modeled droplet size distributions averaged over ~~an ensemble~~the ensembles of elementary volumes corresponding to the first four stages of homogeneous mixing. As seen from Fig. 11a~~,b,c,~~ d for the case with ~~$T_1 = T_2$~~ $T_1 = T_2$ the droplet size distributions are ~~broaden~~broadened towards small sizes. Depending on the stage of mixing and mixing fraction μ the size distributions formed in each elementary volume may be unimodal or multimodal. However, due to the random nature of the modal sizes formed during mixing, the average size distributions become smooth and unimodal (Fig.11a-d).

Broadening of ~~the~~ droplet size ~~distribution~~distributions towards small sizes during homogeneous mixing is well known and it was demonstrated in a number of studies (e.g. Baker and Latham, 1982; Jensen and Baker, 1989; Jeffery, 2007; Kumar et al., 2013). However, if ~~the~~

Formatted: Font: Times New Roman, 12 pt, Font color:
Formatted: Font: Times New Roman, 12 pt, Font color:
Formatted: Font: (Default) Times New Roman, 12 pt, Font color: Black
Formatted: Font: Times New Roman, 12 pt, Font color:
Formatted: Font: Times New Roman, 12 pt, Font color:
Formatted: Font: Times New Roman, 12 pt
Formatted: Font: Times New Roman, 12 pt, Font color:
Formatted: Font: (Default) Times New Roman, 12 pt, Font color: Black
Formatted: Font: (Default) Times New Roman, 12 pt, Font color: Black
Formatted: Font: (Default) Times New Roman, 12 pt, Font color: Black
Formatted: Font: (Default) Times New Roman, 12 pt, Font color: Black
Formatted: Font: (Default) Times New Roman, 12 pt, Font color: Black
Formatted: Font: Times New Roman, 12 pt, Font color:
Formatted: Font: Times New Roman, 12 pt, Font color:
Formatted: Font: Times New Roman, 12 pt, Font color:
Formatted: Font: Times New Roman, 12 pt, Font color:
Formatted: Font: Times New Roman, 12 pt, Font color:
Formatted: Font color: Black
Formatted: Font: Times New Roman, 12 pt, Font color:
Formatted: Font color: Black
Formatted: Font: Times New Roman, 12 pt, Font color:
Formatted: Font color: Black
Formatted: Font: Times New Roman, 12 pt, Font color:
Formatted: Font color: Black
Formatted: Font: Times New Roman, 12 pt, Font color:
Formatted: Font: Times New Roman, 12 pt, Font color:
Formatted: Font: Times New Roman, 12 pt, Font color:
Formatted: Font color: Black
Formatted: Font: Times New Roman, 12 pt, Font color:
Formatted: Font: Times New Roman, 12 pt, Font color:
Formatted ...
Formatted: Font: Times New Roman, 12 pt, Font color:
Formatted: Font: Times New Roman, 12 pt, Font color:
Formatted: Font: Times New Roman, 12 pt, Font color:
Formatted: Font: Times New Roman, 12 pt, Font color:
Formatted: Font: Times New Roman, 12 pt, Font color:
Formatted: Font: Times New Roman, 12 pt, Font color: Black

~~difference $|T_1 - T_2|$ exceeds few degrees and the humidity of the sub-saturated parcel is not too low (e.g. ≥80%), then homogeneous mixing may result in supersaturation of the mixed parcel and subsequent droplet growth. In this case~~ mixing results in supersaturation (section 3.4), then the droplet size distribution may broaden towards ~~large sizes (Fig.11e-h).~~ larger sizes (Fig. 11e–h). For this to occur, both the temperature difference between the cloud and the environment $|T_1 - T_2|$ and the relative humidity of the environment RH_2 must be sufficiently large. Such conditions are inherently unstable, however, this might occur in regions that have been moistened through prior cloud detrainment. Thus homogeneous mixing may result in broadening of droplet size distributions towards either smaller or larger sizes (Fig.11).

~~The examples in Fig.11 show that homogeneous mixing results in broadening of size distribution. Depending on the temperature difference $|T_1 - T_2|$ and the relative humidity of the entrained air the broadening may occur both towards smaller and towards larger sizes. Contrary to homogeneous mixing, extreme inhomogeneous mixing does not result in broadening of droplet size distributions.~~

These results were obtained in the frame of the formalism of homogeneous and inhomogeneous mixing. The following two works in this series (Pinsky et al~~. 2015a,~~., 2016a, b) ~~show that $f(r)$~~ will discuss the broadening ~~towards small droplets may occur~~ of polydisperse and monodisperse $f(D)$ during both homogeneous and inhomogeneous mixing in greater details.

~~**3.7. Summary**~~

~~In~~**5 Identification of type of mixing from in-situ observations**

The purpose of this section is to attempt identifying type of mixing based on examining relationships between basic microphysical parameters N, β, LWC, D_v measured from in-situ.

5.1 Expected relationships between the moments

Prior proceeding with the analysis of in-situ data we summarize the results of the previous consideration on how homogeneous and extreme inhomogeneous mixing is expected to manifest itself in relationships between basic microphysical parameters, such as ~~N, β, q and $\bar{r}_3$. The objective of this analysis is to facilitate examination of in-situ measurements in order to identify the type of mixing within the conventional framework of homogeneous and extreme inhomogeneous mixing.~~ N, β, q and D_v.

Formatted: Font: Times New Roman, 12 pt, Font color: Black

Formatted: Font: Times New Roman, 12 pt, Font color:

Formatted: Font: Times New Roman, 12 pt, Font color:

Formatted: Indent: First line: 0.75 cm, Don't adjust space between Latin and Asian text, Don't adjust space between Asian text and numbers

Formatted: Font: Times New Roman, 12 pt, Font color:

Formatted: Font: Times New Roman, 12 pt, Font color:

Formatted: Font: Times New Roman, 12 pt, Font color:

Formatted: Font: Times New Roman, 12 pt, Font color: Black

Formatted: Font: Times New Roman, 12 pt, Font color:

Formatted: Indent: First line: 0.75 cm, Don't adjust space between Latin and Asian text, Don't adjust space between Asian text and numbers

Formatted: Font: Times New Roman, 12 pt, Font color:

Formatted: Font: Times New Roman, 12 pt, Font color:

Formatted: Font: Times New Roman, 12 pt, Font color:

Formatted: Font: Times New Roman, 12 pt, Font color:

~~Following~~For extreme inhomogeneous mixing the relationship between the pairs of ~~N, β~~ N, β and ~~q~~ q are determined by ~~a~~ linear ~~relationship $M_n = \alpha_{nm} M_m$~~ dependences $M_n = \alpha_{nk} M_k$ (Eq.~~2)~~ 10) at any stage of mixing. As follows from Eq.~~3~~ (11) the slopes ~~α_{nm}~~ α_{nk} for ~~$q(N)$, $\beta(N)$~~ $q(N)$, $\beta(N)$ and ~~$q(\beta)$~~ $q(\beta)$ are equal to the ratios ~~q_0/N_0, β_0/N_0~~ q_1/N_1, β_1/N_1, and ~~q_0/β_0~~. ~~For clouds forming through vertical motions (e.g. *Sc, Ac, Cu, Cb* etc.) N_0, β_0~~ q_1/β_1, respectively, where N_1, β_1 and ~~q_0~~ q_1 correspond to undiluted adiabatic values. The values of ~~N_0, β_0~~ N_1, β_1 and ~~q_0~~ depend ~~of~~ q_1 may vary depending on the location ~~of measurements~~inside the cloud and ~~the~~ environmental conditions at the cloud base. Thus, the adiabatic value of ~~q_0~~ q_1 is a function of elevation above the cloud base ~~ΔZ. The concentration N_0~~ ΔZ, whereas N_1 depends on the vertical velocity at the cloud base ~~u_z~~ u_z and the aerosol load. ~~The extinction coefficient β_0 is determined by both ΔZ and u_z.~~ Therefore, ~~for the measurements collected in the same cloud, but at different altitudes, it is anticipated that the~~ the scattering of ~~N_0, and q_0 will be limited by a sector as shown in Fig.12a. The scattering of measurements $q(N)$~~ $q - N$ points will be aligned along an ensemble of different lines ~~associated with~~determined by q_1/N_1, which are specific to different ~~q_0/N_0~~ cloud volumes. The conceptual diagram of the scattering of ~~$q - N$~~ $q - N$ measurements in a cloud ~~having experienced~~with extreme inhomogeneous mixing is shown in Fig. 12a. The scatter diagrams ~~of $q - \beta$ and $N - \beta$~~ for other moments (e.g. $q - \beta$, $N - \beta$) will have the ~~same~~similar patterns as that in Fig. 12a.

For the case of homogeneous mixing the functional relationship between the pairs of ~~N, q, β and $\bar{r}_3$ is~~ N, β, q and D_v are disrupted by a progressive mixing. As shown in ~~section 3c~~Sect. 4.1 the ensemble of points of ~~N, q, and β~~ N, β and q will be scattered within a sector, which is limited by lines determined by Eq.~~3~~ ((11) (extreme inhomogeneous mixing) and ~~Eq.12 and Eq.15a~~Eqs. (15)-(17) (primary homogeneous), respectively (Fig.~~10~~ 9). What is important, is that the top of the ~~cones of the scatter plots $q(N)$ and $\beta(N)$~~ sectors for $q(N)$ and $\beta(N)$ correspond to points ~~[N_0, q_0]~~[N_1, q_1] and ~~[N_0, β_0],~~[N_1, β_1], respectively. Since ~~N_0, β_0~~ N_1, β_1 and ~~q_0~~ q_1 may vary ~~both~~ within the same cloud ~~as well as from cloud to cloud~~, it is anticipated that the ~~N, q,~~ N, β and ~~β, q~~ measurements will be scattered within an ensemble of ~~cones~~sectors as shown in Fig. 12b.

Formatted: Font: Times New Roman, 12 pt, Font color: Black

Formatted: Indent: First line: 0.75 cm, Don't adjust space between Latin and Asian text, Don't adjust space between Asian text and numbers, Tab stops: Not at 13.65 cm

Formatted ...

Formatted ...

Formatted ...

Formatted: Font: Times New Roman, 12 pt, Font color:

Formatted: Font: Times New Roman, 12 pt, Font color:

Formatted: Font: (Default) Times New Roman, 12 pt, Font color: Black

Formatted: Font: Times New Roman, 12 pt, Font color:

Formatted: Font: Times New Roman, 12 pt, Font color:

Formatted: Font: Times New Roman, 12 pt, Font color:

Formatted ...

Formatted: Font: Times New Roman, 12 pt, Font color:

Formatted: Font: Times New Roman, 12 pt, Font color:

Formatted ...

Formatted: Font: Times New Roman, 12 pt, Font color: Black

Formatted ...

Formatted ...

Formatted ...

Formatted ...

Formatted ...

Formatted: Font: Times New Roman, 12 pt, Font color:

Formatted: Font: Times New Roman, 12 pt, Font color:

Formatted: Font: Times New Roman, 12 pt, Font color:

Formatted: Font: Times New Roman, 12 pt, Font color:

Formatted ...

Formatted ...

~~In the case of inhomogeneous mixing, which occurs within a cloud volume with the same N_0 and q_0, the scattered points are aligned along the same line, e.g. $q = \frac{q_0}{N_0} N$. Such scattering patterns are easy to identify even when there are a limited number of measured points. However, in the case of homogeneous mixing the points will be scattered within a large area limited by the cone with the top point $[N_0, q_0]$ (Fig.12b). Even in case of a relatively large number of measurements the identification of such scattering patterns may be hindered because of the low density of points scattered over a large area. Ultimately, when looking at the feasibility of identifying homogeneous and inhomogeneous mixing by means of microphysical measurements it can be concluded that, when using the analysis of scatter diagrams $q(N)$, $\beta(N)$ and $q(\beta)$, inhomogeneous mixing is easier identify than homogeneous mixing.~~

~~4. In-situ observations~~

~~This section presents an attempt to identify type of mixing based on examining relationships between basic microphysical parameters N, β, LWC, $\bar{r}_3$ measured from in-situ. These parameters present different moments of droplet size distribution and depending on instrumentation set used airborne, they can be either measured directly or calculated from measurements of $f(r)$.~~

~~3.1.~~It is important to note that that during homogeneous mixing prior reaching equilibrium, functional relationships between the microphysical moments do not exist either. After the instant mixing of cloud fraction μ with entrained air (Fig. 1b(2)), $q_{m0} = \mu q_0$ and $N_{m0} = \mu N_0$. This state corresponds to point D in Fig.10. After that droplets start evaporating until liquid mixing ratio reaches point A (Fig.10), which corresponds to the equilibrium state ($RH = 1$). Therefore, during evaporation time $q - N$ points will be scattered along the line AD. Since, point D can be located anywhere on OC, the ensemble of $q - N$ points corresponding to non-equilibrium state will fill the COB area.

Thus, the absence of the functional relationships between the moments during homogeneous mixing may occur both during progressive mixing and during primary mixing prior reaching the equilibrium state. The evaporation time required to reach equilibrium during homogeneous mixing is discussed in details in Pinsky et al. (2016b), and it is usually limited by few tens of seconds. However, progressive mixing is not limited in time. Therefore, it is very likely that no functional relationship between microphysical parameters will be observed during in-situ measurements.

Fig.12 demonstrated a fundamental difference in scattering of $q - N$ for homogeneous and extreme inhomogeneous mixing, which will be used to facilitate identification of type of mixing in the following section.

5.2 Results of observations

The measurements were obtained on the University of Wyoming King Air aircraft during the COPE-MED project in South-Western part of UK during July-August 2013 (Leon et al~~. 2015~~, 2016). The UW King Air was equipped with a suite of microphysical instruments, including a DMT Cloud Droplet probe (CDP~~) and PMS Forward Scattering Spectrometer Probe (FSSP-100). These probes were~~), designed for measurements of droplet sizes and their concentrations in the nominal size ranges 1~~-~~–50~~µm and 3-47µm, respectively~~ µm.

~~The measurements were focused on characterizing microphysical evolution of convective clouds and effect of entrainment on precipitation formation.~~ Figure 13 shows a time series of droplet concentration, extinction coefficient, liquid water content and mean volume droplet diameter measured by the CDP during transit through a convective cell on 18 July 2013. The CDP data were sampled at 10Hz, which corresponds to approximately 10m spatial averaging. Visual examination of the spatial changes of ~~N, β and LWC~~ N, β and LWC shows strong correlation. The amplitude of changes of these parameters reaches nearly one hundred percent with respect to their maximum. Contrary to that, the spatial variations of ~~$\bar{D}$ and $\bar{D}_3$~~ $\bar{D}$ and D_v are quite conservative and their values remain nearly constant. With the exception of two cloud holes between 13:50:42 and 13:50:44, the amplitude of fluctuations of ~~$\bar{D}_3$~~ D_v does not exceed 8% with standard deviation of 2.2%.

Figure 14 shows scatter diagrams of ~~$LWC(N)$, $\beta(N)$, $LWC(\beta)$~~ $LWC(N)$, $\beta(N)$, $LWC(\beta)$ and ~~$\bar{D}_3(N)$~~ $D_v(N)$ measured by the CDP during seven consecutive penetrations of the same convective cell extended over a period of approximately 19 ~~minutes~~min. One of these penetrations is shown in Fig. 13. The measurements were conducted at ~~an altitude $H=$~~ $H =$ 5500m and ~~temperature $T=$-12C.~~ $T =$ -12°C. The relative humidity of the ambient air was approximately 20 %. At the beginning of the sampling no precipitation size particles were observed in the cloud. However, by the end of the sampling period some raindrops and ice crystals were present in the cloud. Despite the presence of some precipitation size particles, the scatter diagrams in Fig. 14a, b~~,~~ and d

Formatted: Indent: First line: 0.75 cm, Don't adjust space between Latin and Asian text, Don't adjust space between Asian text and numbers

Formatted: Font: Times New Roman, 12 pt, Font color: Black

Formatted: Font: Times New Roman, 12 pt, Font color:

Formatted: Font: Times New Roman, 12 pt, Font color:

Formatted: Font: Times New Roman, 12 pt, Font color:

Formatted: Font: Times New Roman, 12 pt, Font color: Black

Formatted: Font: Times New Roman, 12 pt, Font color:

Formatted: Font: Times New Roman, 12 pt, Font color: Black

Formatted: Font: Times New Roman, 12 pt, Font color: Black

Formatted: Font: Times New Roman, 12 pt, Font color:

Formatted: Font: Times New Roman, 12 pt, Font color:

Formatted: Font: Times New Roman, 12 pt, Font color: Black

Formatted: Font: Times New Roman, 12 pt, Font color:

Formatted: Font: Times New Roman, 12 pt, Font color:

Formatted: Font: Times New Roman, 12 pt, Font color:

Formatted: Font: Times New Roman, 12 pt, Font color:

Formatted: Font: Times New Roman, 12 pt, Font color:

Formatted: Font: Times New Roman, 12 pt, Font color:

Formatted: Font: Times New Roman, 12 pt, Font color:

Formatted: Font: Times New Roman, 12 pt, Font color: Black

demonstrate high correlation between pairs ~~N, β and LWC.~~ N, β and LWC. The mean volume diameter in Fig. 14c shows very little changes from 19 ~~µm~~ to 17 ~~µm~~ µm when concentration changes from 1100 to 500 cm^{-3} ~~to 500cm^{-3}~~, However, for ~~N < 200cm^{-3}~~ N < 200 cm^{-3}, the volume diameter decreases to 12~~—~~15 ~~µm~~µm.

Red lines in Fig. 14 indicate ~~$q(N)$, $\beta(N)$, $LWC(\beta)$~~ $q(N)$, $\beta(N)$, $LWC(\beta)$ and ~~$\overline{D}_3(N)$~~ $D_v(N)$ calculated for the 1st stage of homogeneous mixing. The calculations were performed for a monodisperse ~~$f(r)$~~ $f(D)$ with ~~D_0 = 18.5 µm~~ D_1=18.5µm, N_1 = 1100 cm^{-3}, and ~~N_0 = 1100 cm^{-3}. The initial~~ state parameters ~~were considered to be the same~~ as during the measurements. Comparisons of dependences ~~$q(N)$, $\beta(N)$, $LWC(\beta)$~~ $q(N)$, $\beta(N)$, $LWC(\beta)$ and ~~$\overline{D}_3(N)$~~ $D_v(N)$ based on in-situ measurements with those obtained from numerical simulations of homogeneous mixing show minor difference for high concentrations ~~500cm~~700 cm^{-3} ~~< N <1100cm~~< N < 1100 cm^{-3} (Fig. 14a~~,b,~~ c). Simulation also shows that for this specific case the difference between homogeneous and inhomogeneous mixing does not exceed 10% when ~~500cm^{-3} < N <1100cm^{-3}.~~700 cm^{-3}< N < 1100 cm^{-3}. Such difference remains within the errors of measurements. Therefore, in this specific cloud for the regions with ~~N > 500~~ N > 700 cm^{-3} the type of mixing cannot be unambiguously identified from the analysis of the dependences ~~$q(N)$, $\beta(N)$, $LWC(\beta)$~~ $LWC(N)$, $\beta(N)$, $LWC(\beta)$ and ~~$\overline{D}_3(N)$. However,~~ $D_v(N)$. This is consistent with the assessment of feasibility of segregation of homogeneous and inhomogeneous mixing in Fig.3 (dashed line). Since for homogeneous mixing $N \propto \mu$, than Fig.3 suggests good separation of the moments for $N > 700$ cm^{-3}.

For the regions with ~~N <500cm~~ N < 500 cm^{-3} the deviation between homogeneous ~~simulation~~mixing simulations and in-situ measurements in Fig.14 becomes well pronounced and it extends beyond possible errors of measurements. This suggests that the mixing is in these regions is dominated by the extreme inhomogeneous type.

Figure 15 shows the same type of diagrams as in Fig. 14, which were measured during 45 consecutive traverses through an ensemble of deep convective cells. The sampling altitude varied in the range 3000m ~~< H~~ < H < 4500m, temperature ~~-11C <~~ 11°C < T ~~< 0C~~ < 0°C, relative humidity in the vicinity of clouds 15% < RH < 65 %. The cloud measurements were extended over a period of ~~2h 13m~~2 h 13 m, which is suggestive that the convective cells were sampled at different stages of their lifetime. At the sampling level the concentration of raindrops varied from zero to few per liter, and their diameter did not exceed ~~2 mm.~~ 2mm.

Formatted ...
Formatted ...
Formatted: Font: Times New Roman, 12 pt, Font color:
Formatted ...
Formatted: Font: Times New Roman, 12 pt, Font color:
Formatted ...
Formatted: Font color: Black
Formatted ...
Formatted ...
Formatted: Font color: Black
Formatted: Font: Times New Roman, 12 pt, Font color:
Formatted: Indent: First line: 0.75 cm, Don't adjust space between Latin and Asian text, Don't adjust space between Asian text and numbers
Formatted: Font: Times New Roman, 12 pt, Font color:
Formatted ...
Formatted: Indent: First line: 0.75 cm, Don't adjust space between Latin and Asian text, Don't adjust space between Asian text and numbers, Tab stops: Not at 13.65 cm
Formatted: Font: Times New Roman, 12 pt, Font color:
Formatted ...

What is interesting that the scattering of the measurements ~~$LWC(N)$, $\beta(N)$~~ $LWC(N)$, $\beta(N)$ and ~~$LWC(\beta)$~~ $LWC(\beta)$ (Fig. 15a, b~~,~~ and d) is limited by the sector, which originates from the zero point~~.~~ as in Fig.12a. Analysis of the measurements showed that ~~scatter diagrams $LWC(N)$, $\beta(N)$, $LWC(\beta)$ and $\overline{D}_3(N)$ calculated for~~ the data points $LWC(N)$, $\beta(N)$, $LWC(\beta)$ in each individual cloud traverse are ~~very similar to those in Fig.14. It appeared that the~~ well aligned along the lines with different slopes ~~of $LWC(N)$, $\beta(N)$, $LWC(\beta)$ vary from cloud to cloud. So, after~~(e.g. Fig.14). After averaging over the ensemble of clouds, the area of the scattered points ~~will~~turned out to be located inside a sector limited by the lines with smallest and largest slopes.

~~As follows from Eq.3 the slopes of $q(N)$, $\beta(N)$ and $q(\beta)$ are governed by the ratios q_0/N_0, β_0/N_0 and q_0/β_0, respectively, where N_0, β_0 and q_0 correspond to undiluted adiabatic values. As discussed in section 3.7 changes in β_0 and q_0 can be explained by (a) different altitude of measurements above the cloud base, or (b) different cloud base temperatures in different clouds measured during this day. The changes in N_0 can be caused by (a) different vertical velocities w_z at the cloud base in different clouds, or (b) spatial and temporal changes of the aerosol load during measurements. The latter two causes will lead to different concentration of activated CCN. The combination of the above reasons may result in different slopes q_0/N_0, β_0/N_0 and q_0/β_0, which may be the reason of the scattering patterns of $LWC(N)$, $\beta(N)$ and $LWC(\beta)$ in Fig.15.~~

~~A distinguishing characteristic of homogeneous mixing is that during evaporation the concentration tends to approach a non-zero value (Figs.4-6), whereas during inhomogeneous mixing it approaches zero. The above analysis of the type of dependences $LWC(N)$, $\beta(N)$, $LWC(\beta)$ and $\overline{D}_3(N)$ in Fig.14 and 15 clearly shows $N \to 0$, when $q \to 0$. This is another argument in favor that the mixing was dominated by inhomogeneous type.~~

~~3.2. Limitations of identifying type of mixing from in-situ measurements~~

Comparisons of the scatterdiagrams $LWC(N)$, $\beta(N)$ and $LWC(\beta)$ in Figs.14 and 15 with the conceptual diagrams in Fig.12 unambiguously suggest that interaction between cloud and environment in the studied clouds was dominated by inhomogeneous mixing. It should be emphasized that analysis of a stand alone mixing diagram $N - D_v$ would not allow unambiguously draw such conclusion.

Formatted: Font: Times New Roman, 12 pt, Font color: Black

Formatted: Font: Times New Roman, 12 pt, Font color:

Formatted: Font: Times New Roman, 12 pt, Font color:

Formatted: Font: Times New Roman, 12 pt, Font color:

Formatted: Font: Times New Roman, 12 pt, Font color:

Formatted: Font: Times New Roman, 12 pt, Font color:

Formatted: Font: Times New Roman, 12 pt, Font color:

Formatted: Font: Times New Roman, 12 pt, Font color:

Formatted: Font: Times New Roman, 12 pt, Font color:

Formatted: Font: Times New Roman, 12 pt, Font color:

Formatted: Font: Times New Roman, 12 pt, Font color:

Formatted: Font: Times New Roman, 12 pt, Font color:

6. Discussion

One of the assumptions in most past studies is that for a sequence of the cloud samples collected along the flight path, the adiabatic values of N_1, q_1, β_1, D_1 and environmental parameters e_2 and T_2 remain the same. In fact these parameters may vary both within the same cloud or sequence of samples clouds, and the amplitude of their variations depends on microphysical and thermodynamical properties inside and outside the cloud environment. This variation will result in an ensemble of relationships $M_n = F_{nk}(M_k)$, and enhance scattering of the data points. In such cases identification of the type of mixing based on the $N - D_v$ diagram may result in confusion between homogeneous and inhomogeneous mixing. As demonstrated in Sect. 5, consideration of $N - q$ and $N - \beta$ diagrams may provide a better identification type of mixing.

Strictly speaking the identification of type of mixing from particle probe measurements as it was performed in Sect. 5 is incomplete. It allows establishing correlation between microphysical moments and makes a formal conclusion about the mixing type, however it does not allow judgement about stage of mixing (i.e. whether mixing is complete by reaching equilibrium). In most previous studies, including this one, identification of type of mixing was based on the assumption that the sampled cloud volume is in equilibrium state ($RH = 1$), and that it reached the final stage of mixing (Fig.1 a2, a3, b3). It is possible that at the moment of measurement the process of mixing is not complete and the droplet free filaments remained undersaturated (Fig.1 a1, b1, b2). In this case the relationship between different moments may be well described as $M_n = \alpha_{nk} M_{nk}$ and the mixing be confused with inhomogeneous mixing.

In order to identify stage of mixing, high frequency collocated measurements of temperature and humidity are required. Unfortunately current technology does not allow such measurements yet.

Identification of type of mixing from in-situ observations is based on examination of relationships between moments of the size distributions measured along the flight path. The basic assumption underlying this analysis is that the cloud ~~droplets in each averaging interval originate at the same altitude. Otherwise, the effects of mixing on size distributions will be superimposed with~~ environment is not affected by other non-adiabatic processes ~~affecting size distributions, which may affect the relationships between the microphysical parameters. Precipitating particles along with the presence of ice may also~~ .

Formatted: Font: Times New Roman, 12 pt, Font color:

Thus, collision-coalescence, riming or Wegener-Bergeron-Findeisen processes may change the droplet number concentration and liquid water content, and therefore ~~will~~ affect the relationship between the moments. ~~Altogether it limits~~Activation of interstitial CCN will result in breaking correlation between the moments due to formation of large concentration of droplets. Broad size distributions may also hinder identification of type of ~~clouds suitable for examining homogeneous and inhomogeneous~~ mixing. ~~The~~ due to partial evaporation of small droplets (Pinsky et al. 2016a)

It is anticipated that most suitable candidates ~~for that matter~~ to study mixing-entrainment process are non-precipitating convective clouds and stratocumulus clouds. ~~However, as it was seen from above, high correlation between N, β and q may exist even in presence of small amounts of precipitation size particles~~ with relatively narrow droplet size distributions.

~~Another limitation is based on the assumption that the sampled cloud parcel is in equilibrium state and that it reached the final stage of mixing. It is possible that during mixing the cloud mixed with the entrained air, but at the moment of measurement it remained undersaturated and the droplets did not complete changing their sizes. In this case the relationship between different moments may be well described as $M_n = \alpha_{nm} M_m$ and the mixing be confused with inhomogeneous mixing. In order to identify cases like this, accurate high frequency measurements of relative humidity are required. Unfortunately such measurements were not available during the in-situ observations described above.~~

Another limiting factor is that the above consideration did not account for the effect of ~~the vertical velocity. The vertical changes of the relative humidity in adiabatic parcels are described by the equation (Korolev and Field, 2008)~~

$$\frac{1}{S}\frac{dS}{dz} = a \qquad (24)$$

~~After linearization of its solution Eq.(24) yields the distance between the level with S_0 and saturation level (S =1):~~

$$\Delta z = \frac{1 - S_0}{a} \qquad (25)$$

~~According to Eq.25 gives the~~changing humidity in a vertically ascending parcel. Thus in droplet free entrained air relative humidity ~~changes~~increases approximately 10% for ~~$\Delta z \approx$~~ Δz = 200m at ~~T =0C.~~ T = 0 °C. After reaching saturation the mixing turns into a degenerate case, which will appear as extreme inhomogeneous mixing. Joint effects of evaporating droplets and an increase in ~~S~~ S

Formatted: Font: Times New Roman, 12 pt, Font color: Black
Formatted: Font color: Black
Formatted: Font color: Black
Formatted: Font color: Black
Formatted: Font: Times New Roman, 12 pt, Font color:
Formatted: Font color: Black
Formatted: Font color: Black
Formatted: Indent: First line: 0.75 cm, Don't adjust space between Latin and Asian text, Don't adjust space between Asian text and numbers
Formatted: Font: Times New Roman, 12 pt, Font color:
Formatted: Font: Times New Roman, 12 pt, Font color:
Formatted: Font: Times New Roman, 12 pt, Font color: Black
Formatted: Font: Times New Roman, 12 pt, Font color:
Formatted: Font color: Black
Formatted: Indent: First line: 0.75 cm, Don't adjust space between Latin and Asian text, Don't adjust space between Asian text and numbers
Formatted: Font: Times New Roman, 12 pt, Font color:
Formatted: Font: Times New Roman, 12 pt, Font color:
Formatted: Font: Times New Roman, 12 pt, Font color:
Formatted: Font: Times New Roman, 12 pt, Font color:
Formatted: Font: Times New Roman, 12 pt, Font color:
Formatted: Font: Times New Roman, 12 pt, Italic, Font color: Black

during the vertical ascent may facilitate reaching saturation state. This case may also be ~~specifically~~ relevant to the convective cloud ~~measurements~~ described ~~above~~in Sect.5.2.

~~5. Characteristic time scales~~

~~The relative roles of mixing and evaporation is characterized by the Damkölher number (Dimotakis, 2005)~~

$$~~\mathrm{Da} = \frac{\tau_{mix}}{\tau_{react}}~~ \quad ~~(26)$$

~~where τ_{mix} is the characteristic time of turbulent mixing; τ_{react} is the characteristic time of interaction of droplets with the environment through a molecular diffusion. The two extremes with $\mathrm{Da} >> 1$ and $\mathrm{Da} << 1$, correspond to homogeneous and inhomogeneous mixing.~~

~~Over the years, the definition of the reaction time scale τ_{react} was debated in literature on mixing. In some studies τ_{react} was associated with the evaporating time of a droplet (e.g. Latham and Reed, 1977; Baker and Latham, 1979; Burnet and Brenguier, 2007; Andejchuk et al. 2009).~~

$$~~\tau_{ev} - \frac{Fr_0^2}{S-1}~~ \quad ~~(27)$$

~~Another group of works considered that τ_{react} is equal to time of phase relaxation τ_p (Eq.15) (e.g. Baker and Latham, 1982; Jeffery and Reisen, 2006; Kumar et. al. 2013). To compromise these two alternatives Jensen and Baker (1989), Jeffery (2007) considered both τ_{ev} and τ_p.~~

~~In the aforementioned studies in the estimations of τ_{react} the values of S (Eq.27) r and N (Eq.15) were assumed to be constant. However, none of these parameters remain constant during mixing. Thus, Lehman et al. (2009) pointed out that during evaporation the population of droplets is interacting with the environment, and therefore $S(t)$ does not remain constant. They proposed considering τ_{react} as a "dominant" time of either evaporation of population of droplets (τ_{ev}) or time required for saturation of the cloud environment (τ_{eq}).~~

~~In reality the complete evaporation of droplets will be characterized by an ensemble of different τ_{ev}, rather than by a single value. The following two conditions should be satisfied for complete evaporation of a droplet: (1) the volume associated the droplet should be $\Delta V > v$, where~~

Formatted: Font: Times New Roman, 12 pt, Font color:

Formatted: Font: Times New Roman, 12 pt, Font color:

Formatted: Font: Times New Roman, 12 pt, Font color:

Formatted: Font: Times New Roman, 12 pt, Font color:

Formatted: Font: Times New Roman, 12 pt, Font color: Black

$$\upsilon = \frac{4\pi\rho_w r^3}{3\rho_a \delta q^*} \quad (28)$$

is the volume of the air, which will be saturated during a complete droplet evaporation; (2) the residence time of the droplet in the volume ΔV should be $\Delta t > \tau_{ev}$. The volume υ in fact is a minimum volume required for droplet evaporation, which means that the droplet evaporating time t_{ev} will be overly long. If the local concentration of the droplets is sparse enough, so that $\Delta V >> \upsilon$, then the effect of the evaporating water on the humidity in ΔV can be neglected and it can be assumed that the local saturation ratio S =const during $t_{ev} \approx \tau_{ev}$.

Table 1. Evaporating time (t_{ev}), evaporating distance of a free falling droplet (λ_{ev}), size of the volume (λ_υ) saturated by a completely evaporated droplet with radius r and saturation ratio S. T =0C, P =687mb.

r	2μm			5μm			10μm		
S	t_{ev} (s)	λ_{ev} (mm)	λ_υ (mm)	t_{ev} (s)	λ_{ev} (mm)	λ_υ (mm)	t_{ev} (s)	λ_{ev} (mm)	λ_υ (mm)
0.9	0.32	0.10	0.51	1.8	3.8	1.3	6.9	59.4	2.6
0.7	0.11	0.03	0.35	0.60	1.3	0.87	2.3	19.8	1.7
0.5	0.06	0.02	0.29	0.36	0.76	0.72	1.4	11.9	1.4
0.2	0.04	0.01	0.24	0.23	0.48	0.59	0.9	7.4	1.2

7. **Table 1** shows the calculated evaporating time (t_{ev}) and evaporating distance of the free falling droplet (λ_{ev}), size of the volume (λ_υ) saturated by a completely evaporated droplet with radius r at saturation ratio S. The size of the volume $\lambda_{\Delta V}$ required for evaporation of a single droplet should exceed its evaporating distance and saturating droplet volume, i.e.

$$\lambda_{\Delta V} > \lambda_{ev} \text{ and } \lambda_{\Delta V} >> \lambda_\upsilon. \quad (29)$$

Table 1 demonstrates that, depending on S and r, the value of $\lambda_{\Delta V}$ may vary from 10^{-2}cm to few cm. It appears that high humidity S and large r are strong factors limiting complete droplet evaporation, and therefore, declining inhomogeneous mixing.

Figure 16 shows τ_{ev} (black solid line) calculated for $S = S_{m0}$ assuming that S remains constant during its evaporation (i.e. single droplet evaporation). This case corresponds to homogeneous mixing, i.e. when turbulent eddies mixed the entrained environment prior droplets start evaporating. As seen,

Formatted: Font: Times New Roman, 12 pt, Bold

τ_{ev} is a strong function of μ. The smallest value of the evaporating time τ_{ev0} corresponds to unmixed entrained air $S = S_2$ at $\mu = 0$. Due to the fact that during mixing the saturation ratio varies in the range $S_2 < S < 1$, the evaporating time will change in the range $\tau_{ev0} < \tau_{ev} < \infty$. In other words τ_{ev0} presents the shortest evaporation time of a single droplet corresponding to S_2 of the entrained air.

It should be noted that complete evaporation of the entire population of droplets will occur when $\mu \le \mu_{cr}$ regardless type of mixing. The region of complete evaporation calculated for a population of droplets is shown on the left side of Fig.16 in section $\mu \le \mu_{cr}$.

During mixing the droplet sizes r and their concentration N are changing. Therefore, as follows from Eq.16 τ_p will be changing as well. Figure 16 also shows the dependence of time of phase relaxation versus μ calculated for the final stage of inhomogeneous $\tau_p^{(i)}$ (dashed blue) and homogeneous $\tau_p^{(h)}$ (solid blue) mixing, and the initial stage homogeneous mixing before droplet evaporation $\tau_{pm}^{(h)}$ (blue thin line). As seen from Fig.16 $\tau_{p0} \le \tau_{pm}^{(h)} \le \tau_p^{(h)} \le \tau_p^{(i)}$.

The humidity equilibrating time for the population of homogeneously mixed droplets $\tau_{eq}^{(h)}$ was calculated as a time when saturation ratio changed from S_{m0} to 0.999. The calculations were performed with the help of a system of differential equations. As seen from Fig.16 $\tau_{eq}^{(h)} > \tau_p^{(h)} > \tau_{pm}^{(h)}$. The time of phase relaxation results from a solution of the Squires equation for supersaturation (Squires, 1952) as a characteristic time of approaching supersaturation to its quasi-state value S_{qs}, and in general case $\tau_p^{(h)} \ne \tau_{eq}^{(h)}$. For the case in Fig.16 the values of $\tau_{eq}^{(h)}$ and $\tau_{pm}^{(h)}$ may differ by more than an order of magnitude, and for this specific case their ratio varies in the range $0 < \tau_{eq}^{(h)} / \tau_{pm}^{(h)} < 15$. Note, that it is possible that $\tau_{eq}^{(h)} \le \tau_{pm}^{(h)}$, when $S \to 1$ the equilibrating time $\tau_{eq}^{(h)} \to 0$. This presents a degenerate case when there is no difference between homogeneous and inhomogeneous mixing.

The equilibrating time for inhomogeneous mixing $\tau_{eq}^{(i)}$ was calculated for extreme inhomogeneous mixing: at the moment of time $t = \tau_{eq}^{(i)}$ (a) the entrained volume is saturated $S_2(\tau_{eq}^{(i)}) \approx 0$ and (b) the population of droplets with concentration n_{ev} undergoes complete evaporation, i.e. $r(\tau_{eq}^{(i)}) \approx 0$. As seen from Fig.16, $\tau_{eq}^{(i)}$ remains constant at $\mu > \mu_{cr}$. Basically in the frame of the inhomogeneous mixing concept $\tau_{eq}^{(i)}$ coincides with the time of evaporation of the population of droplets, which were transported

into the entrained air. Obviously such a consideration is overly idealized and unlikely to happen in nature. This is suggestive that the consideration of $\tau_{eq}^{(i)}$ has significant limitations.

Comparisons of different characteristic times in Fig.16 allow few conclusions about mixing. Thus, for $\mu_A < \mu \le 1$ $\tau_{eq}^{(h)} < \tau_{ev0}$, i.e. the saturation of the environment occurs faster than the fastest possible evaporation time of a single droplet. This suggests that when $\mu_A < \mu \le 1$ the feasibility of inhomogeneous mixing is low. For $\mu_{cr} < \mu < \mu_B$ $\tau_{ev} < \tau_{eq}^{(h)}$, i.e. saturation of the entire volume takes longer due to evaporation of the droplet population than the complete evaporation of a single droplet. Compete evaporation of some droplets may occur, if the conditions in Eq.29 are satisfied. This suggests that when $\mu_{cr} < \mu < \mu_B$ the feasibility of inhomogeneous mixing is increasing. Since during mixing elementary volumes are mixing at any μ homogeneous and inhomogeneous mixing may occur simultaneously in different parts of the mixing volume.

In the conclusion of this section it could be stated that τ_{react} can be characterized by different characteristic times (i.e. τ_{ev}, τ_{pm}, $\tau_p^{(h)}$, $\tau_p^{(i)}$, $\tau_{eq}^{(h)}$), each of which is a function of μ. The difference between these times can reach two orders of magnitude. This brings up a warning on a proper selection of τ_{react} in Da, and requirements for more studies to address this question.

6. Conclusions

This study analysesanalyzes dependences of different moments of $f(r)$ $f(D)$ in the frame of formalism of homogeneous and extremely inhomogeneous mixing. The analysis was performed for the final stage of mixing based on the mass balance of vapor and liquid water and assumption of adiabatic process of mixing. and energy conservation consideration. The following results were obtained in the frame of this study:

1) It is shown that for the case of extreme inhomogeneous mixing all moments of $f(r)$ are linearly related as $M_n = \alpha_{nm} M_m$ where coefficients α_{nm} are determined by adiabatic valued of M_n and M_m. This relation remains valid for progressive mixing.

Analytical1. Simple analytical relationships $M_n = F_{nm}(M_m)$ between the moments M_n and M_m main microphysical moments were foundobtained for the case offinal state homogenous and extreme inhomogeneous mixing.

Formatted: Font: Times New Roman, 12 pt, Font color:
Formatted: Indent: First line: 0.75 cm, No bullets or numbering, Don't adjust space between Latin and Asian text, Don't adjust space between Asian text and numbers
Formatted: Font: Times New Roman, 12 pt, Font color: Black, English (Canada)
Formatted: Font: Times New Roman, 12 pt, Font color:
Formatted: Font: Times New Roman, 12 pt, Font color: Black
Formatted: Indent: First line: 0.75 cm, Don't adjust space between Latin and Asian text, Don't adjust space between Asian text and numbers
Formatted: Font: Times New Roman, 12 pt, Font color:
Formatted: Font: Times New Roman, 12 pt, Font color:
Formatted: Font: Times New Roman, 12 pt, Font color:
Formatted: Font color: Black
Formatted: Font color: Black
Formatted: Font color: Black
Formatted: Font color: Black
Formatted: Font color: Black

~~2)~~ 2. It was ~~demonstrated~~shown that the functional relationships between ~~M_n and M_m~~ the moments exist only for the first stage of homogeneous mixing~~. The following~~, when equilibrium is reached. Subsequent progressive homogeneous mixing breaks the functional relationship between the moments. ~~It was shown that the scattering of the moments M_n and M_m are limited by the lines for inhomogeneous mixing $M_n = \alpha_{nm} M_m$ and homogeneous mixing $M_n = F_{nm}(M_m)$.~~

3. It was demonstrated that consideration of scattering $N - LWC$, $N - \beta$ diagrams facilitates identification of type of mixing from in-situ measurements. For extreme inhomogeneous mixing the scattering of the data points $N - LWC$, $N - \beta$ will be limited by a sector originating at zero point (Fig.12a). However, for homogeneous mixing the scattering data points will be limited by a sector originating at (N_1, LWC_1) and (N_1, β_1) (Fig.12b). Utilizing a stand-alone conventional $N - D_v$ mixing diagram may not provide unambiguous answer about type of mixing.

~~3)~~ 4. The developed approach was applied to a set of in-situ measurements collected in convective clouds. The analysis of the dependences between ~~N, β, LWC and $\overline{D}_3$ (i.e. M_0, M_2, M_3 N, β, LWC and M_3/M_0) obtained from in-situ measurements of convective clouds~~D_v suggests that the interaction between entrained and cloudy environments ~~is~~for the studied clouds was dominated by inhomogeneous mixing. ~~Homogeneous mixing may to become active, when the mixing fraction μ is close to critical μ_{cr}.~~

~~4) Analysis of different characteristic times related to evaporation and equilibrating of the mixing environment showed their strong dependence on the mixing fraction μ. The difference~~The present study considers relationships between different ~~times may reach two orders of magnitude, which makes the selection of τ_{react} ambiguous. This raises a requirement of further studies on characterization~~moments of ~~τ_{react} in Damköhler number. Comparisons of different characteristic times suggest that within~~$f(D)$ for the ~~same mixing environment depending on μ some volumes may be dominated by homogeneous mixing whereas others by inhomogeneous mixing.~~

~~Due to the various limitations and idealizations of the mixing process explored in the above discussion, this study acknowledges that the current description of the mixing process is far from complete. Since the process of mixing covers a wide range of time and spatial scales a comprehensive simulating efforts are required to achieve a better understanding of the process of mixing of colloidal~~

Formatted: Font: Times New Roman, 12 pt, Font color:
Formatted: Font: Times New Roman, 12 pt, Font color:
Formatted: Indent: First line: 0.75 cm, No bullets or numbering, Don't adjust space between Latin and Asian text, Don't adjust space between Asian text and numbers, Tab stops: Not at 1.76 cm
Formatted: Font: Times New Roman, 12 pt, Font color:
Formatted: Font: Times New Roman, 12 pt, Font color:
Formatted: Font: Times New Roman, 12 pt, Font color: Black
Formatted: Font: Times New Roman, 12 pt, Font color:
Formatted: Indent: First line: 0.75 cm, No bullets or numbering, Don't adjust space between Latin and Asian text, Don't adjust space between Asian text and numbers, Tab stops: Not at 1.76 cm
Formatted: Font: Times New Roman, 12 pt, Font color:
Formatted: Font: Times New Roman, 12 pt, Font color:
Formatted: Font: Times New Roman, 12 pt, Font color:
Formatted: Font: Times New Roman, 12 pt, Font color:
Formatted: Font: Times New Roman, 12 pt, Font color:
Formatted: Font: Times New Roman, 12 pt, Font color: Black
Formatted: Font color: Black
Formatted: Font color: Black
Formatted: Indent: First line: 0.75 cm, Don't adjust space between Latin and Asian text, Don't adjust space between Asian text and numbers

~~systems.~~final stage of mixing. The following two works Pinsky et al. (~~2015a,~~2016a, b) in this series provide a ~~more~~ detailed analysis of ~~evolution~~time dependences of droplet size ~~distribution~~distributions and its moments during homogeneous and inhomogeneous mixing.

~~Acknowledgements~~

Acknowledgement. The authors appreciate two anonymous reviewers for their comments. Alexei Korolev work was supported by Environment Canada and Transport Canada. The COPE-MED project was funded by National Science Foundation grant AGS-1230292 and AGS-1230203. The contribution of Mark Pinsky and Alex Khain was supported by the Israel Science Foundation (grant 1393/14), the Office of Science (BER), US Department of Energy Award DE-SC0006788 and the Binational US-Israel Science foundation (grant 2010446).

Formatted: Font: Times New Roman, 12 pt, Font color:

Formatted: Font: Times New Roman, 12 pt, Font color:

Formatted: Font: Times New Roman, 12 pt, Font color:

Formatted: Font: Times New Roman, 12 pt, Font color:

Formatted: Font: Times New Roman, 12 pt, Font color:

Formatted: Font: Times New Roman, 12 pt, Font color:

Formatted: Indent: Left: 0 cm, First line: 0.75 cm, Don't adjust space between Latin and Asian text, Don't adjust space between Asian text and numbers

Formatted: Justified, Indent: First line: 0.75 cm

Formatted: Font: Times New Roman, 12 pt, Font color:

Formatted: Font: Times New Roman, 12 pt, Font color: Black, English (Canada)

Appendix A

List of Symbols

Symbol	Description	Units
b	$\frac{4\pi\rho_w}{\rho_a}\frac{\frac{1}{q_v}+\frac{L_w^2}{c_p R_v T^2}}{\frac{\rho_w L_w^2}{k_a R_v T^2}+\frac{\rho_w R_v T}{E_w(T) D_v}}$	$m^2 s^{-1}$
c_{pa}	specific heat capacity of dry air at constant pressure	$J kg^{-1} K^{-1}$
c_{pv}	specific heat capacity of water vapor at constant pressure	$J kg^{-1} K^{-1}$
D	droplet diameter	m
Da	Damköhler number	-
D_v	coefficient of water vapor diffusion in the air	$m^2 s^{-1}$
e	water vapor pressure	$N m^{-2}$
e_1	initial water vapor pressure in the cloud parcel	$N m^{-2}$
e_2	initial water vapor pressure in the entrained sub-saturated parcel	$N m^{-2}$
E_s	saturation vapor pressure above flat surface of water	$N m^{-2}$
F	$\left(\frac{\rho_w L_w^2}{k_a R_v T^2}+\frac{\rho_w R_v T}{E_w(T) D_v}\right)^{-1}$ coefficient in the equation droplet growth	$N m^{-2}$
$f(r)$	size distribution of cloud droplets normalized on unity	m^{-1}
k_a	coefficient of air heat conductivity	$J m^{-1} s^{-1} K^{-1}$
L_w	latent heat for liquid water	$J kg^{-1}$
LWC	liquid water content	$kg m^{-3}$
l_p	characteristic spatial phase scale	m
m_1	mass of the cloud parcel (1kg)	kg
m_2	mass of the entrained air (1kg)	kg
M_n	n-th moment of the droplet size distribution $\frac{\int_0^\infty f(r) r^n dr}{\int_0^\infty f(r) dr}$	m^n
N	concentration of droplets	m^{-3}

Formatted: Font: Times New Roman, 12 pt, Font color:

Formatted: Font: Calibri, Font color: Black

Formatted: Font: Times New Roman, 12 pt, Bold

Formatted: Normal, Indent: First line: 0.63 cm

Formatted: Font: Times New Roman

Formatted: Font: (Default) Times New Roman, 12 pt

Formatted Table

Formatted: Font: (Default) Times New Roman, 12 pt, English (United States)

Formatted: Font: (Default) Times New Roman, 12 pt

Formatted: Font: (Default) Times New Roman, 12 pt, English (United States)

Formatted: Left

N_0	concentration of droplets before mixing	m^{-3}
p	pressure of moist air	$N\ m^{-2}$
p_a	pressure of dry air	$N\ m^{-2}$
r	droplet radius	m
$\bar{r}$	mean droplet radius	m
$\bar{r}_2$	mean square droplet radius	m
$\bar{r}_3$	mean cubic droplet radius	m
R_a	specific gas constant of moist air	$J\ kg^{-1}K^{-1}$
R_v	specific gas constant of water vapor	$J\ kg^{-1}K^{-1}$
q	cloud liquid water mixing ratio (mass of liquid water per 1kg of dry air)	-
q_0	cloud liquid water mixing ratio before mixing	-
q_v	water vapor mixing ratio (mass of water vapor per 1kg of dry air)	-
S	e / E_S, relative humidity over water (saturation ratio)	-
S_m	relative humidity after mixing is completed	-
S_{m0}	relative humidity after instant mixing of cloudy and entrained air but before droplets evaporation	-
T	temperature	K
T_1	temperature of the cloud parcel before mixing	K
T_2	temperature of the entrained sub-saturated parcel before mixing	K
T_{m0}	temperature of the parcel after vapor mixing, but before droplet evaporation	K
t	Time	s
u_z	vertical velocity	$m\ s^{-1}$
β	extinction coefficient	m^{-1}
β_0	extinction coefficient before mixing	β_0
δq	amount of liquid water per 1kg of sub-saturated air required to saturate the air in the mixed parcel before droplet evaporation Eq.5	-
δq^*	amount of liquid water per 1kg of dry air required to saturate the air in the entrained cloud free volume Eq.8	-
ε	turbulent energy dissipating rate	$m^2\ s^3$

μ	mixing fraction of cloud and dry parcels $0 \leq \mu \leq 1$	-
μ_{cr}	critical mixing fraction, such that for $\mu \leq \mu_{cr}$ all droplets evaporate	-
ρ_a	density of the dry air	kg m^{-3}
ρ_w	density of liquid water	kg m^{-3}
τ_{ev}	time of complete evaporation	s
τ_{ev}	time of complete evaporation at constant $S = S_{m0}$	s
τ_{ev0}	time of complete evaporation at constant $S = S_2$	s
$\tau_{eq}^{(h)}$	time of saturating environment during evaporation of a population of homogeneously mixed droplets	s
$\tau_{eq}^{(i)}$	time of saturating environment for a population of inhomogeneously mixed droplets	s
τ_p	time of phase relaxation	s
$\tau_p^{(h)}$	time of phase relaxation after completing homogeneous mixing	s
$\tau_p^{(h)}$	time of phase relaxation after completing inhomogeneous mixing	s

1013

~~Appendix B~~

~~:~~ Liquid water deficit

The objective of this section is to find the amount of liquid water, which is required to ~~evaporate~~be evaporated in order to saturate the parcel formed after mixing ~~of a cloud volume with sub-saturated entrained air.~~

~~.~~ Assume that ~~q_{v1}, q_{v2}~~ q_{v1}, q_{v2} are the mixing vapor ratios in the cloudy and entrained parcels, respectively, and ~~T_1, T_2~~ T_1, T_2 are their respective initial temperatures. First, we find the saturation ratio ~~S_{m0}~~ S_{m0} formed after instant mixing of the cloud and entrained before the cloud droplets start evaporating.

The vapor mixing ratio ~~q_{vm}~~ q_{vm} formed in the mixed volume will be

~~$q_{vm} = \mu q_{v1} + (1-\mu) q_{v2}$~~ ~~(B1)~~

$$q_{vm} = \mu q_{v1} + (1-\mu) q_{v2} \quad \text{(A1)}$$

The vapor pressure ~~e_m~~ e_m in the mixed volume can be derived from Eq. ~~B1~~(A1) by substituting ~~$q_v = \frac{e}{p-e}\frac{R_a}{R_v}$~~ $q_v = \frac{e}{p-e}\frac{R_a}{R_v}$, i.e.

~~$e_m = p \dfrac{\mu + \dfrac{e_2(p-e_1)}{p(e_1-e_2)}}{\mu + \dfrac{(p-e_1)}{(e_1-e_2)}}$~~ ~~(B2)~~

$$e_m = p \frac{\mu + \dfrac{e_2(p-e_1)}{p(e_1-e_2)}}{\mu + \dfrac{(p-e_1)}{(e_1-e_2)}} \quad \text{(A2)}$$

The temperature of the mixed volume T_{m0} can be found from the energy conservation law

~~$\mu(q_{v1}c_{pv} + c_{pa})(T_1 - T_{m0}) = (1-\mu)(q_{v2}c_{pv} + c_{pa})(T_{m0} - T_2)$~~ ~~(B3)~~

$$\mu(q_{v1}c_{pv} + c_{pa})(T_1 - T_{m0}) = (1-\mu)(q_{v2}c_{pv} + c_{pa})(T_{m0} - T_2) \quad \text{(A3)}$$

here ~~c_{pv}, c_{pa}~~ c_{pv}, c_{pa} are the specific heat capacitance of water vapor and dry air at constant pressure, respectively, ~~T_1, T_2~~ T_1, T_2 are the initial temperatures in the first and second parcels before mixing~~, T_{m0}~~. Substituting ~~q_{v1}, q_{v2}~~ q_{v1}, q_{v2} yields the temperature in the mixed volume

Formatted: Font: Times New Roman, 12 pt, Font color:
Formatted: Font: Times New Roman, 12 pt, Font color:
Formatted: Indent: First line: 0.75 cm, Don't adjust space between Latin and Asian text, Don't adjust space between Asian text and numbers
Formatted: Font color: Black
Formatted: Font: Times New Roman, 12 pt, Font color:
Formatted: Indent: First line: 0.75 cm, Don't adjust space between Latin and Asian text, Don't adjust space between Asian text and numbers
Formatted: Font: Times New Roman, 12 pt, Font color:
Formatted: Font: Times New Roman, 12 pt
Formatted: Font: Times New Roman, 12 pt, Font color:
Formatted: Font: Times New Roman, 12 pt, Font color:
Formatted: Font: Times New Roman, 12 pt, Font color:
Formatted: Font: Times New Roman, 12 pt, Font color: Black
Field Code Changed
Formatted: Font: Times New Roman, 12 pt, Font color:
Formatted: Font: Times New Roman, 12 pt, Font color:
Formatted: Font: Times New Roman, 12 pt, Font color:
Formatted: Indent: First line: 0.75 cm, Don't adjust space between Latin and Asian text, Don't adjust space between Asian text and numbers
Field Code Changed
Formatted: Font: Times New Roman, 12 pt, Font color: Black
Field Code Changed
Formatted: Font: Times New Roman, 12 pt
Formatted: Font: Times New Roman, 12 pt
Formatted: Font: (Default) Times New Roman, 12 pt, English (United States)
Field Code Changed
Formatted: Font: Times New Roman, 12 pt
Formatted: Don't adjust space between Latin and Asian text, Don't adjust space between Asian text and numbers
Formatted: Font: Times New Roman, 12 pt
Formatted: Font: Times New Roman, 12 pt, Font color:
Formatted: Font: Times New Roman, 12 pt
Formatted: Font: Times New Roman, 12 pt
Formatted: Font: Times New Roman, 12 pt

~~$T_m = \frac{\mu T_1 + a(1-\mu)T_2}{\mu + a(1-\mu)}$~~ ~~(B4)~~

$$T_{m0} = \frac{\mu T_1 + \alpha(1-\mu)T_2}{\mu + \alpha(1-\mu)} \quad (A4)$$

here

~~$a = \frac{1+\frac{c_{pv}R_a e_2}{c_{pa}R_v(p-e_2)}}{1+\frac{c_{pv}R_a e_1}{c_{pa}R_v(p-e_1)}}$~~ ~~(B5)~~

$$\alpha = \frac{1+\frac{c_{pv}R_a e_2}{c_{pa}R_v(p-e_2)}}{1+\frac{c_{pv}R_a e_1}{c_{pa}R_v(p-e_1)}} \quad (A5)$$

With a good accuracy ~~$a \cong 1$~~ $\alpha \cong 1$. The resulting ~~saturation ratio~~relative humidity after mixing the two volumes will be

~~$S_{m0} = \frac{e_m}{E_S(T_{m0})}$~~ ~~(B6)~~

$$RH_{m0} = \frac{e_{m0}}{e_S(T_{m0})} \quad (A6)$$

where ~~$E_s(T_{m0})$~~ $e_S(T_{m0})$ is the saturated vapor pressure at temperature ~~T_{m0}~~ T_{m0}.

~~If the initial saturation ratio is S_{m0}<1, then the cloud droplets start evaporating.~~ The process of evaporation is accompanied by changing humidity and temperature due to latent heat of vaporization. This process is described by the Eq. (C2) in Korolev and Mazin (2003). Assuming the process to be isobaric (i.e. vertical velocity ~~u_z~~ $=u_z = 0$) and absence of ice (~~dq_i~~ $=dq_i = 0$), Eq. (C2) (Korolev and Mazin, 2003) yields

~~$\frac{dS}{S} = \left(\frac{1}{S}\frac{pR_v}{E_S R_a} + \frac{L^2}{c_p R_v T^2}\right) dq$~~ ~~(B7)~~

$$\frac{dS}{S+1} = \left(\frac{1}{S+1}\frac{pR_v}{e_S R_a} + \frac{L^2}{c_{pa} R_v T^2}\right) dq \quad (A7)$$

Field Code Changed

Formatted: Font: Times New Roman, 12 pt, Font color:

Formatted: Don't adjust space between Latin and Asian text, Don't adjust space between Asian text and numbers

Field Code Changed

Formatted: Font: Times New Roman, 12 pt, Font color:

Formatted: Indent: First line: 0.75 cm, Don't adjust space between Latin and Asian text, Don't adjust space between Asian text and numbers

Formatted: Font: Times New Roman, 12 pt, Font color:

Formatted: Font: Times New Roman, 12 pt, Font color: Black

Field Code Changed

Formatted: Font: Times New Roman, 12 pt, Font color:

Formatted: Don't adjust space between Latin and Asian text, Don't adjust space between Asian text and numbers

Formatted: Font: Times New Roman, 12 pt, Font color:

Formatted: Font: Times New Roman, 12 pt, Font color:

Formatted: Indent: First line: 0.75 cm, Don't adjust space between Latin and Asian text, Don't adjust space between Asian text and numbers

Formatted: Font: Times New Roman, 12 pt, Font color:

Formatted: Font: Times New Roman, 12 pt, Font color:

Formatted: Font: Times New Roman, 12 pt, Font color:

Formatted: Font: Times New Roman, 12 pt, Font color:

Formatted: Font: Times New Roman, 12 pt, Font color:

Formatted: Font: Times New Roman, 12 pt, Font color:

Formatted: Font: Times New Roman, 12 pt, Font color:

Formatted: Font: Times New Roman, 12 pt, Font color:

Formatted: Font: Times New Roman, 12 pt, Font color:

Field Code Changed

Field Code Changed

Integrating Eq.~~B1~~ (A7) from initial ~~humidity S_{m0} (Eq.6)~~S_{m0} to saturation state, when ~~$S=1$~~$S = 0$, and taking into account that $RH = S + 1$, gives ~~an expression~~

~~$$\delta q = \frac{L^2}{c_p R_v T_2^2} \ln\left(\frac{1+\frac{E_S(T_{m0})R_a L^2}{pc_p R_v^2 T_{m0}^2}}{1+S_{m0}\frac{E_S(T_{m0})R_a L^2}{pc_p R_v^2 T_{m0}^2}}\right)$$~~ ~~(B8)~~

~~It should be noted that in Eq.B8~~ $$\delta q_m = -b\ln\left(\frac{1+aRH_{m0}}{1+a}\right)$$ (A8)

the ~~changes of temperature during droplet evaporation and related changes~~mixing ratio of liquid water required to evaporate in order to saturate 1kg of the cloud volume ~~were neglected.~~formed after mixing with the entrained air, but before droplet start evaporating. Here $a = \frac{E_S R_a L^2}{pc_p R_v^2 T_m^2}$, $b = \frac{c_p R_v T_m^2}{L^2}$.

Since $\left|\frac{A(RH_{m0}-1)}{1+A}\right| < 1$, Eq.(A8) can be simplified as

$$\delta q_m = ab\frac{1-RH_{m0}}{1+a} = -\frac{S_{m0}}{A_2} \quad \text{(A9)}$$

where $A_2 = \frac{ab}{1+a}$. The analysis of ~~the behavior of Eq.B8~~Eqs. (A8)-(9) shows that for wide range of temperatures ~~-30°C<T <30°C the cases when~~ 30 °C< T < 30 °C, both equations hold with high accuracy as long as the temperatures of the sub-saturated and cloud parcels ~~$|T_1 - T_2| <$~~$|T_1 - T_2| \leq$ 10°C~~, then Eq.B2 is hold with high accuracy.~~.

Figure ~~B1~~A1 shows comparisons of modeled ~~δq~~ δq_m and that calculated from ~~Eq.B8~~Eqs. (A8) and (A9) for three different temperatures. The model ~~consisted in solving~~solved a system of differential equation with ~~decremental~~incremental evaporation of liquid water until saturation is reached.

As seen from Fig. ~~B1~~A1 the agreement between modeled ~~δq~~ δq_m and that calculated from Eq.~~B8~~ (A8)-(A9) is quite good and does not exceed few percent at ~~$S_0 =$~~$RH_{m0} =$ 0.5. This discrepancy results from ~~disregarding the effect of changing T on E_s during evaporation, i.e. in Eq. B8~~ ~~E_s and T~~ assumption that e_S and T are ~~assumed to be~~ constant~~. The changes of the air temperature due to the latent heat of vaporization increase with the increase of the amount evaporated water, when~~

Formatted: Font: Times New Roman, 12 pt, Font color:
Formatted: Indent: First line: 0.75 cm, Don't adjust space between Latin and Asian text, Don't adjust space between Asian text and numbers
Formatted: Font: Times New Roman, 12 pt, Font color:
Formatted: Font: Times New Roman, 12 pt, Font color:
Formatted: Font: Times New Roman, 12 pt, Font color:
Formatted: Font: (Default) Times New Roman, 12 pt, Font color: Black
Formatted: Font: Times New Roman, 12 pt, Font color:
Field Code Changed
Formatted: Font: Times New Roman, 12 pt
Field Code Changed
Formatted: Indent: First line: 0 cm, Don't adjust space between Latin and Asian text, Don't adjust space between Asian text and numbers
Formatted: Font: (Default) Times New Roman, 12 pt, Font color: Black
Formatted: Font: Times New Roman, 12 pt, Font color:
Formatted: Font: Times New Roman, 12 pt, Font color:
Formatted: Font: Times New Roman, 12 pt, Font color:
Formatted: Font: Times New Roman, 12 pt, Font color:
Formatted: Font color: Black
Formatted: Font: Times New Roman, 12 pt, Font color:
Formatted: Font: Times New Roman, 12 pt, Italic, Font color: Black
Formatted: Font: Times New Roman, 12 pt, Font color:
Formatted: Font color: Black
Formatted: Font: Times New Roman, 12 pt, Font color:
Formatted: Font color: Black
Formatted: Font color: Black
Formatted: Font: Times New Roman, 12 pt, Font color:
Formatted: Font color: Black
Formatted: Font: Times New Roman, 12 pt, Font color:
Formatted: Indent: First line: 0.75 cm, Don't adjust space between Latin and Asian text, Don't adjust space between Asian text and numbers
Formatted: Font: Times New Roman, 12 pt, Font color:
Formatted: Font: Times New Roman, 12 pt, Italic, Font color: Black
Formatted: Font: Times New Roman, 12 pt, Font color:
Formatted: Font: Times New Roman, 12 pt, Font color:
Formatted: Font: Times New Roman, 12 pt, Font color:
Formatted: Font: Times New Roman, 12 pt, Italic, Font color: Black
Formatted: Font: Times New Roman, 12 pt, Font color:
Formatted: Font: Times New Roman, 12 pt, Font color: Black

~~the initial humidity is decreasing (Fig. B1). The accuracy provided by Eq. B2 is sufficient for the purposes of the present work.~~ in Eqs.(A8)-(A9).

Appendix B: Liquid water deficit when $T_1 = T_2$

Eq.(A2) by assuming that $p \gg e_1$ and $p \gg e_2$ can be simplified as

$$e_{m0} = \mu e_1 + (1-\mu)e_2 \quad \text{(B2)}$$

As follows from Eq.(A4) for the case $T_1 = T_2$ with high accuracy $T_{m0} = T_1 = T_2$. Therefore, $e_S(T_{m0}) = e_S(T_1) = e_S(T_2)$. Dividing Eq.(B1) by e_S yields

$$RH_{m0} = \mu RH_1 + (1-\mu)RH_2 \quad \text{(B3)}$$

In most liquid clouds $RH_1 = 1$ (Korolev and Mazin 2003). Therefore, Eq.B2 turns into

$$RH_{m0} = \mu + (1-\mu)RH_2 \quad \text{(B4)}$$

Substituting Eq.(B4) in Eq.(B1) yields

$$\delta q_m = -b\ln\left(1 + \frac{a(1-\mu)(RH_2 - 1)}{1+a}\right) \quad \text{(B5)}$$

The expression under logarithm can be presented as the first two terms of the series expansion of $\left(1 + \frac{a(RH_2-1)}{1+A}\right)^{(1-\mu)}$. Substituting this expression into Eq.(B5), gives

$$\delta q_m = (1-\mu)\delta q^* \quad \text{(B6)}$$

where

$$\delta q^* = -b\ln\left(\frac{1+aRH_2}{1+a}\right) \quad \text{(B7)}$$

is the mixing ratio of liquid water required to saturate 1 kg of the entrained dry volume.

Appendix C: Temperature in the mixing volume

The energy conservation for evaporating droplets can be written as

$$(T - T_{m0})(1+q_{vm})c_{pm} + (1-\mu)\delta q^* L = 0 \quad \text{(C1)}$$

here c_{pm} is the specific heat capacity of the moist air

$$c_{pm} = \frac{c_{pa} + q_{vm}c_{pv}}{1+q_{vm}} \quad \text{(C2)}$$

Formatted: Font: Times New Roman, 12 pt, Font color:

Field Code Changed

Field Code Changed

Field Code Changed

Field Code Changed

Field Code Changed

Field Code Changed

Field Code Changed

Since $q_{vm} \ll 1$ and, $c_{pa} \cong c_{pm}$ Eq.(C1) may be simplified, so that the final temperature after mixing

$$T = T_{m0} - \frac{(1-\mu)\delta q^* L}{c_{pa}} \quad \text{(C3)}$$

For the case when $T_1 \neq T_2$ Eq. (C3) should be replaced by

$$T = T_{m0} - \frac{\delta q_m L}{c_{pa}} \quad \text{(C4)}$$

Eqs. (C3) and (C4) are valid for the mixing fraction $\mu > \mu_{cr}$. For $\mu \leq \mu_{cr}$ all entrained liquid water μq_0 evaporates, and the final temperature will be

$$T = T_{m0} - \frac{\mu q_0 L}{c_{pa}} \quad \text{(C5)}$$

References

~~Andejchuk,~~Andrejczuk M., Grabowski, W. W., ~~,~~Malinowski, S. P., and Smolarkiewicz, P. K.: Numerical ~~Simulation of Cloud-Clear Air Interfacial Mixing: Homogeneous versus Inhomogeneous Mixing.~~simulation of cloud–clear air interfacial mixing: homogeneous vs. inhomogeneous mixing., J. Atmos. Sci., 66, 2493–2500, 2009.

Baker, M. B~~.~~, and Latham, J.: The evolution of droplet spectra and the rate of production of embryonic raindrops in small cumulus clouds~~.~~, J. Atmos. Sci., 36, 1612–1615, 1979.

Baker, M. B. and Latham, J.: ~~-~~A diffusive model of the turbulent mixing of dry and cloudy air ~~Quart~~, Q. J. R. Met. Soc., 108, 871–898, 1982.

Baker, M. B., Corbin, R. G., and Latham, J.: The influence of entrainment on the evolution of cloud droplet spectra: I. A model of inhomogeneous mixing~~.~~ ~~Quart~~, Q. J. Roy. Meteor. Soc., 106, 581–598, 1980.

Beals, M.J., and Fugal, J.P., Shaw, R.A., Lu, J., Spuler, S.M., Stith, J.L.: Holographic measurements of inhomogeneous cloud mixing at the centimeter scale. Science, 350, 87-90, 2015

Bohren, C. F~~.~~, and Albrecht, C. H.: Atmospheric Thermodynamics~~.~~, Oxford University Press, New York, 402 pp., 1998.

Field Code Changed
Field Code Changed
Field Code Changed
Formatted: Font: Times New Roman, 12 pt, Font color:
Formatted: Indent: First line: 0.75 cm, Don't adjust space between Latin and Asian text, Don't adjust space between Asian text and numbers
Formatted: Don't adjust space between Latin and Asian text, Don't adjust space between Asian text and numbers
Formatted: Font: Times New Roman, 12 pt, Font color:
Formatted: Indent: Left: 0 cm, Hanging: 0.5 cm
Formatted: Font: Times New Roman, 12 pt, Font color: Auto
Formatted: Font: Times New Roman, 12 pt, Font color:
Formatted: Font: Times New Roman, 12 pt, Font color:
Formatted: Font: Times New Roman, 12 pt, Font color:
Formatted: Font: Times New Roman, 12 pt, Font color:
Formatted: Font: Times New Roman, 12 pt, Font color:
Formatted: Font: Times New Roman, 12 pt, Font color:
Formatted: Font: Times New Roman, 12 pt, Font color:
Formatted: Font: Times New Roman, 12 pt, Not Italic, Font color: Black
Formatted: Font: Times New Roman, 12 pt, Font color:
Formatted: Font: Times New Roman, 12 pt, Font color:
Formatted: Font: Times New Roman, 12 pt, Font color:
Formatted: Font: Times New Roman, 12 pt, Font color:
Formatted: Font: Times New Roman, 12 pt, Font color:
Formatted: Font: Times New Roman, 12 pt, Not Italic, Font color: Black
Formatted: Font: Times New Roman, 12 pt, Font color:
Formatted: Font: Times New Roman, 12 pt, Font color:
Formatted: Font: Times New Roman, 12 pt, Font color:
Formatted: Font: Times New Roman, 12 pt, Font color:
Formatted
Formatted: Font: Times New Roman, 12 pt, Font color:
Formatted
Formatted: Font: Times New Roman, 12 pt, Font color:
Formatted: Font: Times New Roman, 12 pt, Font color:
Formatted
Formatted: Font: Times New Roman, 12 pt, Font color:
Formatted: Font: Times New Roman, 12 pt, Font color:
Formatted: Font: Times New Roman, 12 pt
Formatted
Formatted: Font: Times New Roman, 12 pt
Formatted: Font: Times New Roman, 12 pt, Not Italic
Formatted: Font: Times New Roman, 12 pt
Formatted: Font: Times New Roman, 12 pt

Bower, K. N., and Choularton, T. W.: The effects of entrainment on the growth of droplets in continental cumulus clouds. Quart. J. Roy. Meteor. Soc., 114, 1411–1434, 1988.

Broadwell, J. E., and R. E. Breidenthal: A simple model of mixing and chemical reaction in a turbulent shear layer. J. Fluid Mech., 125, 397–410, 1982

Burnet, F., and Brenguier, J. L.: Observational study of the Entrainment Mixing Processentrainment-mixing process in Warm Convective Cloudswarm convective clouds, J. Atmos. Sci., 64, 1995–2011, 2007.

Devenish, B. J., Bartello, P., Brenguier, J.-L., Collins, L. R., Grabowski, W. W., Ijzermans, R. H. A., Malinovski, S. P., Reeks, M.W., Vassilicos, J. C., Wang, L.-P., and WarhaftandWarhaft, Z.: Droplet growth in warm turbulent clouds. Q. J. Roy. Meteorol.Meteor. Soc., 138, 1401–1429, 2012.

Dimotakis, P. E.: Turbulent mixing. Annu. Rev. Fluid Mech., 37, 329–356, 2005.

Gerber, H., Frick, G., Jensen, J. B., and Hudson, J. G.: Entrainment, mixing, and microphysics in trade-wind cumulus. J. Meteorol. Soc. Jpn., 86A.86, 87–106, 2008.

Hill, T. A., and Choularton, T. W.: An airbone study of the microphysical structure of cumulus clouds. Quart. J. Roy. Meteor. Soc., 111, 517–544, 1985.

Jeffery, C. A.: Inhomogeneous cloud evaporation, invariance, and Damköhler number. J. Geoph. Res., 112, D24S21, doi:10.1029/2007JD008789, 2007.

Jarecka, D., Grabowski, W. W., Morrison, H., Pawlowska, H.: Homogeneity of the Subgrid-Scale Turbulent Mixing in Large-Eddy Simulation of Shallow Convection. J. Atmos. Sci. 70, 2751-2767, 2013

Jensen, J., and Baker, M.: A simple model of droplet spectra evolution during turbulent mixing. J. Atmos. Sci., 46, 2812–2829, 1989.

Korolev, A. V.: The influence of supersaturation fluctuations on droplet spectra formation. Journal of the Atmospheric Sciences, 52, 3620-3634, 1995.

Korolev, A. V. and Isaac, G. A.: Drop Growth Duegrowth due to High Supersaturation Causedhigh supersaturation caused by Isobaric Mixing.isobaric mixing, J. Atmos. Sci., 57, 10, 1675–1685, 2000.

Korolev, A. V., and Filed, I.P.R.: The effect Mazin,: Supersaturation of dynamics on mixed phasewater vapor in clouds: theoretical considerations., J. Atmos. Sci., 65, 66–86, 2008 60, 2957-2974, 2003.

Formatted ...

Formatted: Font: Times New Roman, 12 pt, Font color:

Formatted ...

Formatted: Indent: Left: 0 cm, Hanging: 0.5 cm

Formatted: Normal, Justified, Indent: Left: 0 cm, Hanging: 0.5 cm, Don't adjust space between Latin and Asian text, Don't adjust space between Asian text and numbers, Tab stops: Not at 2 cm + 15.75 cm + 16.19 cm + 16.25 cm +

Formatted ...

Formatted ...

Formatted ...

Formatted ...

Formatted ...

Formatted: Font: Times New Roman, 12 pt, Font color:

Formatted: Indent: Left: 0 cm, Hanging: 0.5 cm, Tab stops: Not at 15.75 cm + 16.5 cm

Formatted ...

Formatted ...

Formatted ...

Formatted: Indent: Left: 0 cm, Hanging: 0.5 cm, Widow/Orphan control, Don't adjust space between Latin and Asian text, Don't adjust space between Asian text and numbers, Tab stops: Not at 1.25 cm

Formatted ...

Krueger, S., Su, C.-W., and McMurtry, P.: Modeling entrainment and finescale mixing in cumulus clouds, J. Atmos. Sci., 54, 2697–2712, 1997.

Kumar, B., Schumacher, J., and Shaw, R. A.: Cloud microphysical effects of turbulent mixing and entrainment, Theor. Comput. Fluid Dyn., 27, 361–376, 2013.

Lasher-Trapp, S. G., Cooper, W. A., and Blyth, A. M.: Broadening of droplet size distributions from entrainment and mixing in a cumulus cloud, Q. J. R. Meteorol Roy. Meteor. Soc., 131, 195–220, 2005.

Latham, J., and Reed, R. L.: Laboratory studies of the effects of mixing on the evolution of cloud droplet spectra, Quart. Q. J. Roy. Meteor. Soc., 103, 297–306, 1977.

Lehmann, K., Siebert, H., and Shaw, R. A.: Homogeneous and inhomogeneous mixing in cumulus clouds: Dependencedependence on local turbulence structure, J. Atmos. Sci., 66, 3641–3659, 2009.

Leon, D. C., French, J. R., Lasher-Trapp, S., Blyth, A. M., Abel, S. J., Ballard, S., Bennett, L. J., Bower, K., Brooks, B., Brown, P., Choularton, T., Clark, P., Collier, C., Crosier, J., Cui, ZhZ., Dufton, D., Eagle, C., Flynn, M. J., Gallagher, M., Hanley, K., Huang, Y., Kitchen, M., Korolev, A., Lean, H., Liu, Z., Marsham, J., Moser, D., Nicol, J., Norton, E. G., Plummer, D. Price, J., Ricketts, H., Roberts, N., Rosenberg, P. D., Taylor, J. W., Williams, P. I., and Young, G.: The Convective Precipitation Experiment (COPE): Investigatinginvestigating the origins of heavy precipitation in the southwestern UK, Bull. Amer. Meteor., B. Am. Meteorol. Soc., (in press), 2015, 2016.

Lu, C., and Liu Y., Niu, S.: Examination of turbulent entrainmentimixing mechanisms using a combined approach. J. Geoph. Res., 116, D20207, 2011.

Paluch, I. R.,: Mixing and the droplet size spectrum: generalizations from the CCOPE data, J. Atmos. Sci., 43, 1984–1993, 1986.

Paluch, I. R., and Baumgardner, D. G.: Entrainment and fine-scale mixing in a continental convective cloud, J. Atmos. Sci., 46, 261–278, 1989.

Paluch, I. R., and Knight, C. A.: Mixing and evolution of cloud droplet size spectra in a vigorous continental cumulus, J. Atmos. Sci., 41, 1801–1815, 1984.

Pinsky, M., Khain, A., Korolev, A., and Magaritz-Ronen, L.: Theoretical studyinvestigation of mixing in liquidwarm clouds – Part 2: Homogeneous mixing, Atmos. Chem. Phys., (submitted), . Discuss., 15, 30269-30320, doi:10.5194/acpd-15-30269-2015, 2015.

Formatted ...

Formatted ...

Formatted ...

Formatted: Indent: Left: 0 cm, Hanging: 0.5 cm

Formatted ...

Formatted: Indent: Left: 0 cm, Hanging: 0.5 cm, Don't adjust space between Asian text and numbers

Formatted ...

Formatted ...

Formatted: Font: Times New Roman, 12 pt, Font color:

Formatted: Indent: Left: 0 cm, Hanging: 0.5 cm, Don't adjust space between Asian text and numbers

Formatted ...

Formatted: Indent: Left: 0 cm, Hanging: 0.5 cm

Formatted ...

Formatted ...

Formatted: Font: Times New Roman, 12 pt, Font color: Black, English (Canada)

Formatted: Indent: Left: 0 cm, Hanging: 0.5 cm, Don't adjust space between Asian text and numbers

Formatted ...

Pinsky, M., Khain, A., and Korolev, A~~.,~~ .: Theoretical ~~study~~analysis of mixing in liquid clouds~~.~~ – Part 3: ~~Inomogeneous~~Inhomogeneous mixing~~.~~, Atmos. Chem. Phys~~., (submitted),~~ Discuss., 15, 30321–30381, doi:10.5194/acpd-15-30321-2015, 2015.

Pinsky, M., Khain, A., Korolev, A., and Magaritz-Ronen, L.: Theoretical investigation of mixing in warm clouds – Part 2: Homogeneous mixing, Atmos. Chem. Phys., submitted, 2016

Pinsky, M., Khain, A., and Korolev, A.: Theoretical analysis of mixing in liquid clouds – Part 3: Inhomogeneous mixing, Atmos. Chem. Phys. Submitted, 2016

Rogers, R. R~~.,~~ .: A ~~*short course*~~Short Course in ~~*cloud physics.* Oxford~~Cloud Physics, Pergamon press, Oxford, 227 pp~~.~~, 1976.

Squires, P.: The growth of cloud drops by condensation. Aust. J. Sci. Res., 5, 66–86, 1952.

Su, C.-W., Krueger, S. K., McMurtry, P. A., and Austin, P. H.: Linear eddy modeling of droplet spectral evolution during entrainment and mixing in cumulus clouds~~.~~, Atmos. Res., 47-48, 41-58, 1998.

Formatted: Font: Times New Roman, 12 pt, Font color: Black, English (Canada)

Formatted: Font: Times New Roman, 12 pt, Font color: Black, English (Canada)

Formatted: Font: Times New Roman, 12 pt, Font color:

Formatted: Font: Times New Roman, 12 pt, Font color:

Formatted: Font: Times New Roman, 12 pt, Font color:

Formatted: Font: Times New Roman, 12 pt, Font color:

Formatted: Font: Times New Roman, 12 pt, Font color:

Formatted: Font: Times New Roman, 12 pt, Not Italic, Font color: Black

Formatted: Font: Times New Roman, 12 pt, Font color:

Formatted: Font: Times New Roman, 12 pt

Formatted: Font: Times New Roman, 12 pt

Formatted: Indent: Left: 0 cm, Hanging: 0.5 cm, Don't adjust space between Latin and Asian text, Don't adjust space between Asian text and numbers

Formatted: Font: Times New Roman, 12 pt

Formatted: Font: Times New Roman, 12 pt, Not Italic

Formatted: Font: Times New Roman, 12 pt, Not Italic

Formatted: Font: Times New Roman, 12 pt

Formatted: Font: Times New Roman, 12 pt

Formatted: Font: Times New Roman, 12 pt

Formatted: Font: Times New Roman, 12 pt

Formatted: Font: Times New Roman, 12 pt, Font color:

Formatted: Indent: Left: 0 cm, Hanging: 0.5 cm, Don't adjust space between Latin and Asian text, Don't adjust space between Asian text and numbers

Formatted: Font: Times New Roman, 12 pt, Font color:

Formatted: Font: Times New Roman, 12 pt, Font color:

Formatted: Font: Times New Roman, 12 pt, Font color:

Formatted: Font: Times New Roman, 12 pt, Font color:

Formatted: Font: Times New Roman, 12 pt, Font color:

Formatted: Font: Times New Roman, 12 pt, Font color:

Formatted: Font: Times New Roman, 12 pt, Not Italic, Font color: Black

Formatted: Font: Times New Roman, 12 pt, Font color:

Formatted: Font: Times New Roman, 12 pt, Not Bold, Font color: Black

Formatted: Font: Times New Roman, 12 pt, Font color:

Formatted: Font: Times New Roman, 12 pt, Font color: Auto

1201 **Table 1**

Formatted: Font: Times New Roman, 12 pt, Bold

Table 1. Evaporating time (t_{ev}), evaporating distance of a free falling droplet (λ_{ev}), size of the volume (λ_v) saturated by a completely evaporated droplet with radius r and saturation ratio S. T =0C, P =687mb.

r	2μm			5μm			10μm		
S	t_{ev} (s)	λ_{ev} (mm)	λ_v (mm)	t_{ev} (s)	λ_{ev} (mm)	λ_v (mm)	t_{ev} (s)	λ_{ev} (mm)	λ_v (mm)
0.9	0.32	0.10	0.51	1.8	3.8	1.3	6.9	59.4	2.6
0.7	0.11	0.03	0.35	0.60	1.3	0.87	2.3	19.8	1.7
0.5	0.06	0.02	0.29	0.36	0.76	0.72	1.4	11.9	1.4
0.2	0.04	0.01	0.24	0.23	0.48	0.59	0.9	7.4	1.2

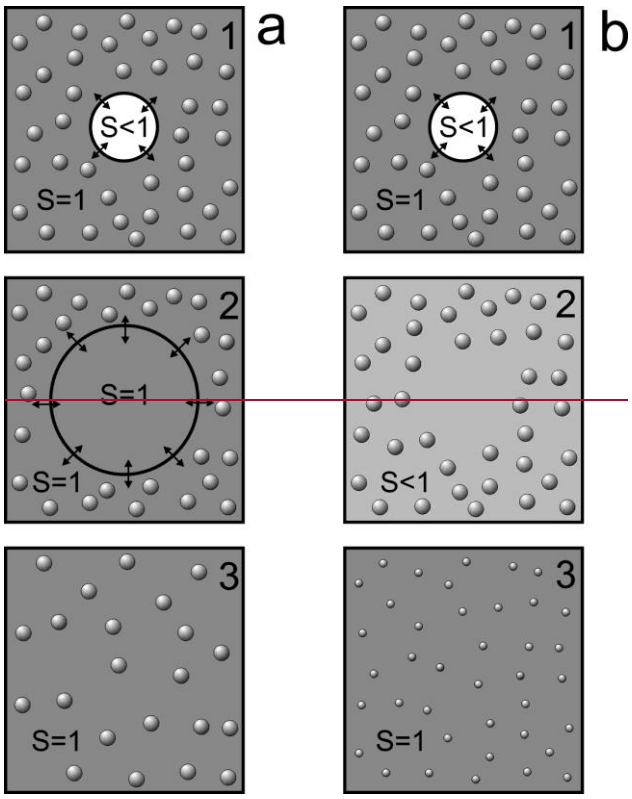

List of Symbols

Symbol	Description	Units
A_2	$\frac{pR_v}{e_s R_a} + \frac{L^2}{c_{pa} R_v T^2}$	-
a	$\frac{e_s R_a L^2}{p c_{pa} R_v^2 T^2}$	-

Formatted: Font: Times New Roman, 12 pt, Bold
Formatted: Font: Times New Roman
Formatted: Normal, Indent: First line: 0.63 cm
Formatted: Font: (Default) Times New Roman, 12 pt
Formatted: Font: (Default) Times New Roman, 12 pt
Formatted: Font: (Default) Times New Roman, 12 pt, English (United States)
Formatted: Left
Formatted Table
Formatted: Font: (Default) Times New Roman, 12 pt, English (United States)

b	$\frac{c_{pa}R_vT^2}{L^2}$	-
c_{pa}	specific heat capacity of dry air at constant pressure	J kg^{-1}K^{-1}
c_{pv}	specific heat capacity of water vapor at constant pressure	J kg^{-1}K^{-1}
$\overline{D}$	mean droplet diameter	m
D_2	mean square droplet diameter	m
D_v	mean volume droplet diameter	m
e	water vapor pressure	N m^{-2}
e_1	initial water vapor pressure in the cloud parcel	N m^{-2}
e_2	initial water vapor pressure in the entrained sub-saturated parcel	N m^{-2}
e_s	saturation vapor pressure above flat surface of water	N m^{-2}
$f(D)$	size distribution of cloud droplets normalized on unity	m^{-1}
L	latent heat for liquid water	J kg^{-1}
M_n	n-th moment of the droplet size distribution $\frac{\int_0^\infty f(r)r^n dr}{\int_0^\infty f(r)dr}$	m^n
N	concentration of droplets	m^{-3}
N_1	concentration of droplets before mixing	m^{-3}
p	pressure of moist air	N m^{-2}
R_a	specific gas constant of moist air	J kg^{-1}K^{-1}
R_v	specific gas constant of water vapor	J kg^{-1}K^{-1}
RH	e/E_S, relative humidity over water (saturation ratio)	-
RH_1	initial relative humidity in the cloud volume (RH_1=1)	-
RH_2	relative humidity in the entrained sub-saturated parcel	-
RH_{m0}	relative humidity after instant mixing of cloudy and entrained air but before droplets evaporation	-
q	cloud liquid water mixing ratio (mass of liquid water per 1kg of dry air)	-
q_1	cloud liquid water mixing ratio before mixing	-
q_v	water vapor mixing ratio (mass of water vapor per 1kg of dry air)	-

S	$e/e_s - 1$, supersaturation	-
S_2	supersaturation of the dry out-of-cloud air	-
S_{m0}	supersaturation after instant mixing of cloudy and entrained air, but before droplets start evaporating	-
T	temperature	K
T_1	temperature of the cloud parcel before mixing	K
T_2	temperature of the entrained sub-saturated parcel before mixing	K
T_{m0}	temperature of the parcel after vapor mixing, but before droplet evaporation	K
β	extinction coefficient	m^{-1}
β_1	extinction coefficient before mixing	m^{-1}
δq_m	mixing ratio of liquid water required to saturate 1kg of the cloud volume after instant mixing, but before droplet evaporation.	-
δq^*	mixing ratio of liquid water required to saturate 1kg of the dry out-of-cloud air	-
μ	cloud fraction of mixing air, $0 \le \mu \le 1$	-
μ_{cr}	critical cloud fraction, such that for $\mu \le \mu_{cr}$ all droplets evaporate	-
ρ_a	density of the dry air	$kg\ m^{-3}$
ρ_w	density of liquid water	$kg\ m^{-3}$
ξ	coefficient $0 \le \xi \le 1$ characterizing proximity of homogeneous mixing to inhomogeneous (when $\xi \to 0$).	-

7

Figure Captions

Figure 1. Classical conceptual diagram of (a) inhomogeneous and (b) homogeneous mixing. 1 initial state; 2 mixing state; 3 final state.

Formatted: Font: Times New Roman, 12 pt

Formatted: Indent: Left: 0 cm, Hanging: 1.5 cm

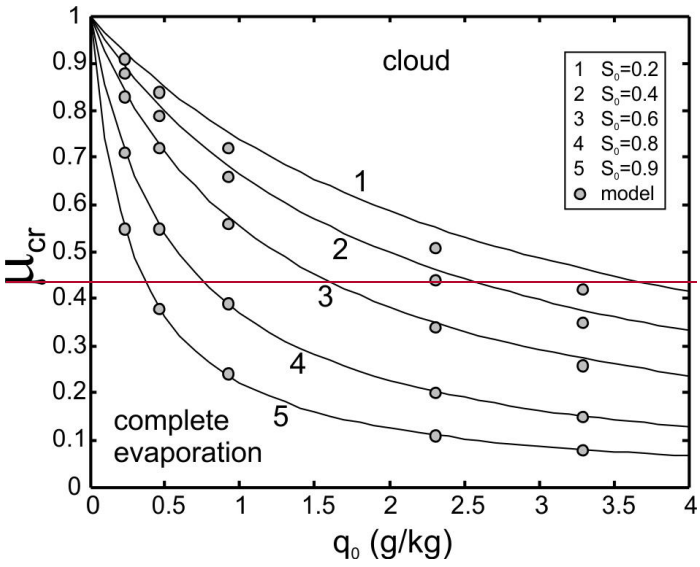

Figure 2. Dependence of ~~initial ratio of mixing q_0 versus~~ critical ~~ratio of~~ mixing fraction μ_{cr} versus mixing ~~μ_{cr}~~ ratio q_0 calculated from Eq~~.23.~~(7). Circles indicate modeled points. The calculations were performed for ~~T~~=0C and ~~H~~=3000m.

Formatted: Font: Times New Roman, 12 pt

Formatted: Font: Times New Roman, 12 pt

Formatted: Indent: Left: 0 cm, Hanging: 1.5 cm

Formatted: Font: Times New Roman, 12 pt

Formatted: Font: Times New Roman, 12 pt

Formatted: Font: Times New Roman, 12 pt

Formatted: Font: Times New Roman, 12 pt

Formatted: Font: Times New Roman, 12 pt

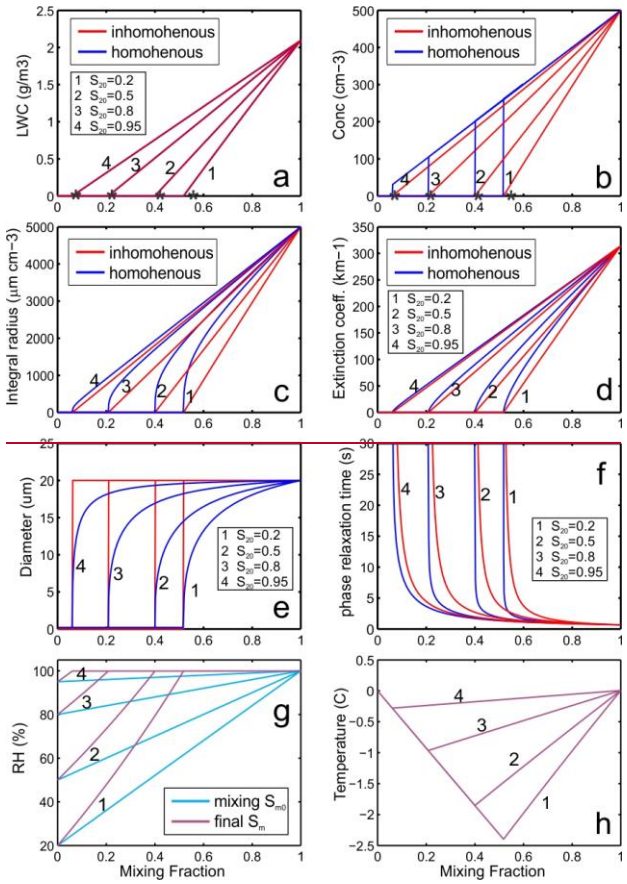

Figure 3. Dependence of ξ versus μ. Numbers are the dimensionless ratios $\delta q^*/q_1$. Critical mixing ratios μ_{cr} are indicated by stars. Grey area indicates area where the moments of homogeneous and extreme inhomogeneous mixing may not be segregated from in-situ measurements. Dashed line was calculated for the cloud in Figs.13-14.

Figure 4. Simulation of (a) liquid water mixing ratio, (b) droplet number concentration ~~and (b) liquid water mixing ratio, (~~, (c) integral droplet ~~radius~~diameter, (d) extinction coefficient, (e) mean ~~cube~~volume diameter, (f) time of phase relaxation, (g) relative humidity in the mixed volume before droplet evaporation ~~S_{m0}~~ RH_{m0} and ~~final S_m~~, at the equilibrium state RH_m, (h) final temperature ~~T_m~~ T_{m0} versus ratio of mixing μ formed after homogeneous

Formatted: Font: Times New Roman, 12 pt
Formatted: Font: Times New Roman, 12 pt, Not Bold
Formatted: Font: Times New Roman, 12 pt
Formatted: Font: Times New Roman, 12 pt
Formatted: Indent: Left: 0 cm, Hanging: 1.5 cm
Formatted: Font: Times New Roman, 12 pt
Formatted: Font: Times New Roman, 12 pt
Formatted: Font: Times New Roman, 12 pt
Formatted: Font: Times New Roman, 12 pt
Formatted: Font: Times New Roman, 12 pt
Formatted: Font: Times New Roman, 12 pt
Formatted: Font: 12 pt
Formatted: Font: Times New Roman, 12 pt

and extreme inhomogeneous mixing between dry and cloudy parcel with monodisperse droplets. Black stars ~~on (a) and (b)~~ indicate critical ~~ratio of~~ mixing ~~μ_{cr}~~ fraction μ_{cr} calculated from Eq.~~23.~~ (7). The calculations were performed for ~~RH_{20} =20%, 50%, 80%,~~ RH_2 =0.2, 0.5, 0.8, 0.95~~%; r_0 =10~~; D_1=20μm, ~~N_0=~~N_1=500cm^{-3}; ~~$T_{10} = T_{20} =$~~ $T_1 = T_2$ =0C; ~~H~~H=1000m.

Formatted: Font: Times New Roman, 12 pt

Formatted: Font: Times New Roman, 12 pt

Formatted: Font: Times New Roman, 12 pt

Field Code Changed

Formatted: Font: Times New Roman, 12 pt

Formatted: Font: Times New Roman, 12 pt

Formatted: Font: Times New Roman, 12 pt

Formatted: Font: 12 pt

Formatted: Font: Times New Roman, 12 pt

Formatted: Font: Times New Roman, 12 pt

Formatted: Font: Times New Roman, 12 pt

Formatted: Font: Times New Roman, 12 pt

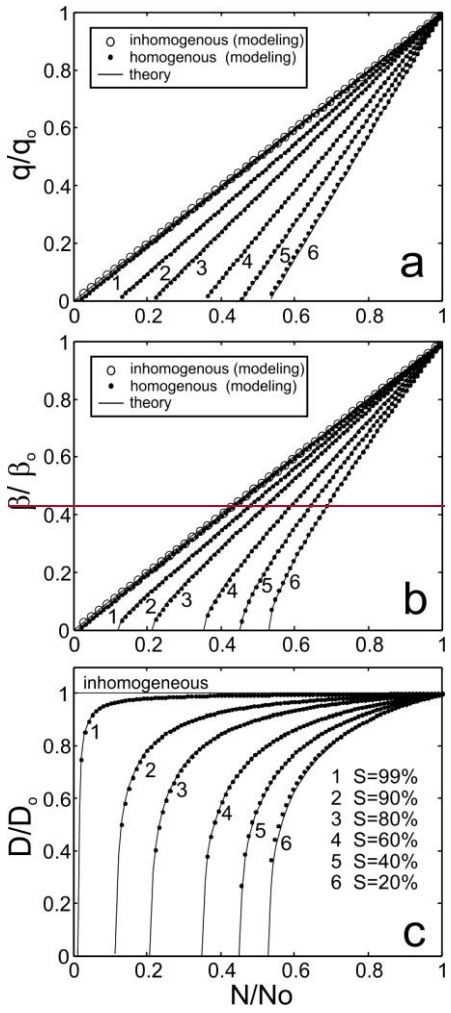

Figure 45. Dependence of normalized liquid water mixing ratio ~~q/q_0~~ q/q_1 (a,d,g), extinction coefficient ~~β/β_0~~ β/β_1 (b,e,h) and mean volume diameter ~~r_3/r_0~~ D_v/D_{v1} (c,f,j) versus normalized number concentration ~~N/N_0~~ N/N_1 for various humidity of the entrained air (a,b,c), for various liquid water mixing ratios (d,e,f) and for various temperatures (g,h,j). The calculations were performed ~~for different relative humidity of the entrained air *RH*: (1) 99%; (2) 90%; (3) 80%; (4) 60%; (5) 40%; (6) 20%.~~

Formatted: Font: Times New Roman, 12 pt

Formatted: Font: Times New Roman, 12 pt

Formatted: Font: Times New Roman, 12 pt

The the initial conditions used for the calculations were: H_0: H=1000m, $T_1(0)=T_2(0)=0C$; $r_0=10D_1=20\mu m$;

$N_0=$; for (a-c; g-j) $N_1=500cm^{-3}$.

Formatted: Font: Times New Roman, 12 pt

Formatted: Font: Times New Roman, 12 pt

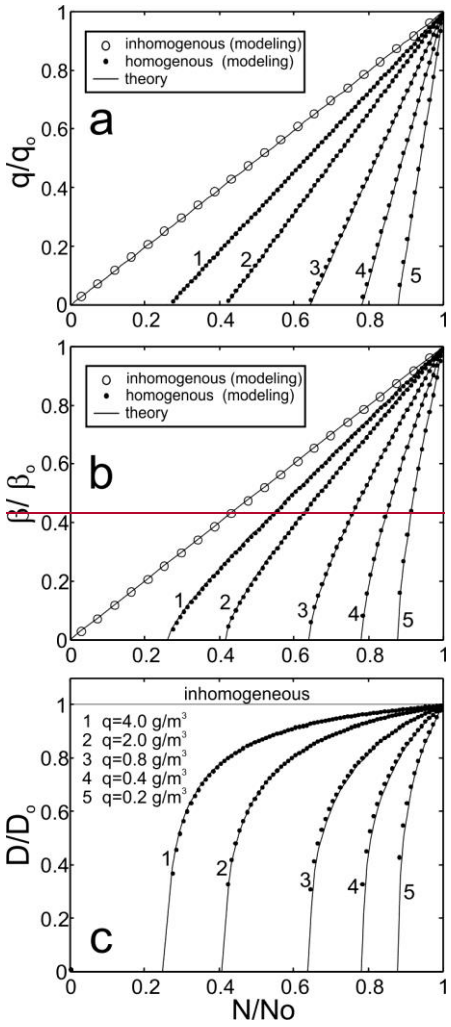

Figure 5. Effect of the water content q_0 on mixing. Same as in Fig.4. The calculations were performed for different initial liquid water content: (1) 4.0g/kg; (2) 2.0g/kg; (3) 0.8g/kg; (4) 0.4g/kg; (5) 0.2g/kg. The initial conditions used for the calculations were: H_o=1000m, $RH(0)$=50%; $T_1(0)=T_2(0)$=0C; r_o=10μm.

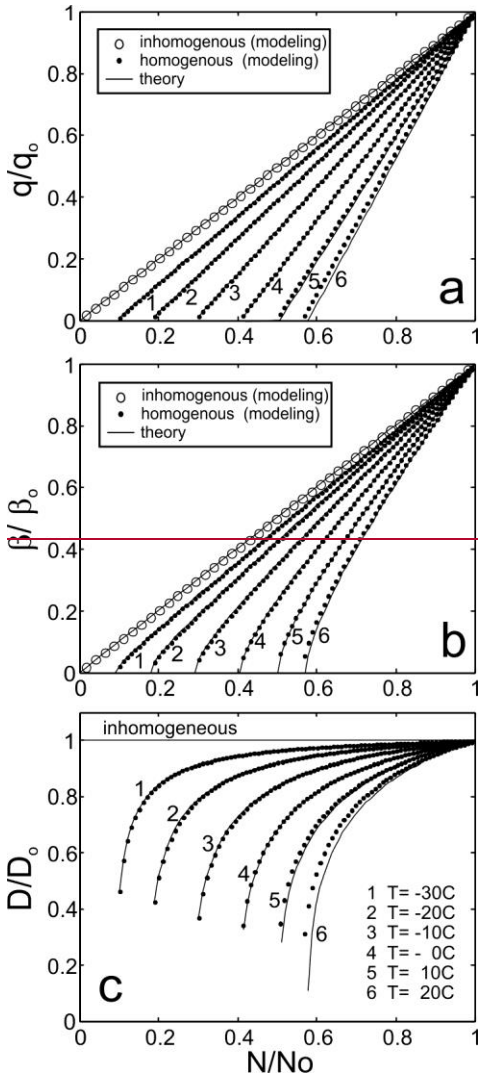

Figure 6. Effect of temperature on mixing. Same as in Fig.4. The calculations were performed for different initial temperatures T: (1) -30C; (2) -20C; (3) -10C; (4) 0C; (5) 10C; (6) 20C. The initial conditions used for the calculations were: H_o=1000m, $RH(0)$=50%; r_o=10μm, N_o=500cm^{-3} (a-f) $T_1 = T_2 =$0C.

Formatted: Right: -0.24 cm

Formatted: Font: Times New Roman

Formatted: Font: Times New Roman, Bold

Formatted: Font: Times New Roman

Formatted: Font: Times New Roman, 12 pt

Formatted: Indent: Left: 0 cm, Hanging: 1.5 cm, Right: 0 cm

Formatted: Font: Times New Roman, 12 pt

7

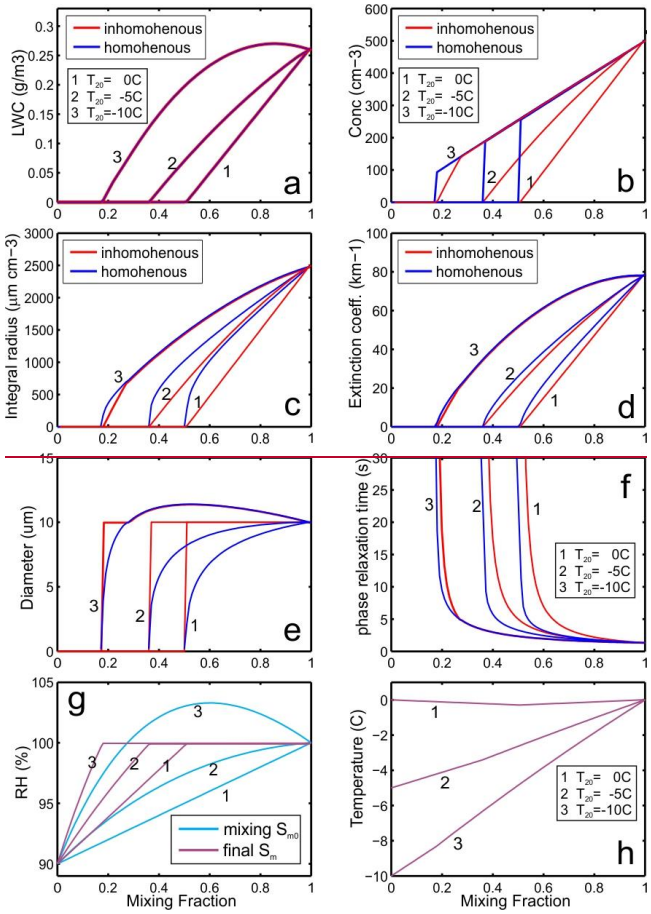

Figure ~~7~~6. Simulation of (a) droplet number concentration and (b) liquid water mixing ratio, (c) integral droplet ~~radius~~diameter, (d) extinction coefficient, (e) mean ~~cube~~volume diameter, (f) time of phase relaxation, (g) relative humidity in the mixed volume before droplet evaporation ~~S_{m0}~~ RH_{m0} and ~~final S_m~~, at the equilibrium state RH_m, (h) final temperature ~~T_m~~ T_m versus ratio of mixing μ formed after homogeneous and extreme inhomogeneous mixing between dry and cloudy parcel with monodisperse droplets. ~~Black stars on (a) and (b) indicate critical ratio of mixing μ_{cr} calculated from Eq.22.~~ The calculations were

Formatted: Font: Times New Roman, 12 pt
Formatted: Indent: Left: 0 cm, Hanging: 1.5 cm
Formatted: Font: Times New Roman, 12 pt
Formatted: Font: Times New Roman, 12 pt
Formatted: Font: Times New Roman, 12 pt
Formatted: Font: Times New Roman, 12 pt
Formatted: Font: Times New Roman, 12 pt
Field Code Changed
Formatted: Font: Times New Roman, 12 pt
Formatted: Font: 12 pt
Formatted: Font: Times New Roman, 12 pt
Formatted: Font: Times New Roman, 12 pt
Formatted: Font: Times New Roman, 12 pt

performed for ~~RH=90%; r_0=5~~RH_2=0.9; D_1=10μm, ~~N_0=~~N_1=500cm^{-3}; ~~T_{10}=~~T_1 =0C; ~~T_{20} =~~ -T_2 = -10C, -5C, 0C; ~~H~~=1000m.

Formatted: Font: 12 pt

Formatted: Font: Times New Roman, 12 pt

Formatted: Font: Times New Roman, 12 pt

Formatted: Font: Times New Roman, 12 pt

Formatted: Font: Times New Roman, 12 pt

Formatted: Font: Times New Roman, 12 pt

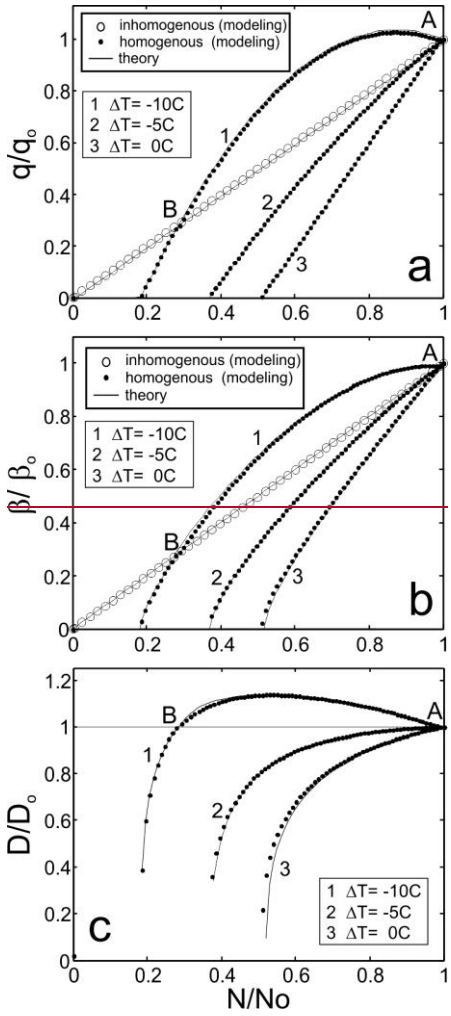

Figure 7. ~~**Figure 8.**~~ Effect of temperature difference between cloud and entrained air on mixing. ~~Same as in Fig.4.~~ The calculations were performed for ~~different~~ initial temperatures ~~ΔT~~ T_2: (1) -10C; (2) -5C; (3) ~~-0C.~~0C. Grey circles indicate extremely inhomogeneous mixing on line 1 at the *AB* interval. The rest cases on extremely inhomogeneous mixing are indicated

Formatted: Font: Times New Roman, 12 pt

Formatted: Font: Times New Roman, 12 pt, Bold

Formatted: Font: Times New Roman, 12 pt

Formatted: Indent: Left: 0 cm, Hanging: 1.5 cm

Formatted: Font: Times New Roman, 12 pt

Formatted: Font: Times New Roman, 12 pt

Formatted: Font: Times New Roman, 12 pt

by open circles. The initial conditions used for the calculations were: ~~H_0~~H=1000m, ~~$RH(0)$~~RH_2=90%; ~~r_0~~=~~5~~D_1 =10μm, ~~N_0~~=N_1 =500cm^{-3}; ~~T_{10}~~ = T_1=0C.

Formatted: Font: Times New Roman, 12 pt
Formatted: Font: Times New Roman, 12 pt
Formatted: Font: Times New Roman, 12 pt
Formatted: Font: 12 pt
Formatted: Font: Times New Roman, 12 pt
Formatted: Font: Times New Roman, 12 pt
Formatted: Font: Times New Roman, 12 pt
Formatted: Font: 12 pt

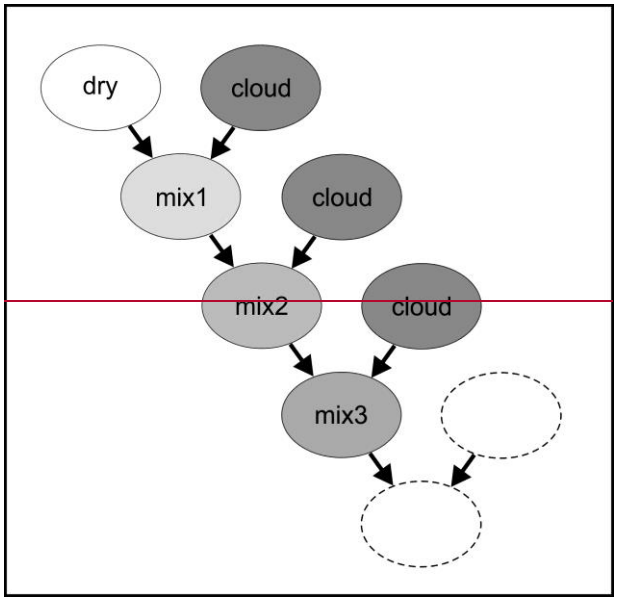

Figure 8. Conceptual diagram of cascade mixing of the out-of-cloud entrained parcel with the cloudy environment

Figure 9. Simulation of stochastic mixing corresponding to stages 1-4 as indicated in Fig.8. Solid red lines indicate the normalized dependences q, β, D_v vs. N for the primary stage of homogeneous mixing. Dashed red lines indicate the same dependences for inhomogeneous mixing. The initial conditions used for the simulations were: H=1000m, $T_1 = T_2$ =0C; RH_2=0.5; D_1 =10μm, N_1 =500cm^{-3}.

Figure 10. Conceptual diagram explaining breaking the functional relationships between the microphysical moment during progressive missing (see text).

Figure 11. Droplet size distributions formed during the progressive homogeneous mixing corresponding to the (a,e) primary stage; (b,f) 2nd stage; (c,g) 3rd stage; (d,h) 4th stage. Left column (a,b,c,d) corresponds to the case, when the cloud temperature is equal to the dry air temperature $T_1 = T_2 = 0$℃,; right column (e,f,g,h) corresponds to the case when $T_1 = 0$℃, $T_2 = -10$℃. For both cases the simulation was performed for D_1 =10μm; N=500cm^{-3}; RH_2=0.9.

Formatted: Font: Times New Roman, 12 pt

Formatted: Font: Times New Roman, 12 pt, Bold

Formatted: Font: Times New Roman, 12 pt

Figure 12. Conceptual diagrams of scattering of measurements of q versus N for (a) extreme inhomogeneous and (b) homogeneous mixing.

Figure 13. Spatial changes of particle concentration (a), extinction coefficeint (b), liquid water content (c) and average and mean mass diameter (d) during transit through one of the convective clouds measured by CDP. The measurements were conducted during the COPE-MED project on 18 July, 2015. The sampling rate 10Hz (~10m spatial resolution). H=5500m, T=-12C, RH=0.2.

Figure 14. Relatonships between (a) $LWC(N)$; (b) $\beta(N)$; (c) $D_v(N)$; (d) $LWC(\beta)$ calculated from the CDP measurements obtained during sampling several convective clouds. The meadurements were conducted during the COPE-MED project on 18 July, 2015, H=5500m, T=-12C, RH=0.2. The measurements were sampled at 10Hz (~10m spatial resolution). Dashed lines are linear regressions. Red lines indicate primary inhomogeneous mixing dependencies calculated for the same environmental conditions.

Figure 15. Relatonships between (a) $LWC(N)$; (b) $\beta(N)$; (c) $D_v(N)$; (d) $LWC(\beta)$ calculated from the CDP measurements sampled during traverse through 45 convective clouds. The meadurements were conducted during the COPE-MED project on 02 August, 2015. Dashed lines indicate (a), (b) and (d) indicate the sectors, where the majority of the points are scattered. ~~**Figure 9.**~~The altitude of sampling varied in the range 3000m <H< 4500m, temperature -11C<T<0C, relative humidity in the vicinity of clouds 15%<RH<65%. The measurements were sampled at 10Hz (~10m spatial resolution).

Figure A1. Amount of evaporated liquid water δq_m required for saturation of a cloud volume with initial humidity RH_m. Comparisons of the modeled δq_m and that calculated from Eqs. (A8) and (A9) for three temperatures T_{m0} =-20C, 0C and 20C. Calculations were performed for P=880mb.

Formatted: Font: Times New Roman, 12 pt

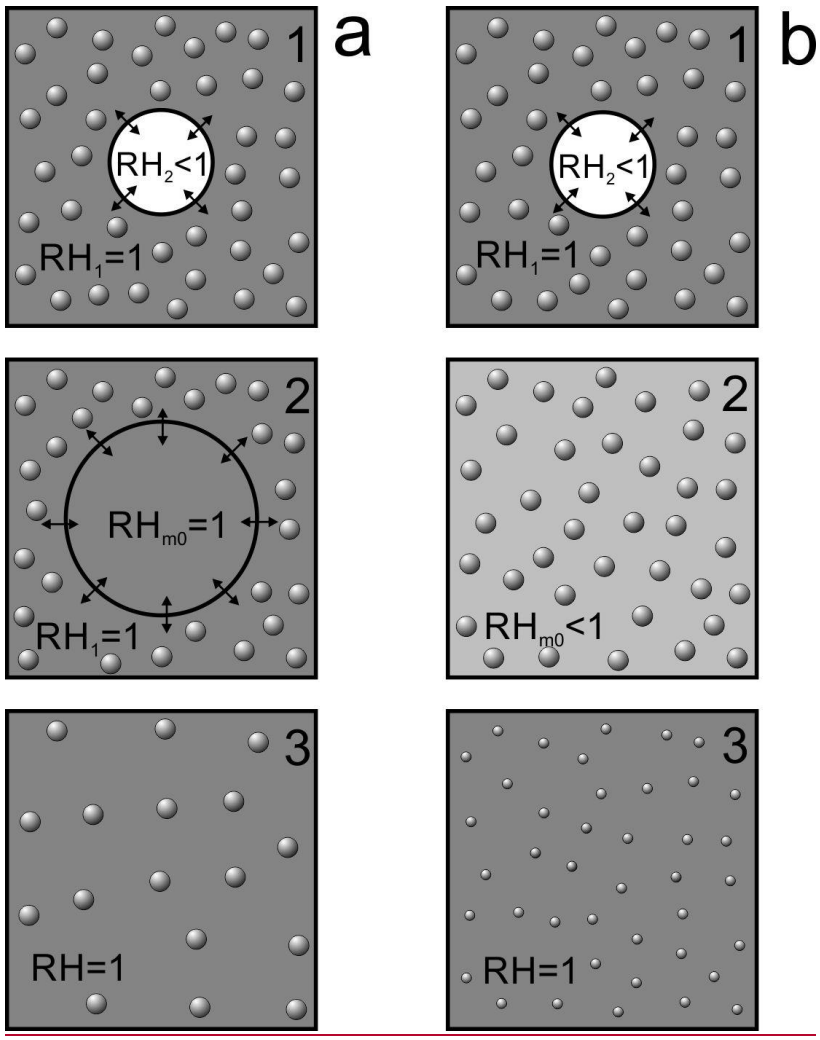

Figure 1. Classical conceptual diagram of (a) inhomogeneous and (b) homogeneous mixing. 1 initial state; 2 mixing state; 3 final state.

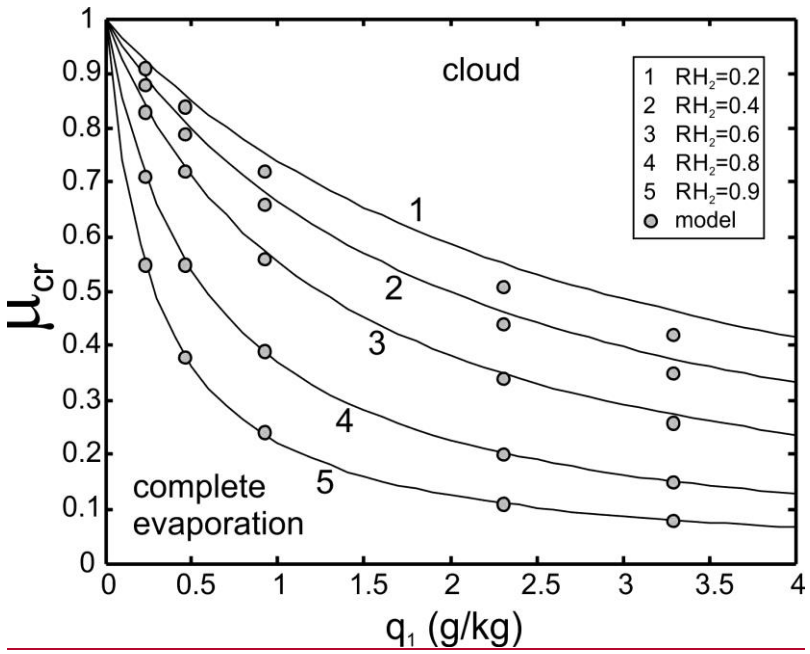

Figure 2. Dependence of critical mixing fraction μ_{cr} versus mixing ratio q_0 calculated from Eq.(7). Circles indicate modeled points. The calculations were performed for T=0C and H=3000m.

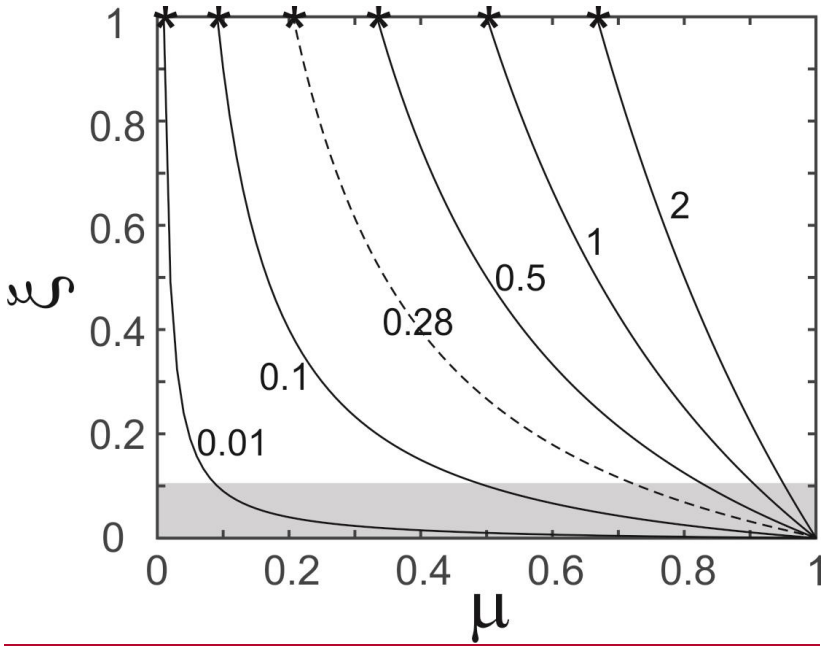

Figure 3. Dependence of ξ versus μ. Numbers are the dimensionless ratios $\delta q^*/q_1$. Critical mixing ratios μ_{cr} are indicated by stars. Grey area indicates area where the moments of homogeneous and extreme inhomogeneous mixing may not be segregated from in-situ measurements. Dashed line was calculated for the cloud in Figs.13-14.

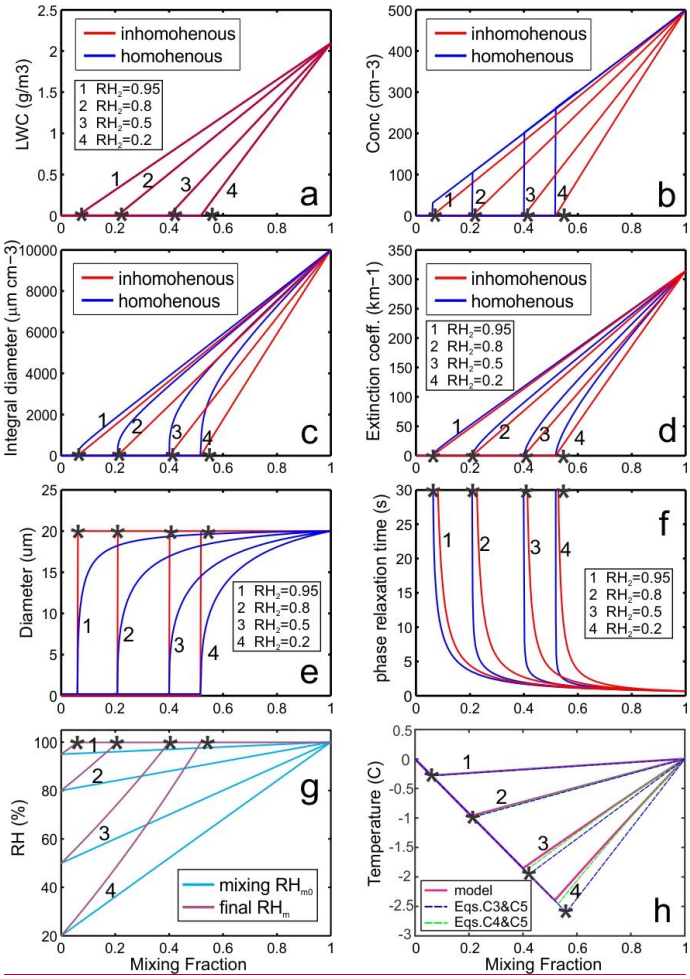

Figure 4. Simulation of (a) liquid water mixing ratio, (b) droplet number concentration, (c) integral droplet diameter, (d) extinction coefficient, (e) mean volume diameter, (f) time of phase relaxation, (g) relative humidity in the mixed volume before droplet evaporation RH_{m0} and at the equilibrium state RH_m, (h) final temperature T_{m0} versus ratio of mixing μ formed after homogeneous and extreme inhomogeneous mixing between dry and cloudy parcel with monodisperse droplets. Black stars indicate critical mixing fraction μ_{cr} calculated from Eq.(7). The calculations were performed for RH_2 =0.2, 0.5, 0.8, 0.95; D_1=20μm, N_1=500cm^{-3}; $T_1 = T_2$ =0C; H=1000m.

Field Code Changed

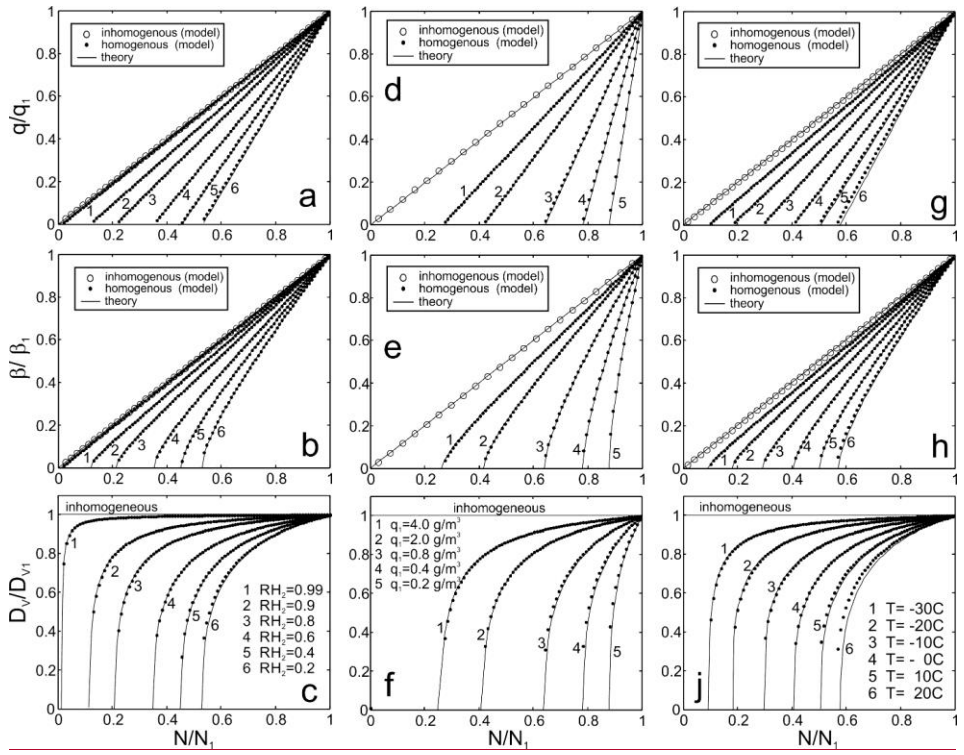

Figure 5. Dependence of normalized liquid water mixing ratio q/q_1 (a,d,g), extinction coefficient β/β_1 (b,e,h) and mean volume diameter D_v/D_{v1} (c,f,j) versus normalized number concentration N/N_1 for various humidity of the entrained air (a,b,c), for various liquid water mixing ratios (d,e,f) and for various temperatures (g,h,j). The calculations were performed the initial conditions: H=1000m, D_1=20μm; for (a-c; g-j) N_1=500cm^{-3}; for (a-f) $T_1 = T_2$ =0C.

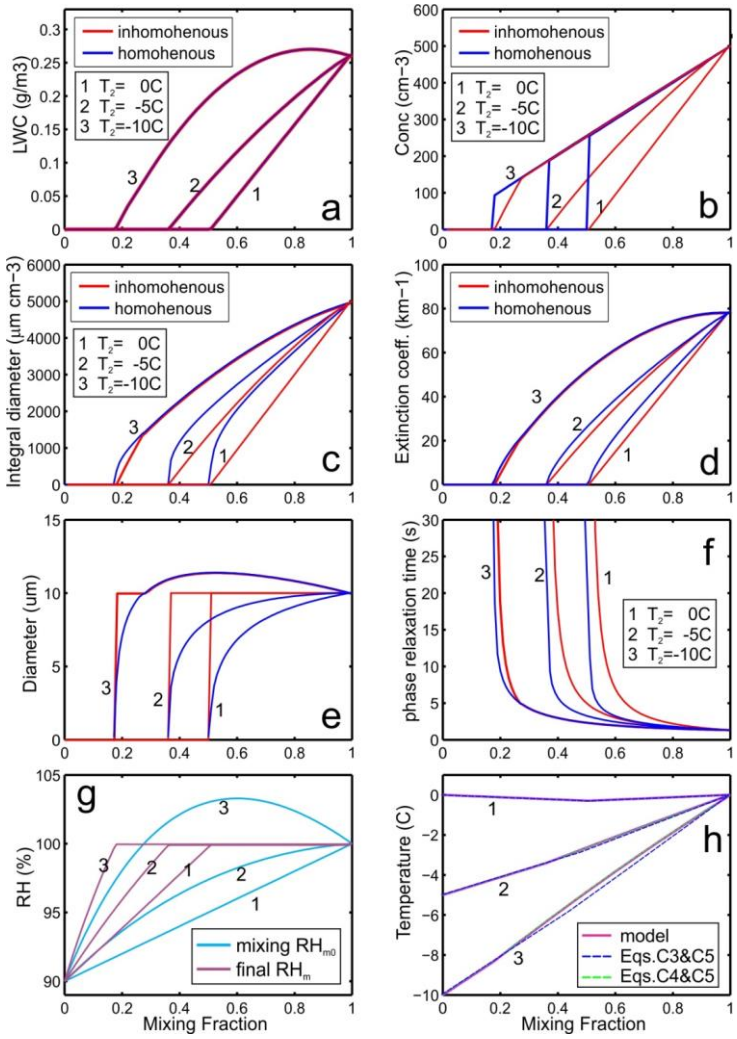

Figure 6. Simulation of (a) droplet number concentration and (b) liquid water mixing ratio, (c) integral droplet diameter, (d) extinction coefficient, (e) mean volume diameter, (f) time of phase relaxation, (g) relative humidity in the mixed volume before droplet evaporation RH_{m0} and at the equilibrium state RH_m, (h) final temperature T_m versus ratio of mixing μ formed after homogeneous and extreme inhomogeneous

Formatted: Right: -0.24 cm

Formatted: Font: Times New Roman

Formatted: Font: Times New Roman, Bold

Formatted: Font: Times New Roman

Field Code Changed

mixing between dry and cloudy parcel with monodisperse droplets. The calculations were performed for RH_2=0.9; D_1=10μm, N_1=500cm^{-3}; T_1 =0C; T_2 = -10C, -5C, 0C; H=1000m.

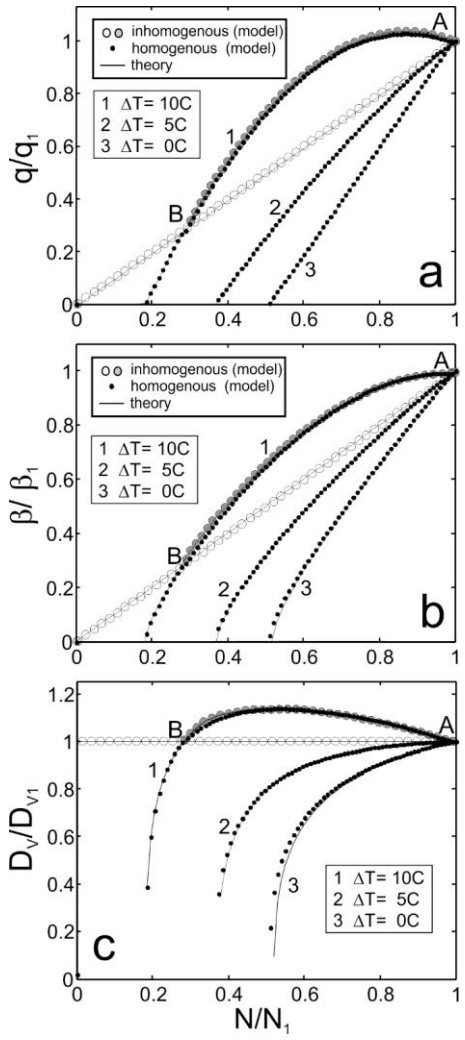

Figure 7. Effect of temperature difference between cloud and entrained air on mixing. The calculations were performed for initial temperatures T_2: (1) -10C; (2) -5C; (3) 0C. Grey circles indicate extremely inhomogeneous mixing on line 1 at the AB interval. The rest cases on extremely inhomogeneous mixing are indicated by open circles. The initial conditions used for the calculations were: H=1000m, RH_2=90%; D_1 =10μm, N_1 =500cm^{-3}, T_1=0C.

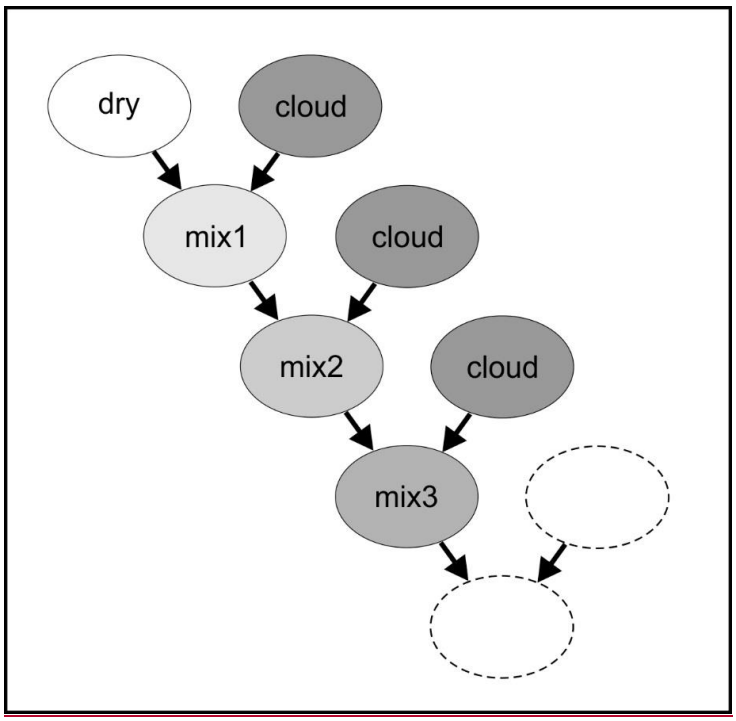

Figure 8. Conceptual diagram of cascade mixing of the out-of-cloud entrained parcel with the cloudy environment

Formatted: Font: Times New Roman

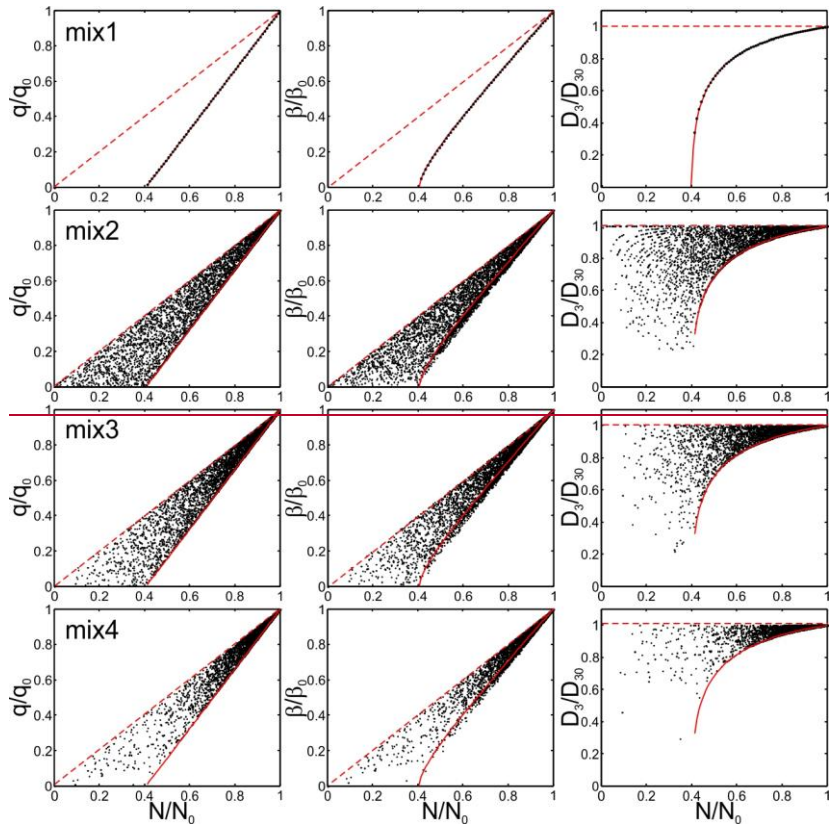

1

2

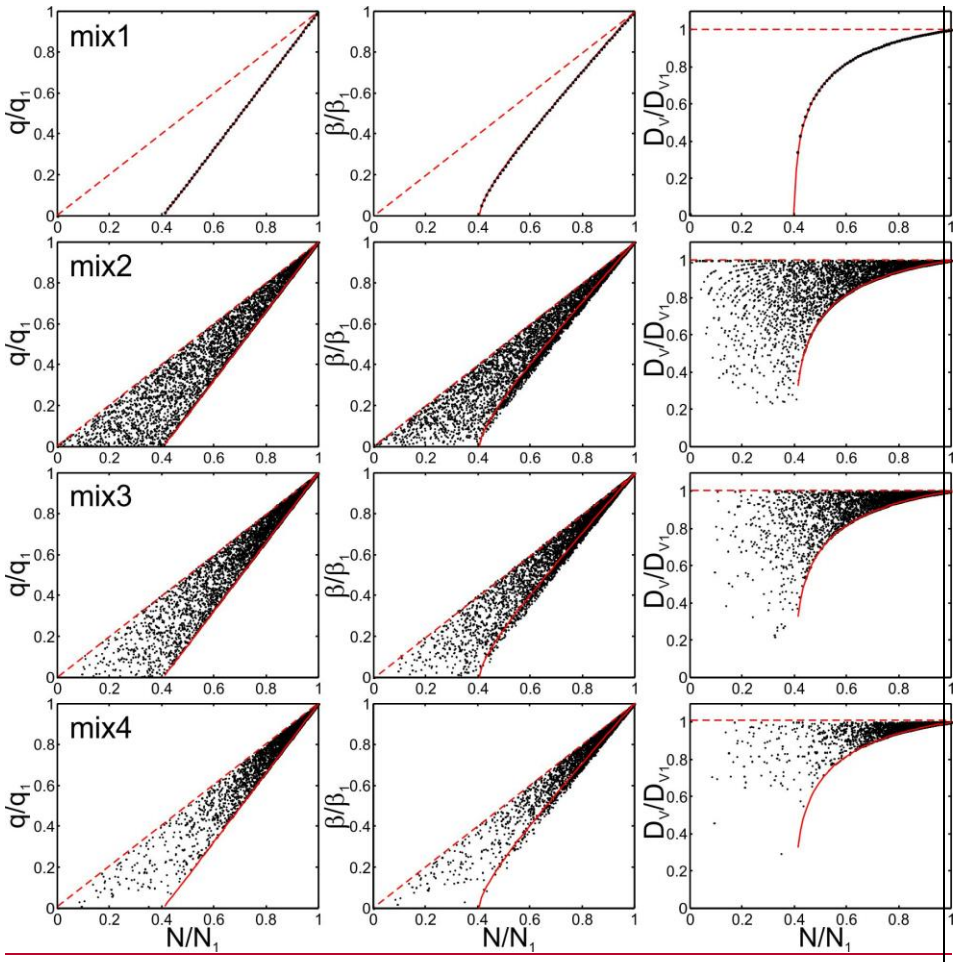

Figure ~~10~~9. Simulation of stochastic mixing corresponding to stages 1-4 as indicated in Fig.~~7~~8. Solid red lines indicate the normalized dependences ~~$q, \beta, \overline{D}_3$~~ q, β, D_v vs. ~~N~~N for the primary stage~~.~~ of homogeneous mixing. Dashed red lines indicate the same dependences for inhomogeneous mixing. The initial conditions used for the simulations were: ~~H_0~~H=1000m, ~~$T_1(0)=T_2(0)=$~~$T_1 = T_2$ =0C; ~~$RH_2(0)=50\%$;~~ ~~$r_0=$~~$RH_2=0.5$; D_1 =10μm, ~~$N_0=$~~N_1 =500cm^{-3}.

Formatted: Font: Times New Roman
Formatted: Font: Times New Roman
Formatted: Font: Times New Roman
Formatted: Font: Times New Roman
Formatted: Font: (Default) Times New Roman, 12 pt, English (United States)

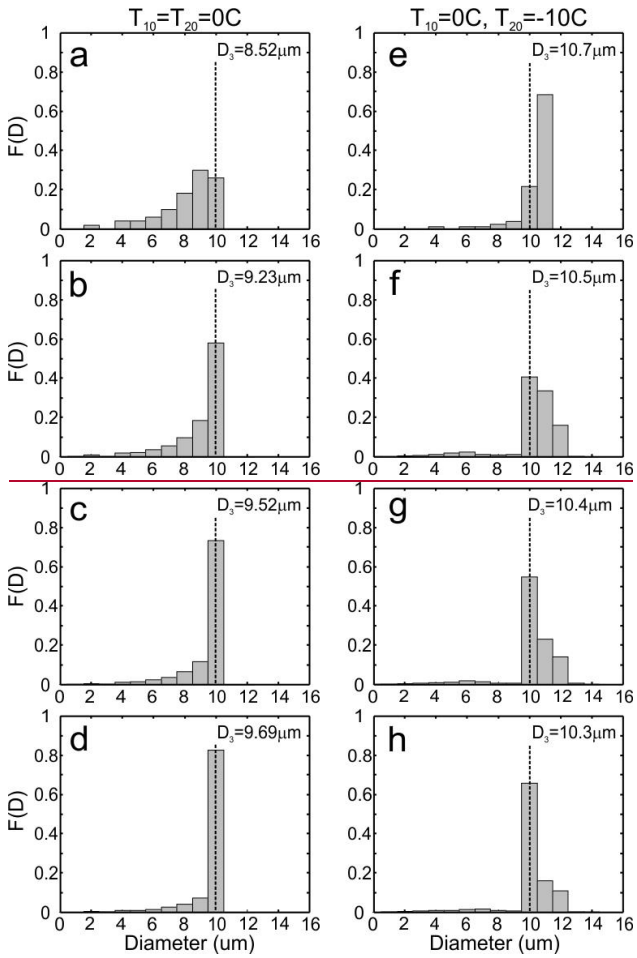
T10=T20=0C
T10=0C, T20=-10C
a
D3=8.52μm
b
D3=9.23μm
c
D3=9.52μm
d
D3=9.69μm
e
D3=10.7μm
f
D3=10.5μm
g
D3=10.4μm
h
D3=10.3μm
F(D)
Diameter (um)

1

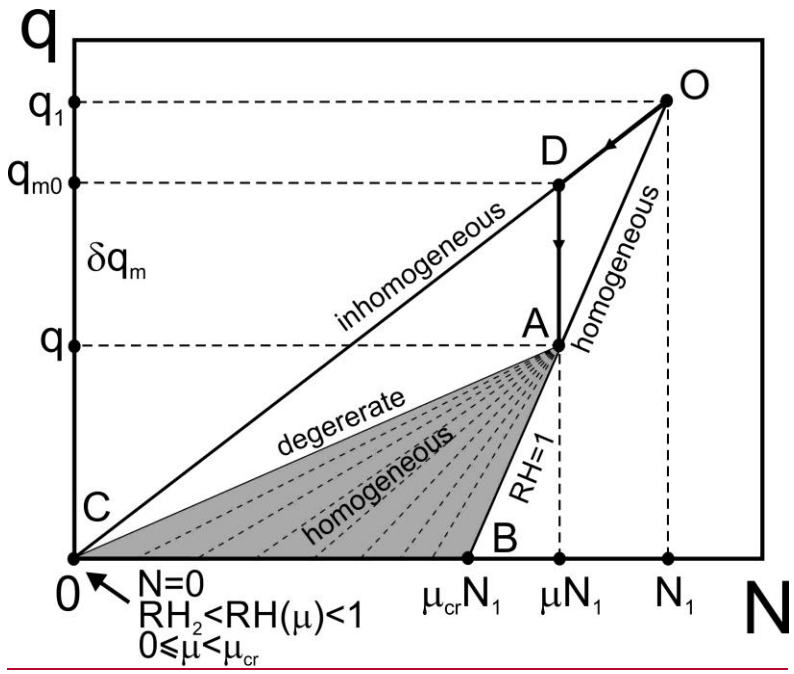

Figure 10. Conceptual diagram explaining breaking the functional relationships between the microphysical moment during progressive missing (see text).

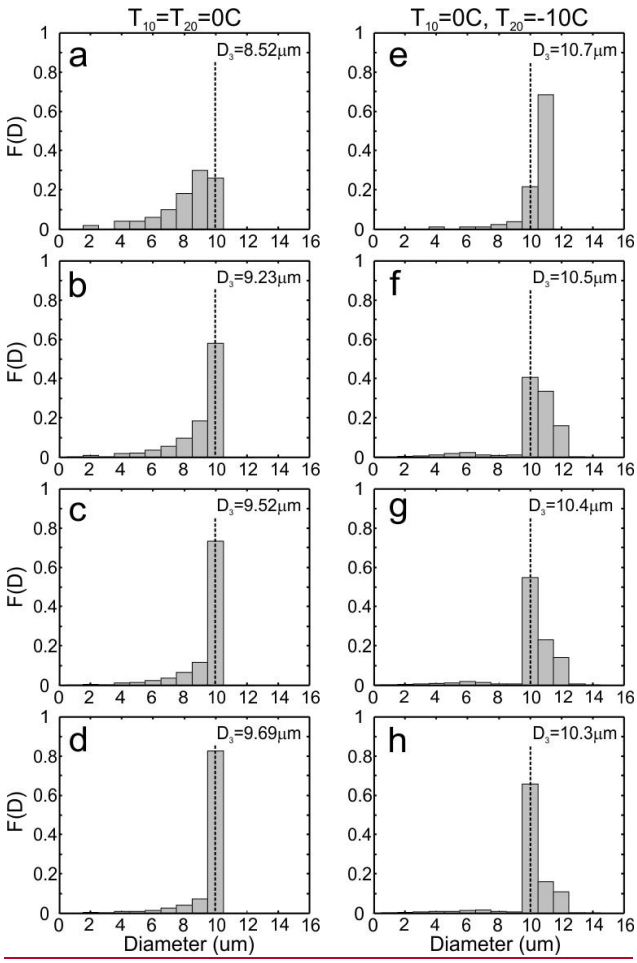

Figure 11. Droplet size distributions formed during the progressive homogeneous mixing corresponding to the (a,e) primary stage; (b,f) 2nd stage; (c,g) 3rd stage; (d,h) 4th stage. Left column (a,b,c,d) corresponds to the case, when the cloud temperature is equal to the dry air temperature ~~T_{10}=T_{20}=0C,~~$T_1 = T_2 = 0°C$, right column (e,f,g,h) corresponds to the case when ~~the dry air temperature is colder than that of cloud T_{10}=0C; T_{20}= 10C.~~ $T_1 = 0°C$, $T_2 = -10°C$. For both cases the simulation was performed for ~~r_0 =5~~D_1 =10μm; ~~N~~=500cm^{-3}; ~~RH_2~~(RH_2=0)~~=90%~~.9.

Formatted: Font: Times New Roman
Formatted: Line spacing: Multiple 1.15 li
Formatted: Font: Times New Roman
Formatted: Font: Times New Roman
Formatted: Font: Times New Roman
Formatted: Font: Times New Roman
Formatted: Font: Times New Roman
Formatted: Font: Times New Roman
Formatted: Font: Times New Roman

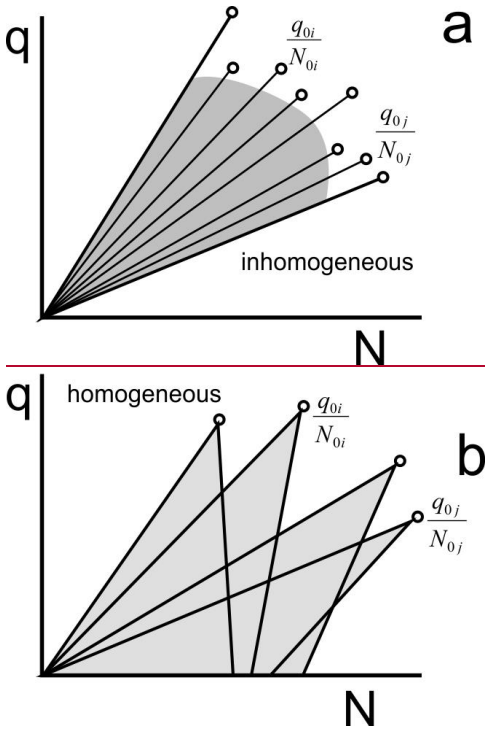
q
a
$\frac{q_{0i}}{N_{0i}}$
$\frac{q_{0j}}{N_{0j}}$
inhomogeneous
N
q
homogeneous
$\frac{q_{0i}}{N_{0i}}$
b
$\frac{q_{0j}}{N_{0j}}$
N

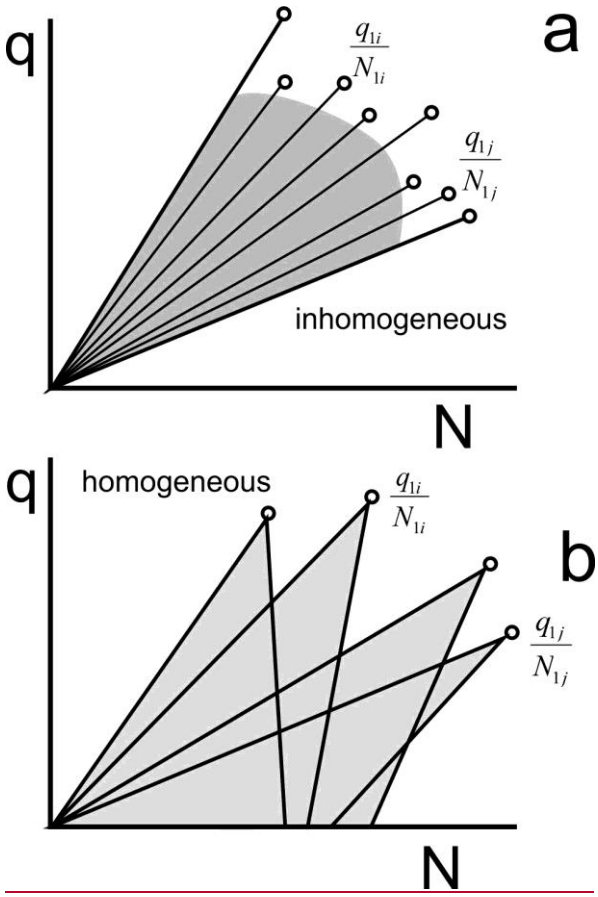

Figure 12. Conceptual diagrams of scattering of measurements of q versus N for (a) extreme inhomogeneous and (b) homogeneous mixing.

Formatted: Font: Times New Roman

Formatted: Font: Times New Roman

Formatted: Font: Times New Roman

Formatted: Font: (Default) Times New Roman, 12 pt, English (United States)

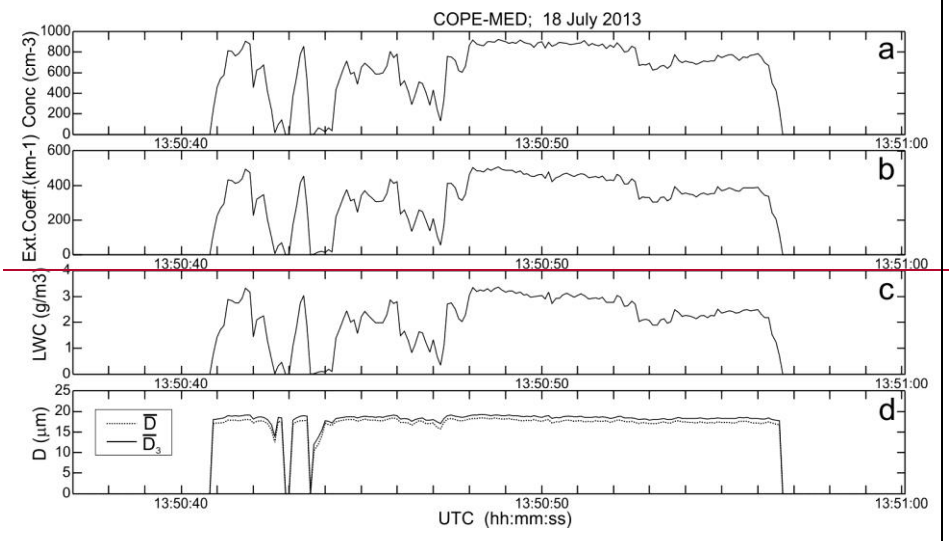
COPE-MED; 18 July 2013
Ext.Coeff.(km-1) Conc (cm-3)
LWC (g/m3)
D (μm)
a
b
c
d
13:50:40
13:50:50
13:51:00
UTC (hh:mm:ss)

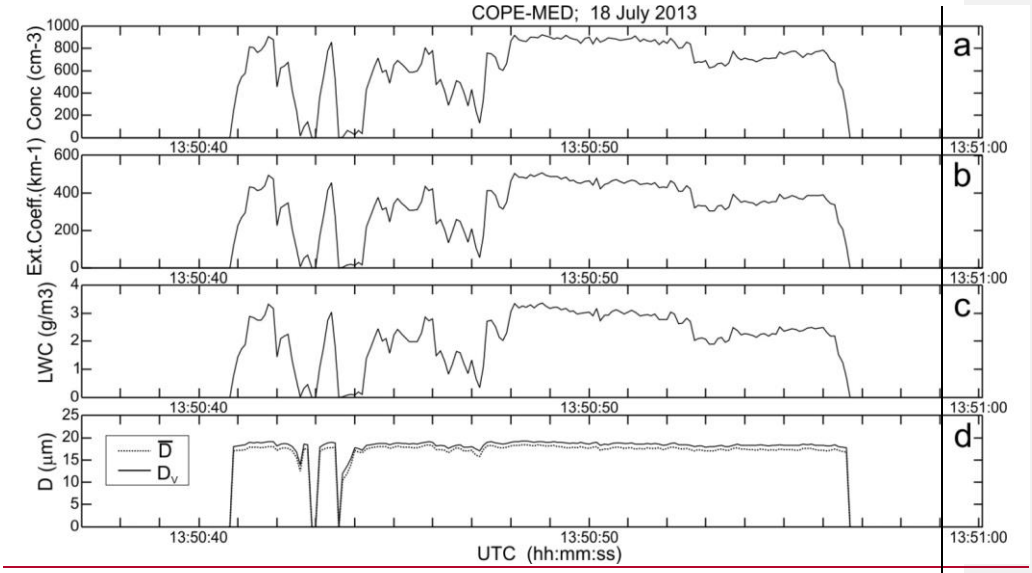

Figure 13. Spatial changes of particle concentration (a), extinction coefficeint (b), liquid water content (c) and average and mean mass diameter (d) during transit through one of the convective clouds measured by CDP. The measurements were conducted during the COPE-MED project on 18 July, 2015. The sampling rate 10Hz (~10m spatial resolution). ~~*HH*~~=5500m, ~~*TT*~~=-12C, ~~*RH=20%.*~~*RH*=0.2.

Formatted: Font: Times New Roman

Formatted: Font: (Default) Times New Roman, 12 pt, English (United States)

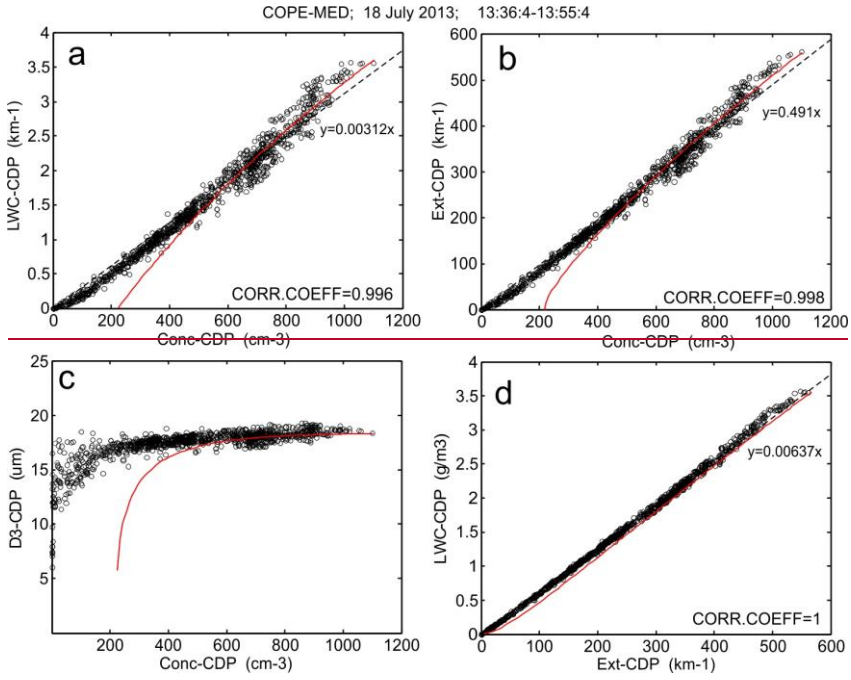
COPE-MED; 18 July 2013; 13:36:4-13:55:4
a
LWC-CDP (km-1)
y=0.00312x
CORR.COEFF=0.996
Conc-CDP (cm-3)
b
Ext-CDP (km-1)
y=0.491x
CORR.COEFF=0.998
Conc-CDP (cm-3)
c
D3-CDP (um)
Conc-CDP (cm-3)
d
LWC-CDP (g/m3)
y=0.00637x
CORR.COEFF=1
Ext-CDP (km-1)

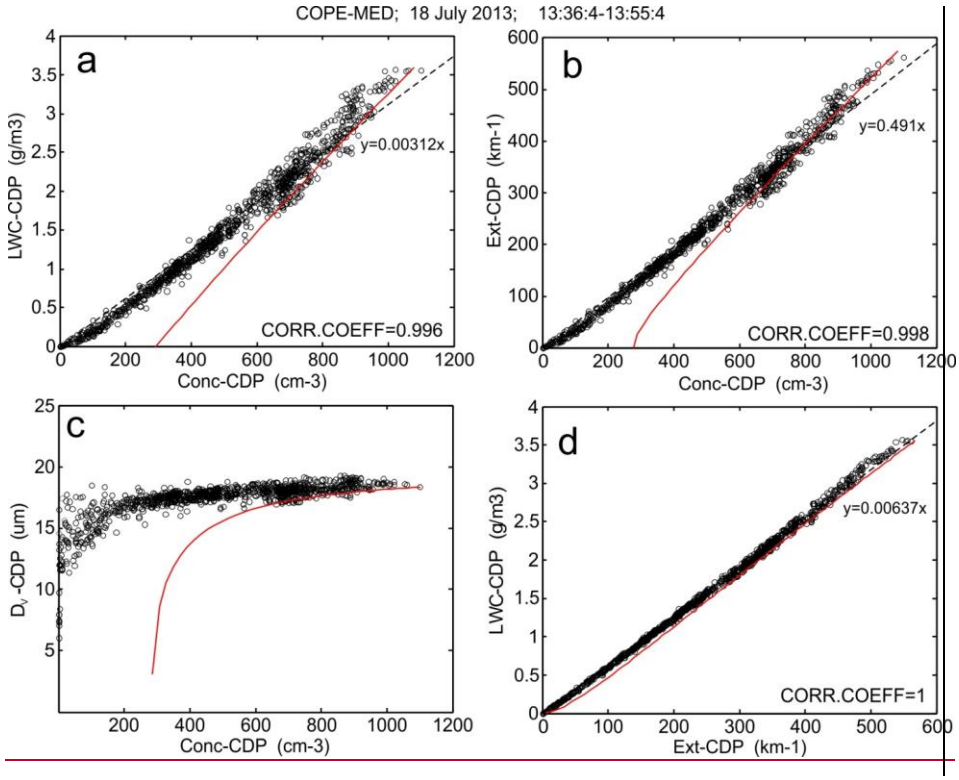

Figure 14. Relatonships between (a) ~~$LWC(N)$~~;$LWC(N)$; (b) ~~$\beta(N)$~~;$\beta(N)$; (c) ~~$\overline{D}_3(N)$~~;$D_v(N)$; (d) ~~$LWC(\beta)$~~$LWC(\beta)$ calculated from the CDP measurements obtained during sampling several convective clouds. The meadurements were conducted during the COPE-MED project on 18 July, 2015, ~~H~~H=5500m, ~~T~~T=-12C, ~~RH=20%.~~RH=0.2. The measurements were sampled at 10Hz (~10m spatial resolution). -Dashed lines are linear regressions. Red lines indicate primary inhomogeneous mixing dependencies calculated for the same environmental conditions.

Formatted: Font: Times New Roman
Formatted: Font: Times New Roman
Formatted: Line spacing: Multiple 1.15 li
Formatted: Font: Times New Roman
Formatted: Font: Times New Roman
Formatted: Font: Times New Roman
Formatted: Font: Times New Roman
Formatted: Font: Times New Roman
Formatted: Font: Times New Roman
Formatted: Font: Times New Roman

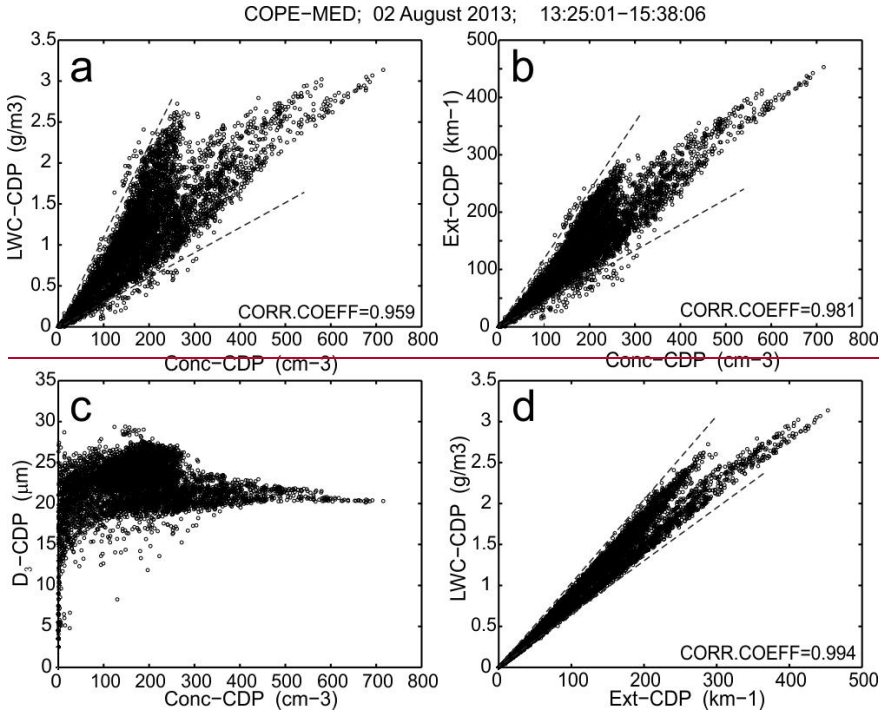
COPE−MED; 02 August 2013; 13:25:01−15:38:06
a
LWC−CDP (g/m3)
CORR.COEFF=0.959
Conc−CDP (cm−3)
b
Ext−CDP (km−1)
CORR.COEFF=0.981
Conc−CDP (cm−3)
c
D3−CDP (μm)
Conc−CDP (cm−3)
d
LWC−CDP (g/m3)
CORR.COEFF=0.994
Ext−CDP (km−1)

1

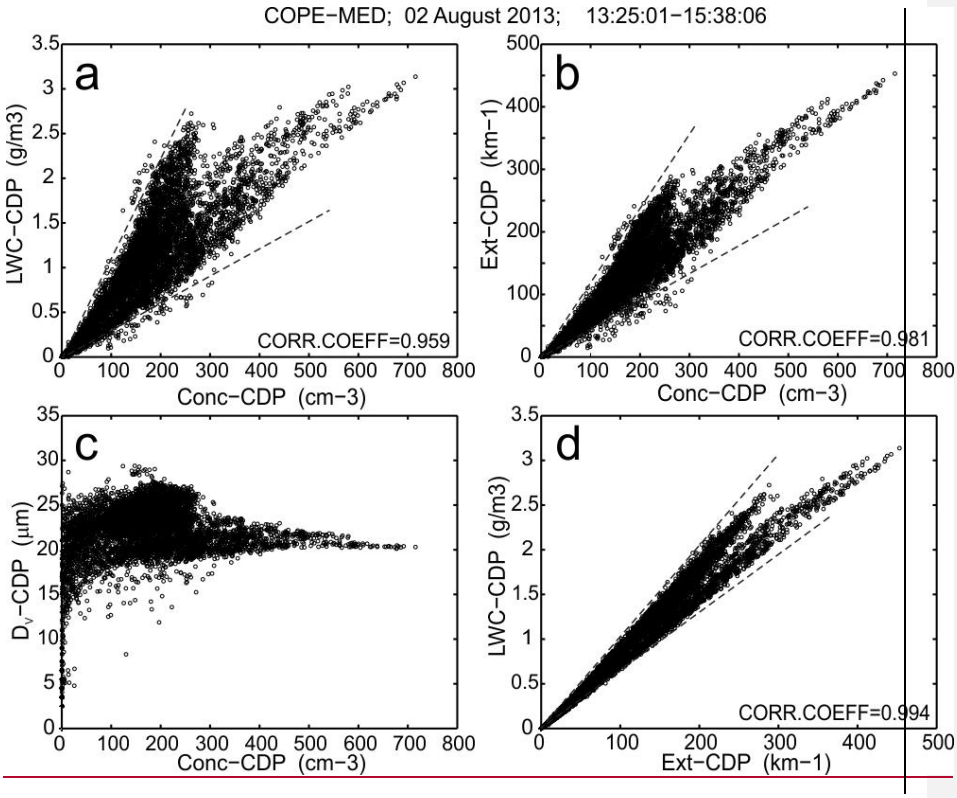

Figure 15. Relatonships between (a) ~~$LWC(N)$~~; $LWC(N)$; (b) ~~$\beta(N)$~~; $\beta(N)$; (c) ~~$\overline{D}_3(N)$~~; $D_v(N)$; (d) ~~$LWC(\beta)$~~ $LWC(\beta)$ calculated from the CDP measurements sampled during traverse through 45 convective clouds. ~~The meadurements were conducted during the COPE-MED project on 02 August, 2015. Dashed lines indicate (a), (b) and (d) indicate the sectors, where the majority of the points are scattered.~~ The meadurements were conducted during the COPE-MED project on 02 August, 2015. Dashed lines indicate (a), (b) and (d) indicate the sectors, where the majority of the points are scattered. The altitude of sampling varied in the range 3000m <~~H~~ H< 4500m, temperature -11C<~~T~~ T<0C, relative humidity in the vicinity of clouds 15%<~~RH~~ RH<65%. The measurements were sampled at 10Hz (~10m spatial resolution).

Formatted: Font: Times New Roman
Formatted: Font: Times New Roman
Formatted: Line spacing: Multiple 1.15 li
Formatted: Font: Times New Roman
Formatted: Font: Times New Roman
Formatted: Font: Times New Roman
Formatted: Font: Times New Roman, 12 pt
Formatted: Font: Times New Roman
Formatted: Font: Times New Roman
Formatted: Font: Times New Roman
Formatted: Font: Times New Roman

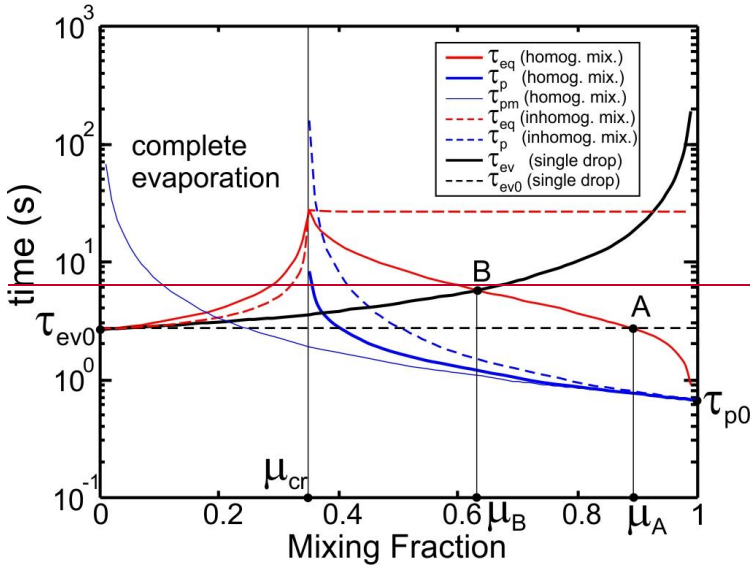

Formatted: Indent: First line: 0.63 cm

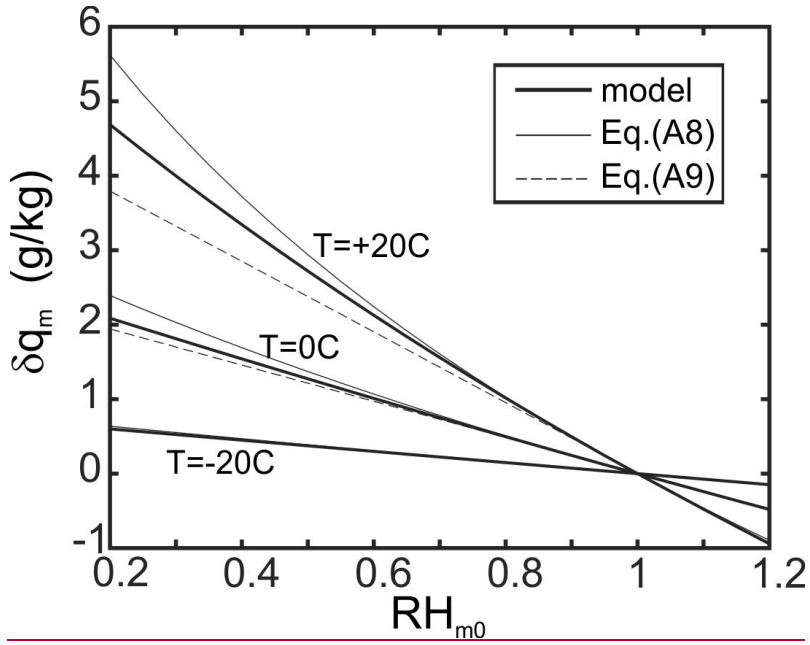

Figure ~~16. Dependencies of different characteristic times versus ratio of mixing. The calculations were performed for RH_{20}=50%; r_0=10μm, N_0=500cm^{-3}; $T_{10} = T_{20}$ = 0C; H=1000m.~~

Formatted: Font: Times New Roman

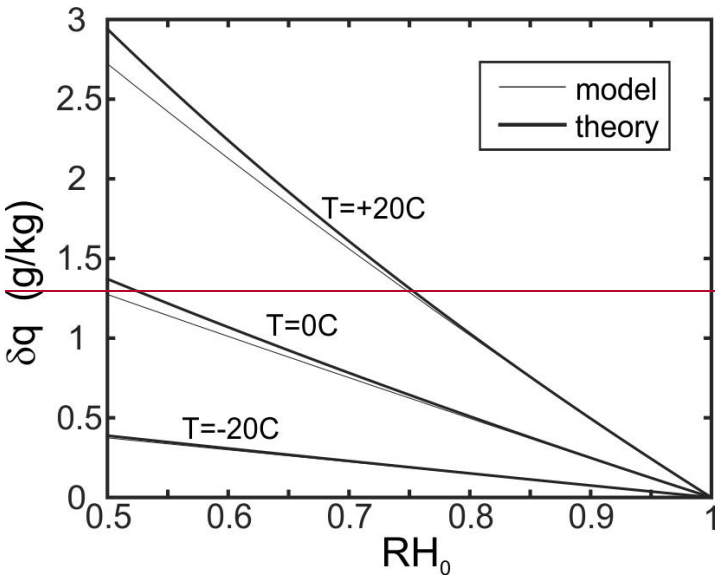

~~Figure B1~~A1. Amount of evaporated liquid water ~~δq~~ δq_m required for saturation of a cloud volume with initial humidity ~~RH_0~~RH_m. Comparisons of the modeled ~~δq~~ δq_m and that calculated from ~~Eq.B8~~Eqs. (A8) and (A9) for three ~~different~~ temperatures ~~T_{m0}~~ =20C, 0C and 20C. Calculations were performed for ~~P~~ =P=880mb.

Formatted: Header distance from edge: 1.25 cm, Footer distance from edge: 1.25 cm, Numbering: Restart each page

Formatted: Font: Times New Roman

Formatted: Font: Times New Roman

Formatted: Font: Times New Roman

Formatted: Font: Times New Roman, 12 pt

Formatted: Indent: First line: 0 cm, Don't adjust space between Latin and Asian text, Don't adjust space between Asian text and numbers